M.O.637

HANDBOOK

OF

WEATHER FORECASTING

METEOROLOGICAL OFFICE

1964

U.D.C.
551.509.3(02)

PREFACE

The Handbook of Weather Forecasting was written mainly for distribution within the Meteorological Office to provide forecasters with a comprehensive and up-to-date reference book on techniques of forecasting and closely related aspects of meteorology. The work, which appeared originally as twenty separate chapters, is now re-issued in three volumes in loose-leaf form to facilitate revision.

Certain amendments of an essential nature have been incorporated in this edition but, in some chapters, temperature values still appear in degrees Fahrenheit. These will be changed to degrees Celsius when the chapters concerned are completely revised.

CHAPTER 5

SOME DYNAMICAL ASPECTS OF ATMOSPHERIC SYSTEMS

CONTENTS

Chapter 5

SOME DYNAMICAL ASPECTS OF ATMOSPHERIC SYSTEMS

LIST OF DIAGRAMS

CHAPTER 5

SOME DYNAMICAL ASPECTS OF ATMOSPHERIC SYSTEMS

5.1. INTRODUCTION

The main purpose of this chapter is to explain to forecasters, in terms as simple as possible consistent with the requisite thoroughness and accuracy, the concepts on which a number of modern techniques of forecasting are based. A direct derivation of formulae by the manipulation of the equations of motion may tend to leave the forecaster with the impression that the theoretical mathematical approach is not directly applicable to work on the bench. However, the bases of most modern techniques of forecasting changes in the synoptic chart are formulated mathematically and it is important that the forecaster should understand the physical and dynamical interpretation of them. To assist the forecaster to obtain a satisfactory understanding of the dynamical aspects of synoptic systems this chapter approaches the problem in three main steps. The opening sections are mainly descriptive of some features of the tropospheric flow from which the reader is led to consider the importance of temperature distribution and the concept of baroclinity. The middle sections develop the mathematical concepts. The final sections indicate how these concepts can be interpreted either quantitatively or qualitatively on the bench.

5.2. HISTORICAL EVOLUTION OF FORECASTING TECHNIQUES

Forecasters who have some historical knowledge of the evolution of forecasting techniques over recent decades should be better able to appreciate the present state of the science and also to form an opinion of the importance of new techniques of the future. To provide some historical background for the inexperienced forecaster the following resumé has been included. A more complete review has been given by Douglas.[1*]

The introduction of frontal ideas by the Norwegian school of meteorologists proved the mainspring of advances in forecasting techniques during the period between World Wars I and II. The technique was very suitable for application on surface charts which were the only ones available at that time. Practical forecasters found that the models worked well and were reasonably easy to use in operational forecasting. By the 1930's the techniques had been adopted generally and formed the fundamental techniques for forecasting in temperate latitudes. They are still extremely useful – particularly for short-period detailed forecasting for periods up to about 12 hours and to a lesser extent for 12-24 hours ahead.

Although the scientists who propounded the frontal theory and its subsequent refinements laid stress on the importance of upper air conditions the practitioners tended to think of fronts as surface phenomena and to pay too little attention to upper air conditions. This was understandable since the surface chart was the only chart available, as routine and upper air information was very limited. Routine measurements of upper winds, made by pilot-balloon ascents, were limited in number and usually restricted to lower tropospheric altitudes by the existence of cloud or limited visibility. Nephoscope observations, although valuable, were inadequate to delineate the upper flow pattern. Current day-to-day information on temperatures in the upper air over this country was negligible until the first routine aircraft ascents were started at Duxford in 1925. These observations were plotted on the tephigram which soon became a valuable tool to forecasters. This was the only routine information on upper air temperatures in the United

---

* The superscript figures refer to the bibliography at the end of this chapter.

Kingdom until the establishment of a second aircraft ascent at Aldergrove in 1937. A few reports were available from other aircraft ascents over the European continent.

The movement of weather systems is predominantly from west to east and the United Kingdom was in a bad position geographically to develop new techniques of using upper air information. Areas upwind of the British Isles are mainly oceanic and, during the 1920 and 1930 decades, routine upper air ascents were not made over water. It is not surprising that our continental neighbours made greater practical progress in establishing aircraft ascents. The information obtained was eagerly applied to upper air charting during the 1930's and notably so by the Germans who had established seven aircraft ascents and could utilize others from their neighbours. It had now become apparent that three-dimensional charting of weather systems on a day-to-day basis was a practical possibility and that some major advance might be made in the physical understanding of the movement, development and decay of synoptic systems. Such ideas stimulated research in several countries and the foundation of the basic concepts underlying the modern theory of development was laid down.

The stresses of war and the exacting demands of national air forces for accurate upper air information to relatively high levels resulted in development of the radio-sonde network at an accelerated rate. Improvements in other techniques (for example radar) contributed toward more regular and accurate observations of upper winds. The need for accurate information over certain sea areas was partly met by the operation of meteorological reconnaissance flights. After World War II some regular upper observations over sea areas have been provided by means of radio-sondes released from a few weather ships located at key positions. One result of all this development and progress was that during the 1940's the construction of routine and reliable upper charts at various levels throughout the troposphere over a considerable portion of the northern hemisphere had been proved to be practicable. The pipe dreams of a few outstanding pioneers and advanced thinkers had come true and a systematic three-dimensional and dynamical attack on weather systems could be attempted and tested on a day-to-day basis. The network of upper air observing stations was still quite open and, although some fairly small systems might not be observed nor be inferred, there was no doubt but that the main features of major systems were always detected. The newly available information proved a great stimulus to research workers and much effort has been expended toward the understanding of these upper flow patterns.

5.3. SOME CHARACTERISTICS OF THE UPPER FLOW

Forecasters of quite limited experience soon realize that the successful application of frontal ideas to forecasting requires a knowledge of current frontal positions over an area several times larger than the area for which the forecast is required. If forecasts are being prepared for a substantial part of north-west Europe for about 24 hours ahead detailed charting is necessary over the greater part of the North Atlantic Ocean, Europe, the Mediterranean Sea, the northern parts of Africa and the eastern parts of North America. In addition to these current synoptic observations, a background of climatological knowledge is also required. This is achieved from textbooks, extensive readings of published papers and by practical experience over long periods of operational analysis and forecasting over the region. (Chapter 12 of the handbook contains some climatological information of value to the practical forecaster.)

Some Dynamical Aspects of Atmospheric Systems

The successful application of three-dimensional dynamical ideas to forecasting also requires a knowledge of current upper air conditions and of climatology over an area much larger than the forecast area. At the major forecasting centres in this country, analysed upper air charts over substantial areas of the temperate and polar regions of the northern hemisphere are required and are employed against a background of experience of the types of flow which are known to occur around the hemisphere. Even at the smaller outstations forecasters should have some knowledge of the characteristics of the hemispherical flow against which to assess the main upper flow pattern over a substantial part of the North Atlantic Ocean and Europe. The main features of the upper flow pattern can be delineated at outstations on outline charts which can be prepared from coded messages which are broadcast from the Central Forecasting Office and which contain sufficient data for the reproduction of the main patterns of isopleths at several upper levels. The finer detail may be filled in when necessary by a programme of upper air plotting and analysis within the compass of the limited staff at the outstation. A very general description of some characteristics of the upper flow will now be given and, for reasons which will be apparent later, the account will be concerned mainly with the flow at a level of about 500 millibars.

As would be expected, 500-millibar charts for the northern hemisphere show an infinite variation in detail from day to day, but if some of the detail or embroidery on the main hemispherical patterns is ignored it is possible to recognize a number of characteristic types of flow.

The first striking feature of the hemispherical patterns is the existence of a broad current of strong winds blowing mainly from west to east through temperate latitudes with markedly lighter winds both to the south towards the tropics and to the north towards the polar regions. The width of this current around the hemisphere is not constant. At times the strong flow is concentrated into a narrow belt with a width of about 300-500 nautical miles (5° to 8° latitude) but at others the flow may be much broader and extend over perhaps 15° to 20° latitude. The speed also varies both from place to place and time to time. Where the flow is concentrated into a narrow belt speeds may exceed 100 knots at 500 millibars, and at other times and in other places speeds may be quite light and the general flow is scarcely recognizable over some parts of the hemisphere as a broad belt of strong wind. Yet if a broad enough view is taken over a period of days this hemispherical belt of strong winds can be recognized in temperate latitudes on nearly every chart.

5.3.1. *The upper westerlies or zonal flow*

The simplest form in which this current of strong wind can be observed is as a belt of westerly winds. Figure 5.1 illustrates such a belt. It will be seen that there is an extensive almost straight current at 500 millibars with a direction very close to west in middle latitudes over almost the whole of the western northern hemisphere. In the troposphere such westerly currents usually increase with height to the tropopause, there is often very little change of direction and the strong wind is generally confined to a latitudinal or zonal belt. Such a circulation pattern would be described as zonal or one of "high index".

5.3.2. *Waves in the upper westerlies*

A fairly simple variation on this zonal flow is observed as a number of waves in this broad flow. The broad current is no longer mainly westerly but the direction varies in a periodic manner so that the flow exhibits simple wave-like patterns. Figure 5.2 illustrates such a flow in which there are waves between 120°W. and 10°W. in the northern hemisphere. Eastwards of 10°W. the 500-millibar flow shown in Figure 5.2 is more distorted. It will be noted that, in the wave-like flow, the ridges and troughs are orientated in a predominantly north-south direction and that the amplitude of the wave from the crest of the ridge to the bottom of the trough is limited to about 10° or 15° of latitude. Although no ridge or trough is identical in size or shape with its upstream or downstream neighbour and the wavelength varies somewhat around the hemisphere, the relative simplicity and uniformity of pattern is a striking feature of our complex atmosphere. This pattern of flow typifies long-wave patterns in the upper westerlies about which a great deal of literature has been published, notably in the United States (see Riehl[2] for a list of some references to literature).

5.3.3. *Meridional flow*

A further variation on this wave-like flow is seen when an increase takes place in the amplitude of the waves. In the various sections of the wave pattern the wind deviates still further from a westerly direction and the ridges penetrate to higher and the troughs to lower latitudes. Figure 5.3 illustrates such a flow. The striking characteristic features of such a pattern are the extensive currents of air with predominantly northerly or southerly flow over much of the zone between the subtropics and the Arctic Circle. Much of this type of flow is approximately along meridians of longitude and the pattern is often described as "meridional" or of "low index".

Experience indicates that there are many variations in the long-wave pattern from the three basic types discussed above. It would not be profitable to attempt to catalogue a great variety as this would tend to confuse. There are, however, three variations which occur fairly frequently and should be mentioned.

5.3.4. *The "cut-off" low*

One such variation is a further development from a well marked meridional pattern. It is found at times that the upper isopleths indicate a closed circulation in the trough in lower latitudes. Initially the upper low lies on the poleward side of the main flow, but later, as the circulation round the low becomes more complete, a new branch of the westerly current is formed across the "neck" of the original trough and the new vortex finds itself equatorward of the meandering westerlies. These upper vortices usually form in association with depressions shown by the surface chart and are usually referred to as "cut-off" lows. Such upper vortices exhibit a number of features of importance in forecasting and these aspects are discussed in Chapter 11, Section 11.3 and Chapter 12, Section 12.4.2. Figure 5.4 indicates a cut-off low to the south and west of the British Isles.

5.3.5. *The "cut-off" high*

The cut-off high is somewhat analogous to the cut-off low and occurs when a well marked closed anticyclonic vortex forms in the ridge pattern of a marked meridional circulation. When these upper anticyclonic circulations form they usually do so in association with low-level anticyclones and these tend to be in latitudes somewhat higher than normal. Figure 5.5 illustrates a cut-off high centred to north-west of the British Isles.

It is found that both the low-latitude cut-off low and the high-latitude cut-off high often tend to be persistent over a period of several days.

Chapter 5

Some Dynamical Aspects of Atmospheric Systems

FIGURE 5.1 *500-millibar contours in decametres, 0300 G.M.T., 13 December 1956*

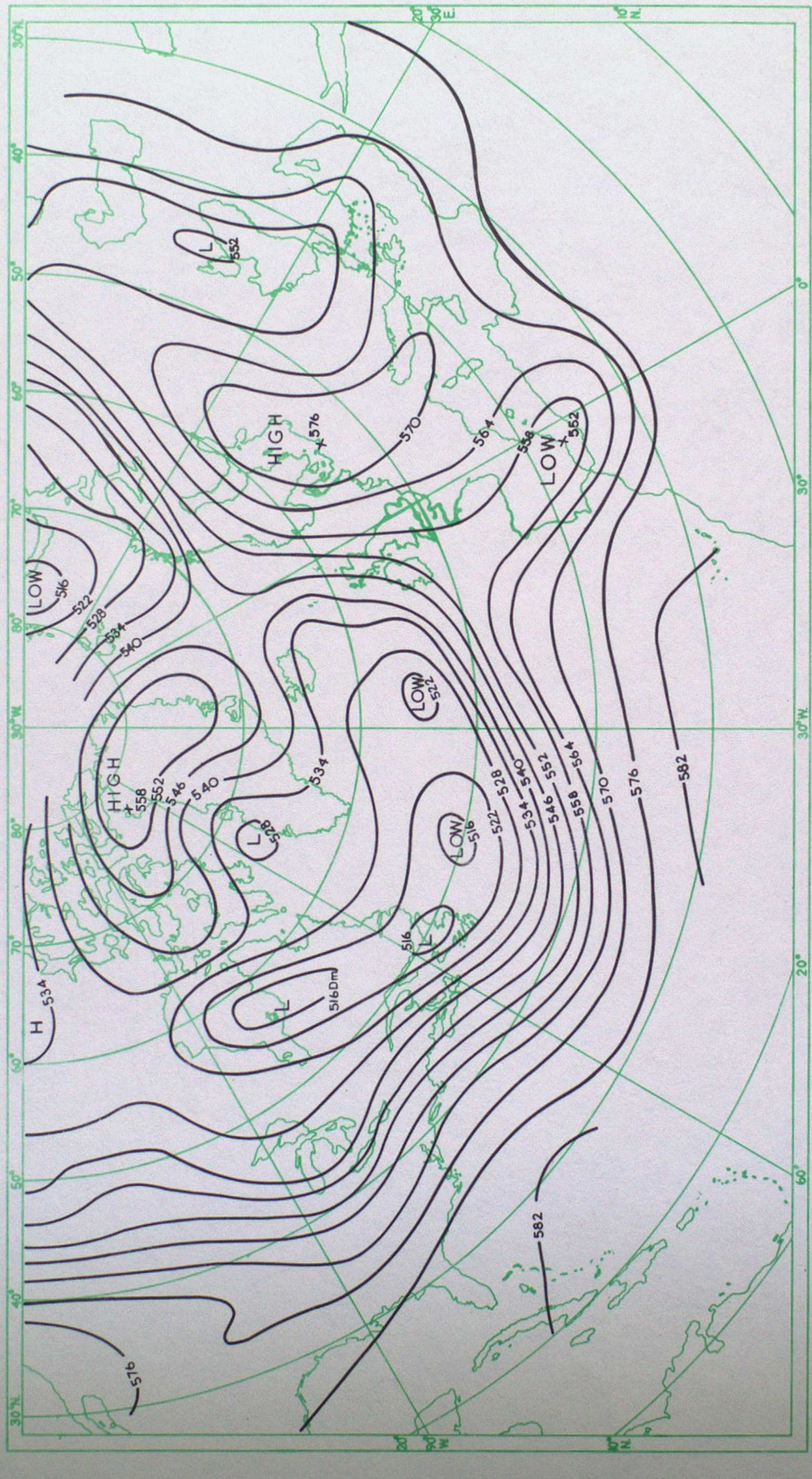

FIGURE 5.2 *500-millibar contours in decametres, 1200 G.M.T., 21 November 1959*

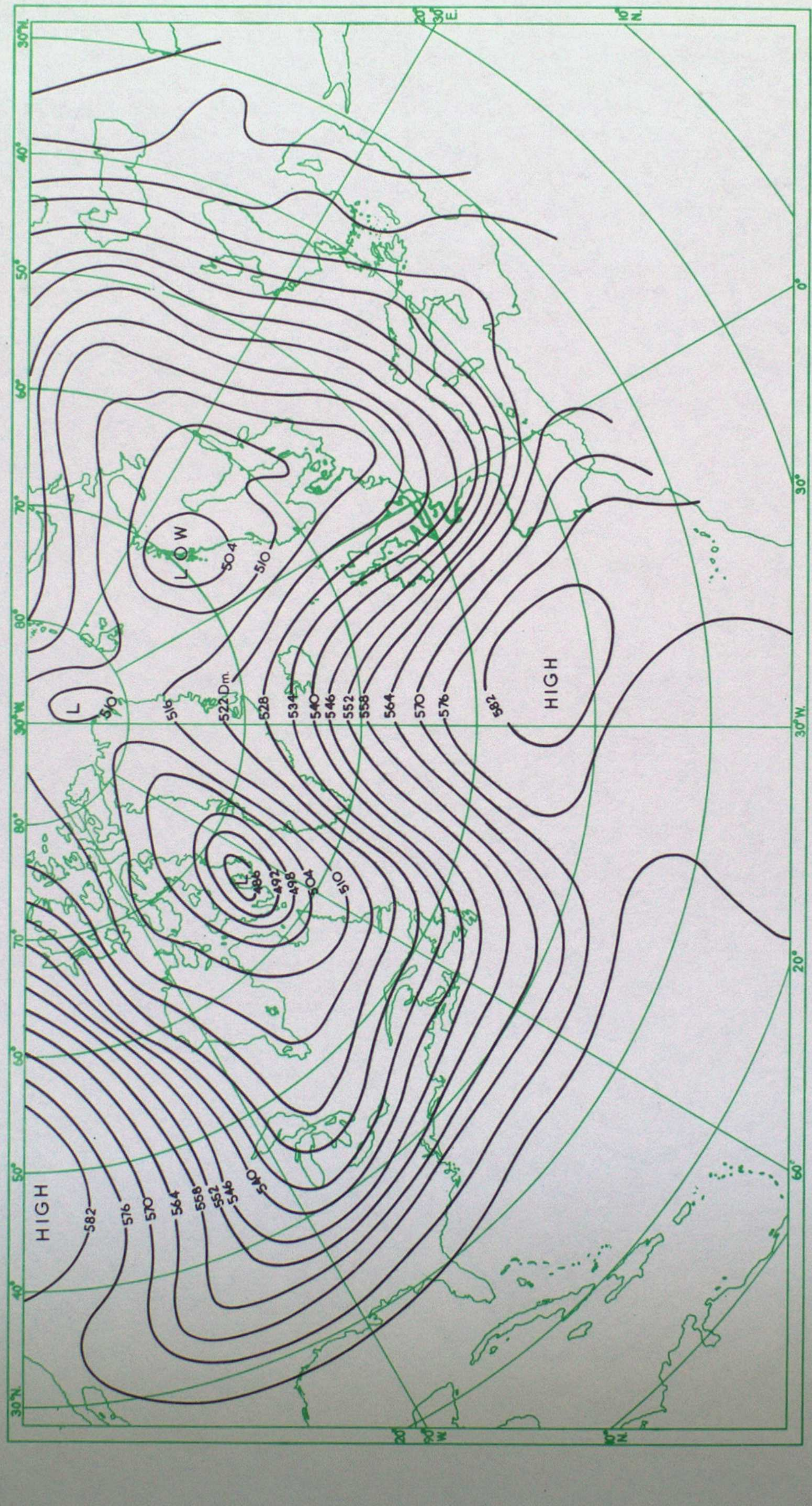

FIGURE 5.3 *500-millibar contours in decametres, 0300 G.M.T., 29 November 1956*

FIGURE 5.4 *500-millibar contours in decametres, 0000 G.M.T., 21 April 1958*

Some Dynamical Aspects of Atmospheric Systems

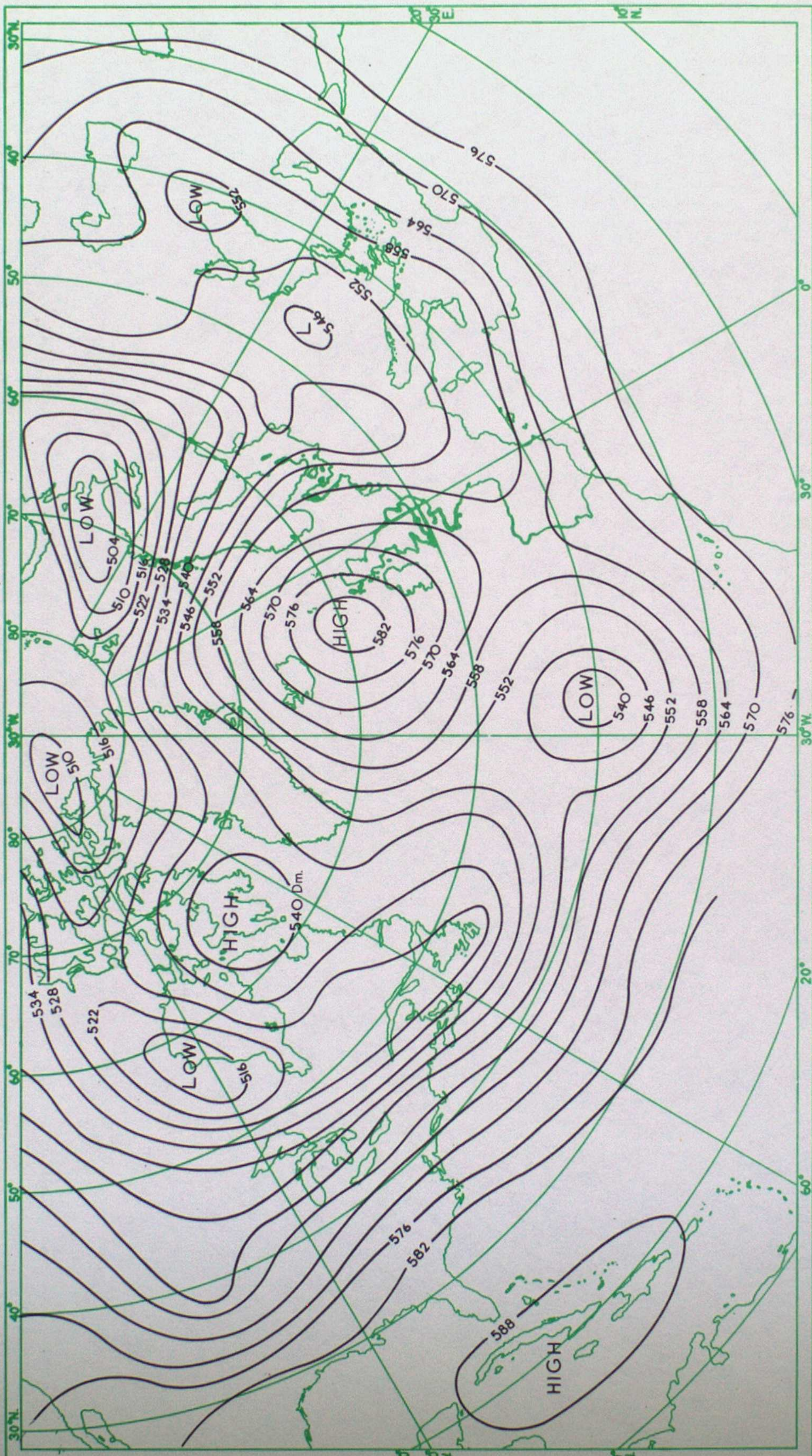

FIGURE 5.5 *500-millibar contours in decametres, 0000 G.M.T., 8 April 1957*
Observations from North America and American weather ships are for 0300 G.M.T.

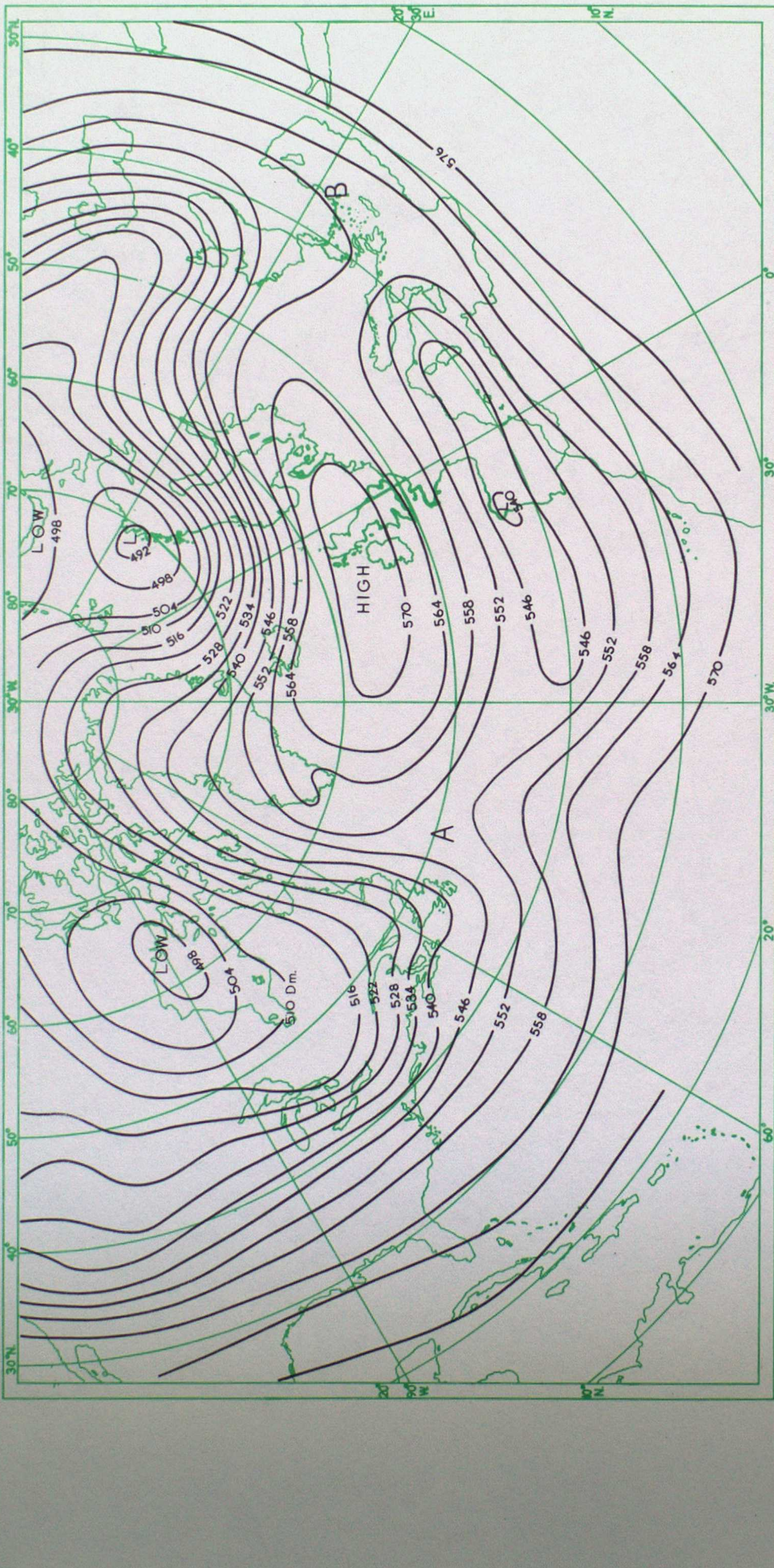

FIGURE 5.6 *500-millibar contours in decametres, 1200 G.M.T., 9 February 1960*

5.3.6. *A split in the upper westerlies*

When both a cut-off low and high occur in conjunction in the same range of longitudes the pattern is often very persistent. Figure 5.6 shows this type of situation. The low-latitude cut-off low and the high-latitude anticyclonic cell are clearly marked and it is seen that between them there is well established and extensive easterly flow at 500 millibars. It should also be noted that at A upwind of the complex the broad upper flow splits into two currents. One current swings north and skirts the western and northern flanks of the anticyclone. The other current moves along the southern edge of the cut-off low. Well to the east of the upper complex the two currents merge near B and once again form a single broad current. It is a feature of this pattern that depressions forming to westward of the complex tend to move north of the anticyclonic centre or south of the cyclonic centre and thus the pattern acts as an effective block to the normal eastward movement of depressions. The anticyclone is then often referred to as a "blocking high". It is unfortunate that there is no widely accepted formal definition of what constitutes a "block" but practically all workers would agree that this complex does constitute a block. Some information on blocks is included in Chapter 12, Sections 12.4.2 and 12.4.3.

5.3.7. *Further general comments on long-wave patterns*

Experience shows that many upper air charts exhibit some properties of the three simple types of hemispherical flow described in Sections 5.3.1, 5.3.2 and 5.3.3 and that some qualitative information can be conveyed by describing the flow as zonal or meridional, with some qualifying adjective adding yet further general information. To convey much more quantitative information on long-wave patterns an extensive series of charts must be maintained and supported by a fair amount of computation which is beyond the scope of all but the major forecasting centres. It is, however, possible to convey a little more information by adding some remarks about the wavelength of the pattern. On the hemispherical scale the number of waves according to Riehl[2] varies from three to seven with four or five as the most common. Glaser,[3] however, quotes the following frequency distribution for the northern hemispheric wave number (defined as the number of major troughs in the mid-tropospheric westerlies between 30° and 45°N. and counted each day).

Year	*Wave number* 4	5	6	7–8	*Total*
	No. of occasions				
1946, 1947, 1952, 1953, 1954, 1955 (Some years incomplete)	72	888	915	249	2124

These figures imply that five or six hemispheric waves are most common. With waves varying between three and eight in number and being more or less uniformly distributed around the hemisphere it is clear that typical wavelengths will vary between about 120° and 45° longitude.

Two further facts about long-wave patterns are stressed at this stage. Firstly the well marked features are relatively slow-moving. On some occasions the hemispherical pattern settles down with the long-wave troughs and ridges almost stationary – sometimes for several days. On other occasions – particularly with relatively shallow waves in the upper westerlies and when the long-wave pattern is being substantially modified – movement may be considerable and amount to 10° or 20° longitude per day with noticeable variation in the amplitude of the long-wave features. The second noteworthy fact is that a well marked long-wave pattern changes to another type fairly slowly. For example a typical wave pattern in the westerly would not change to a well marked meridional pattern in 24 hours, nor would a newly formed cut-off low of normal dimensions at the 500-millibar level disappear from the chart in 24 hours. It is not possible to fix any general time scales for the modification from one type to another but forecasters should know that the time to effect a change from one well established pattern to another is normally a matter of days rather than hours.

A more complete but still descriptive account of some 500-millibar flow patterns and their synoptic evolution has been given by Smith.[4]

5.3.8. *The short-wave pattern*

A detailed examination of the upper flow patterns reveals that the trend of change is not always in the same direction in one area from one day to the next. For example, when a marked meridional pattern is being developed from a typical mobile westerly pattern over a period of several days, a sequence of detailed charts often shows that troughs and ridges do not steadily become larger and larger. True, there is over a period of days the trend to greater amplitude but it is often found that, perhaps for 12–24 hours over an area which is small compared with the long-wave pattern, there is a small-scale pattern superimposed on and travelling through the long-wave pattern. Thus when a small-scale ridge moves through a long-wave pattern the long-wave trough appears to be relaxing and the ridge building at an increased rate. After the passage of the small-scale ridge the trough might continue to develop and the ridge appear to weaken but the long-wave pattern is often substantially unchanged after the passage of the smaller system.

The sequence of charts in Figures 5.7*(a)* to *(f)* shows a deep depression both at the surface and at the 500-millibar level with centres in the Iceland – Greenland region. Further south in the North Atlantic the surface charts show a number of surface depressions moving quickly east-north-eastwards. The 500-millibar contour charts show a strong west-south-westerly flow which is substantially unchanged after the passage of the mobile disturbances. Figures 5.8*(a)* to *(f)* show a sequence of surface and 500-millibar charts with a marked anticyclonic and meridional pattern near the British Isles. In this series depressions are moving northwards on the western side of the major ridge in the long-wave pattern at 500 millibars, eastwards on its northern flank and southwards on the eastern side. This sequence also demonstrates that a system of relatively small depressions can travel round the upper flow and, when the small perturbation has moved downwind, the long-wave pattern may be little changed. The long-wave pattern appears to carry a superimposed pulsation of short wavelength which usually moves through the pattern. This short-wave pattern is linked with the smaller atmospheric systems such as travelling depressions, troughs, ridges and anticyclones. For short-period forecasting such small-scale systems are usually vital and often form the crux of the problem.

It is thus possible on some occasions to regard the long-wave pattern as dictating the general type of weather to be expected over a period of days and the short-wave travelling systems as filling in the short-period detail. But there is no such general rule. The short-wave features do exert their effect on the long-wave pattern and sometimes the small systems themselves develop into systems of major dimensions – say 1,000–1,500 nautical miles in horizontal extent – and the long-wave pattern is then substantially modified. The assessment of the extent to which a long-wave feature will dominate a small-scale feature, or the smaller-scale system will deform the long-wave, forms one of the most difficult practical problems in the preparation of prebaratic/prontour charts.

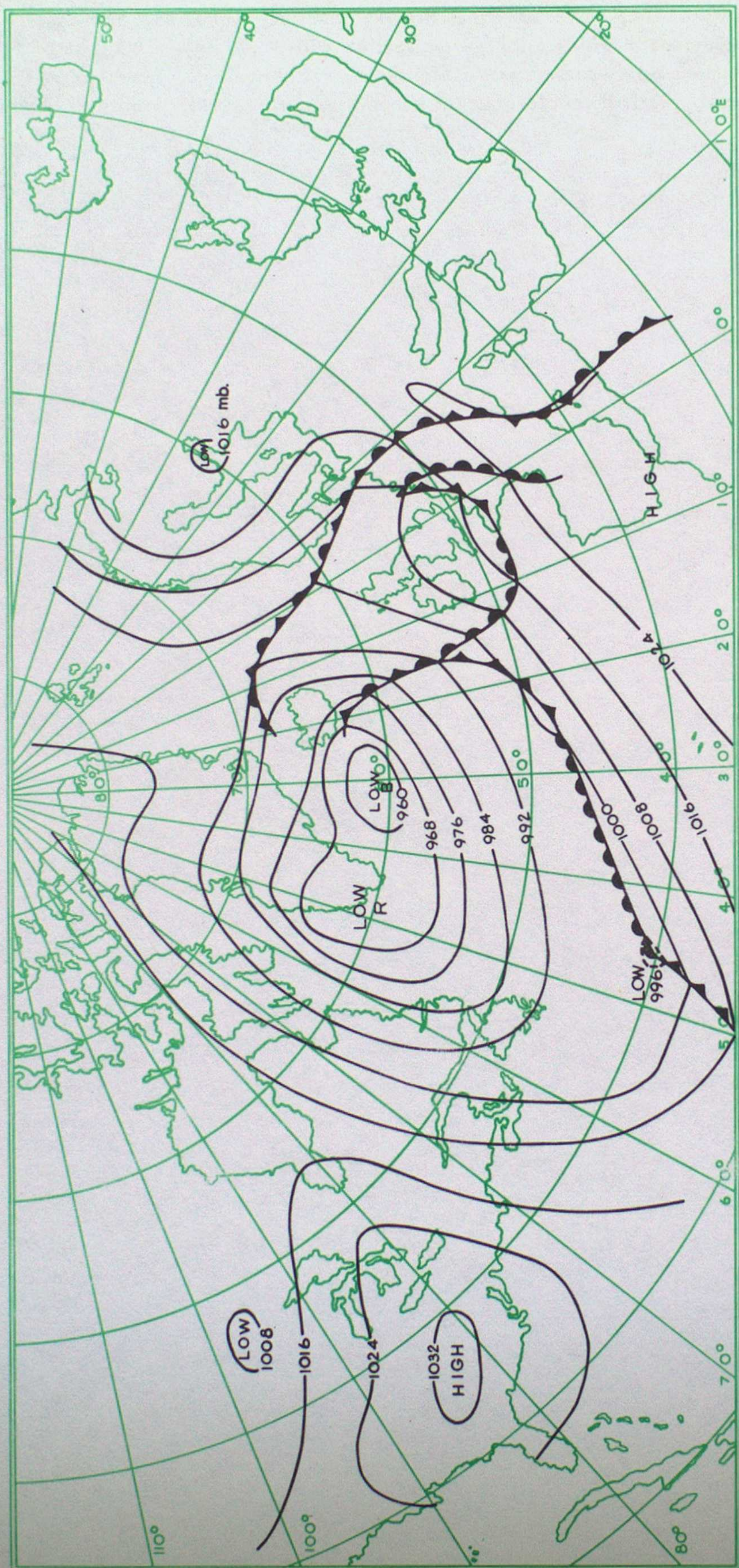

FIGURE 5.7(a) *Surface chart for 1200 G.M.T., 3 January 1957*

Some Dynamical Aspects of Atmospheric Systems

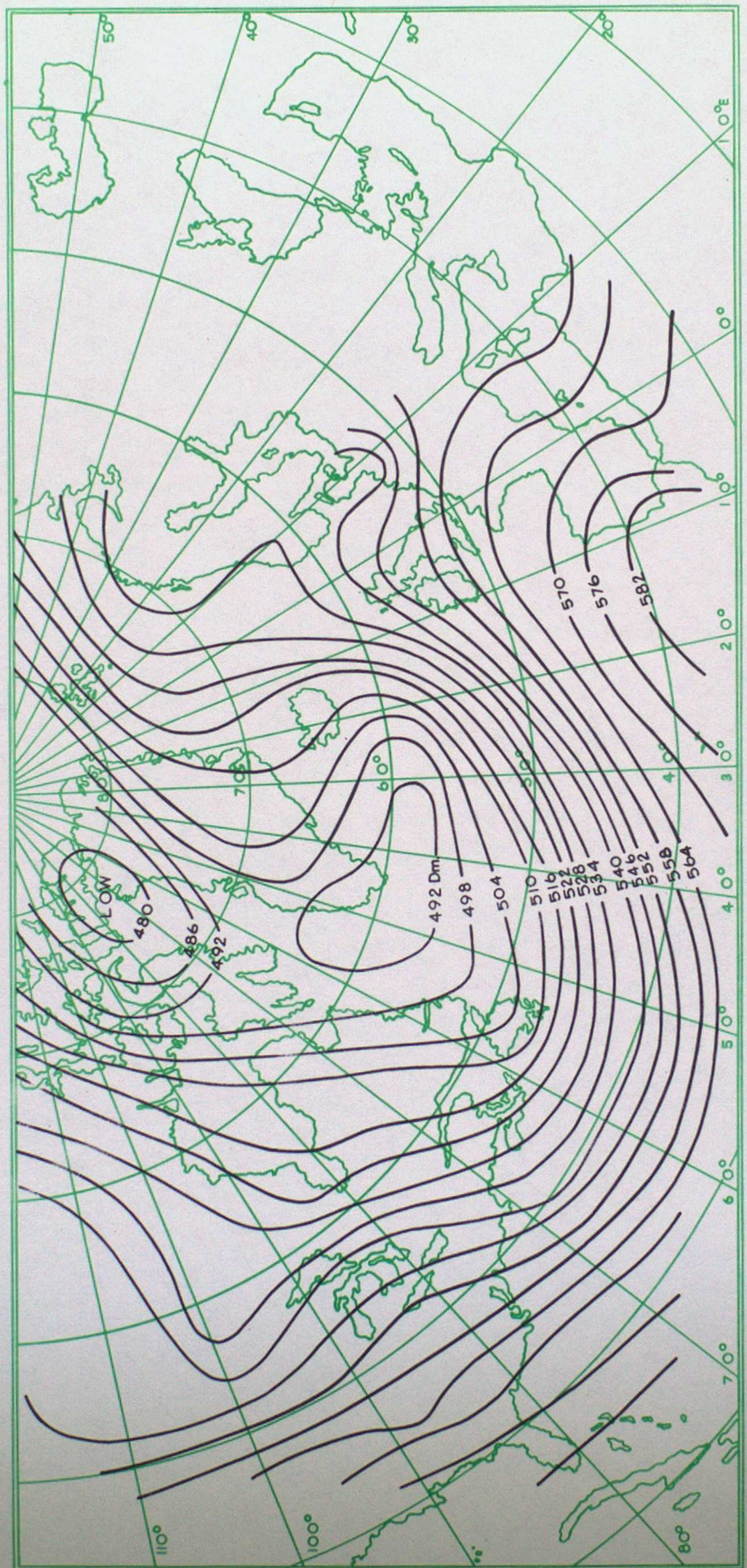

FIGURE 5.7(*b*) *500-millibar contours in decametres, about 1500 G.M.T., 3 January 1957*

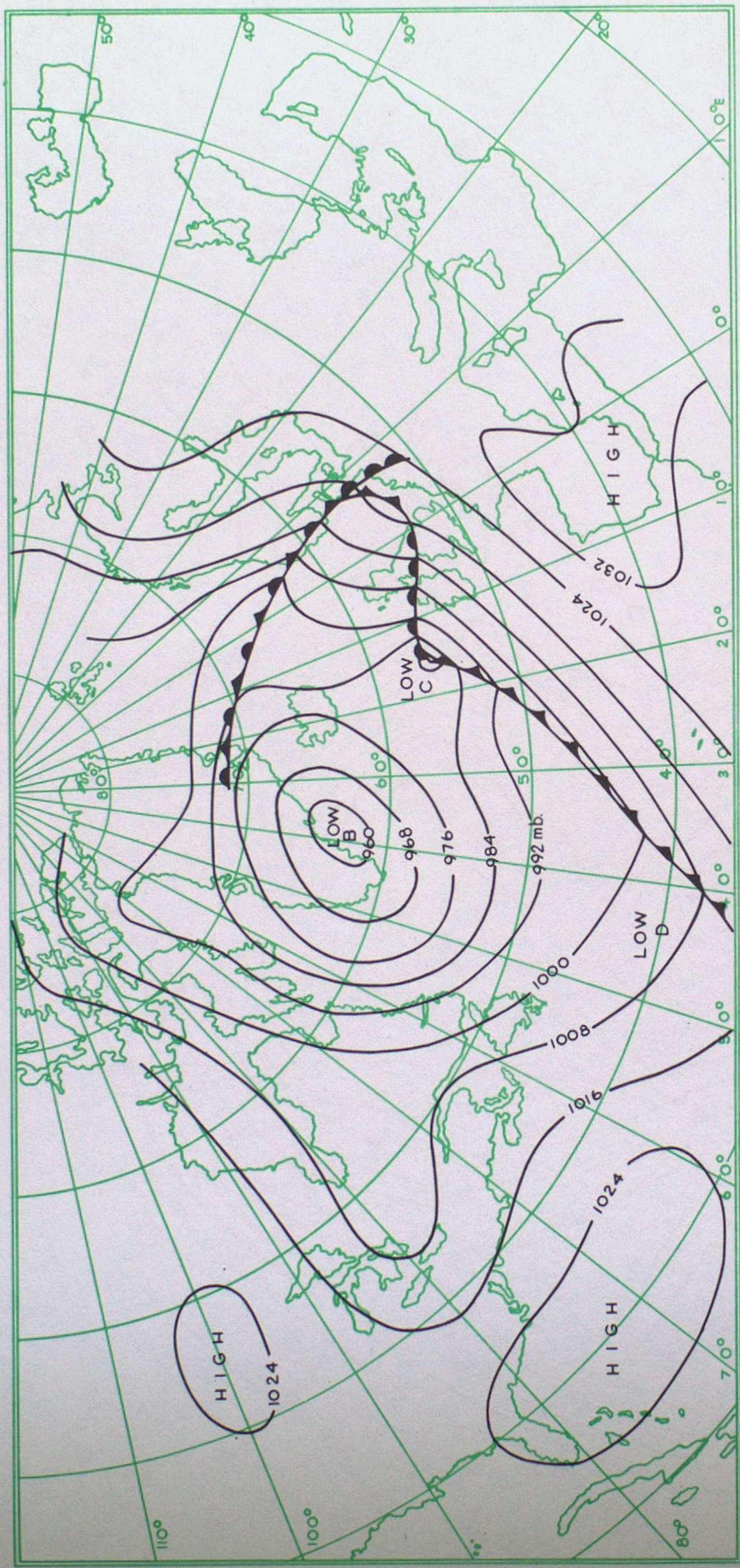

FIGURE 5.7(c) *Surface chart for 1200 G.M.T., 4 January 1957*

Some Dynamical Aspects of Atmospheric Systems

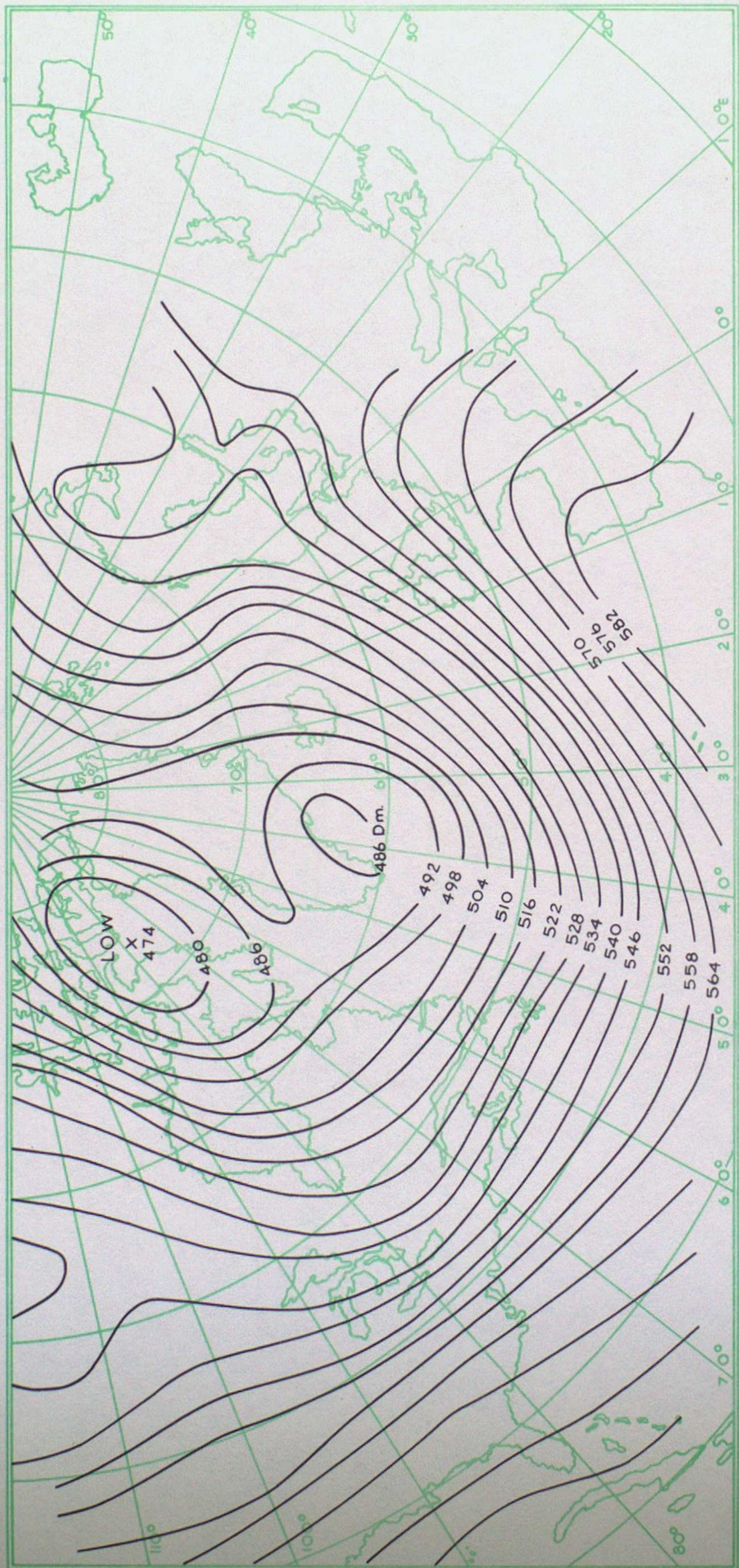

FIGURE 5.7(*d*) *500-millibar contours in decametres, about 1500 G.M.T., 4 January 1957*

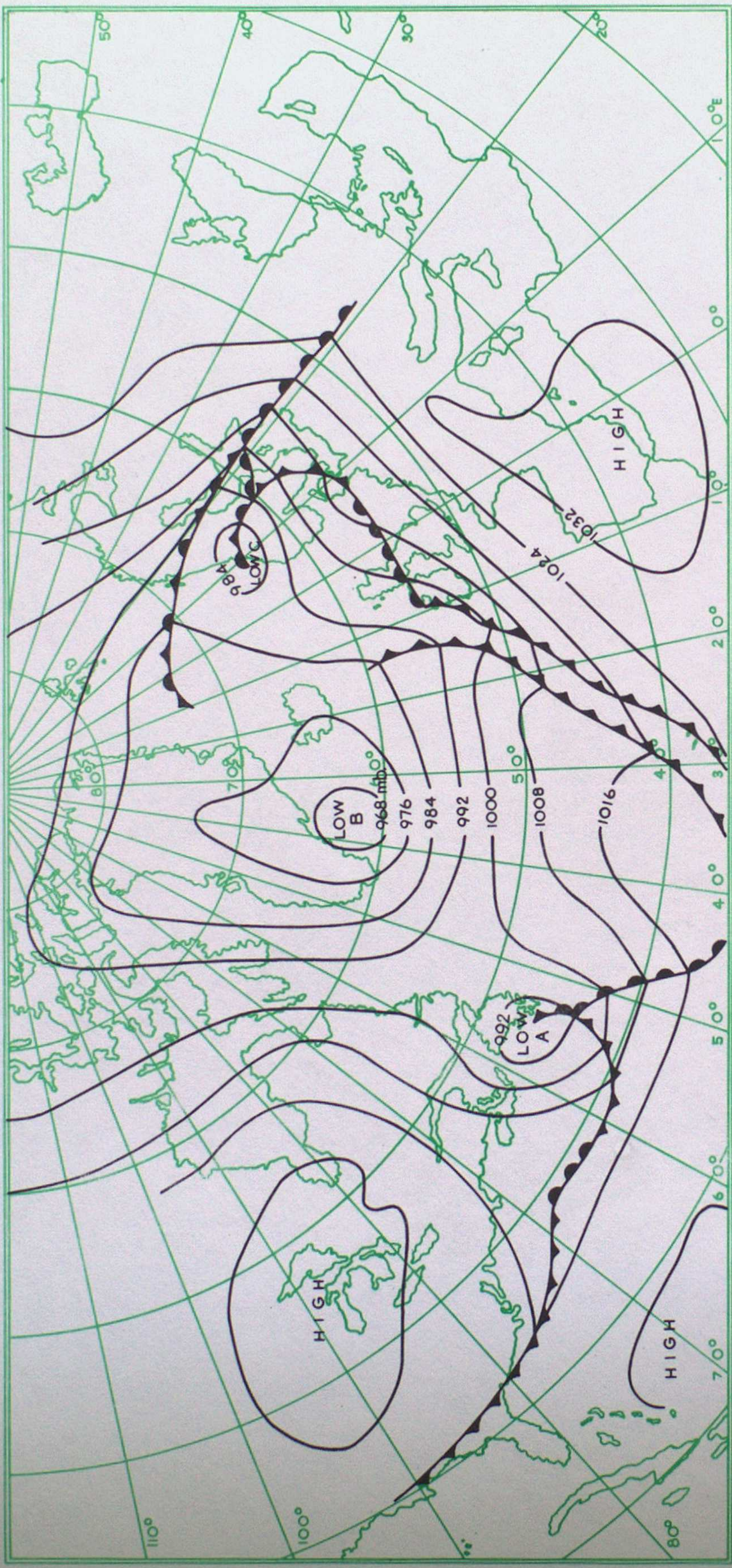

FIGURE 5.7(e) *Surface chart for 1200 G.M.T., 5 January 1957*

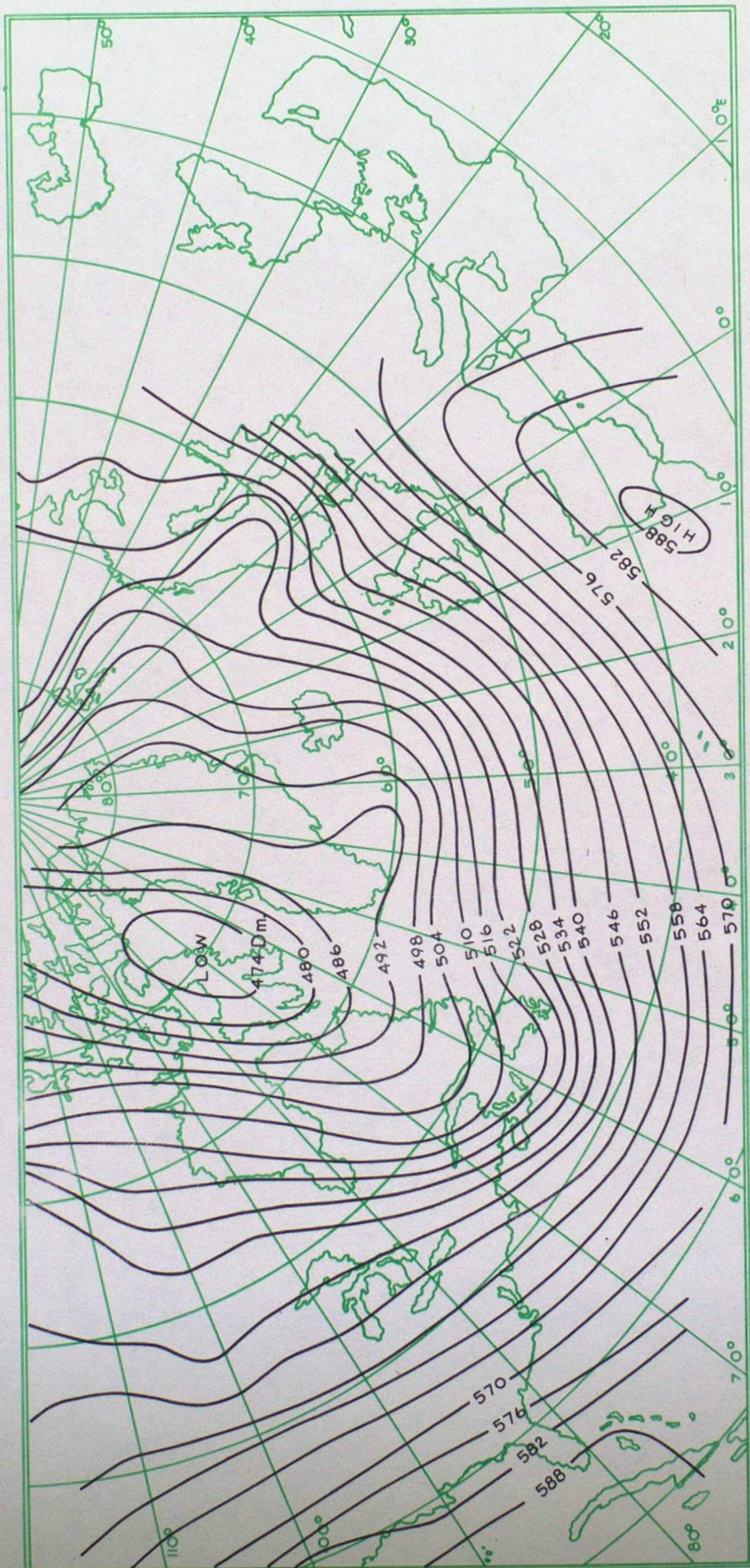

FIGURE 5.7(f) 500-millibar contours in decametres, about 1500 G.M.T., 5 January 1957

FIGURE 5.8(a) *Surface chart for 1200 G.M.T., 8 January 1960*

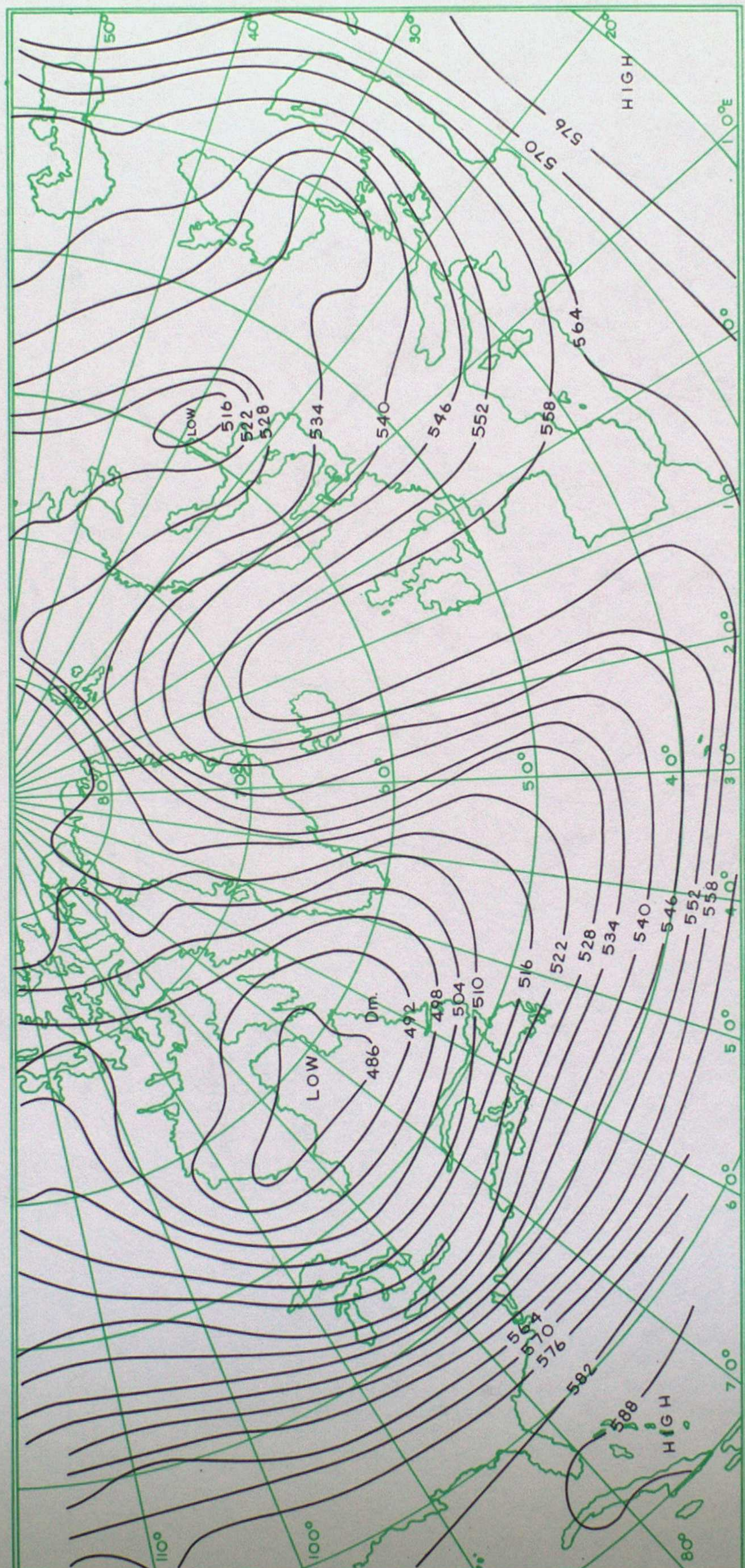

FIGURE 5.8(*b*) *500-millibar contours in decametres, about 1200 G.M.T., 8 January 1960*

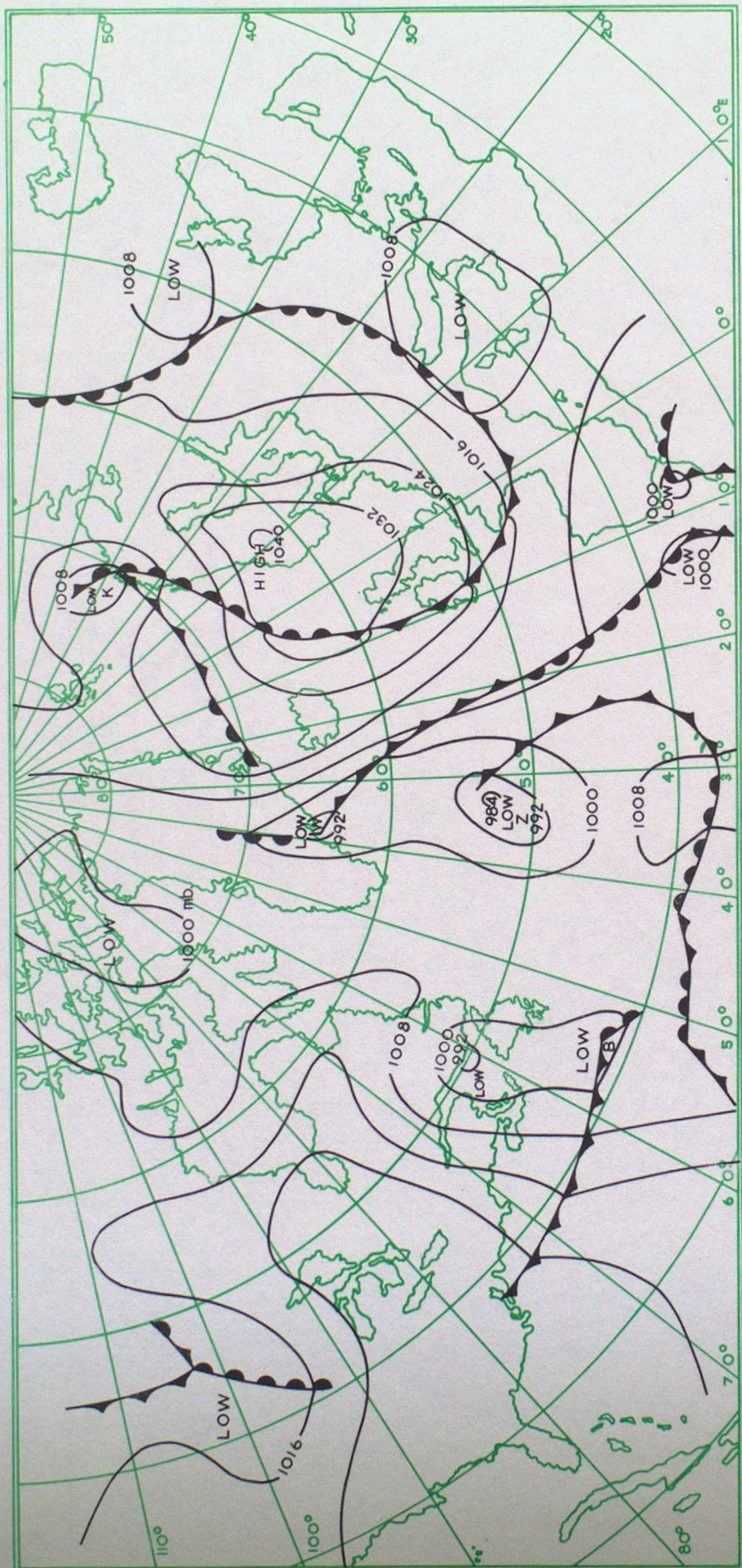

FIGURE 5.8(c) *Surface chart for 1200 G.M.T., 9 January 1960*

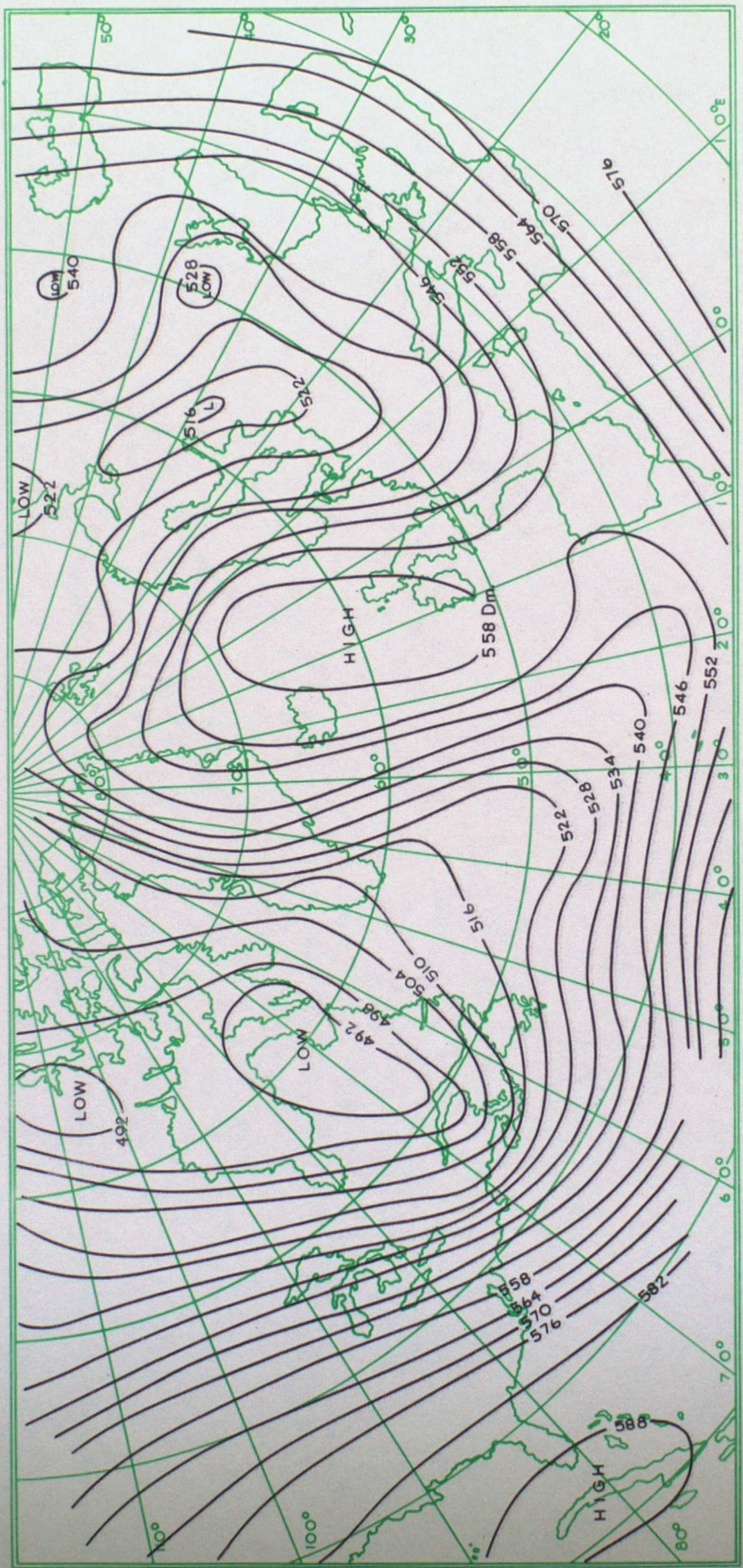

FIGURE 5.8(*d*) *500-millibar contours in decametres, about 1200 G.M.T., 9 January 1960*

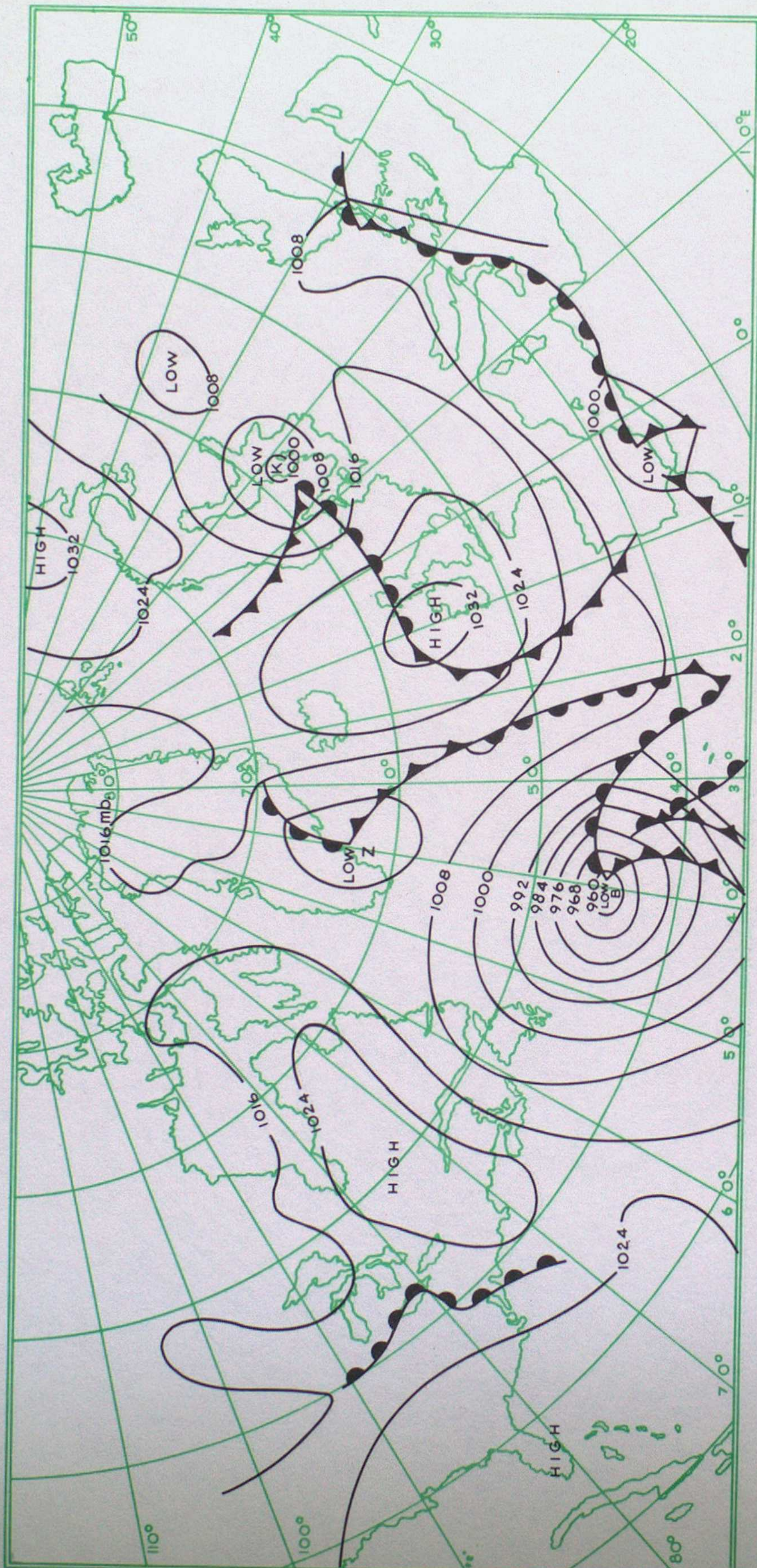

FIGURE 5.8(e) *Surface chart for 1200 G.M.T., 10 January 1960*

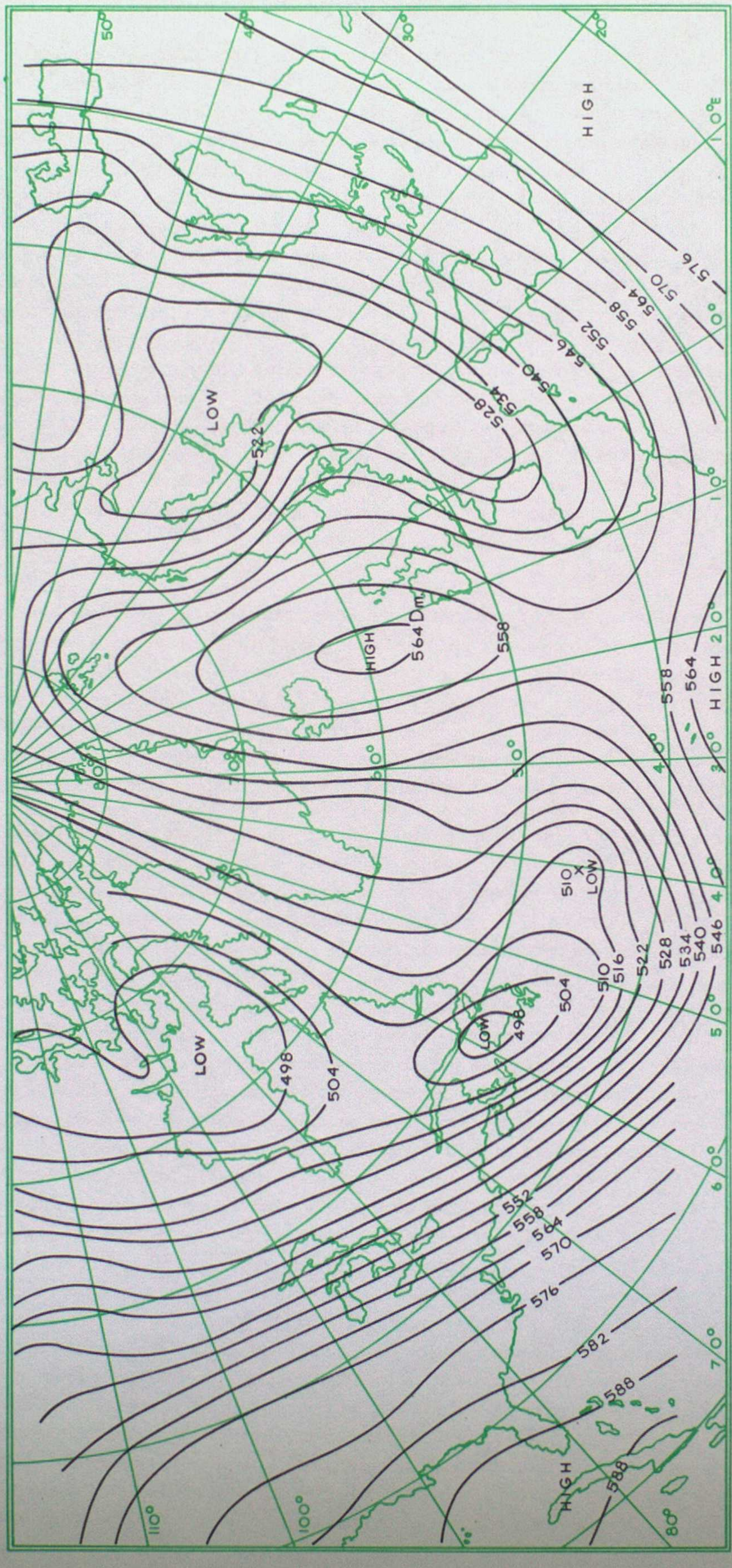

FIGURE 5.8(*f*) *500-millibar contours in decametres, about 1200 G.M.T., 10 January 1960*

5.4. LARGE-SCALE DISTRIBUTION OF TEMPERATURE

The energy which is required to drive atmospheric circulations is originally derived from radiation received from the sun. This radiation absorbed by the earth and its atmosphere is first manifest in the form of heat. Taking the earth and its atmosphere as a whole there is a net gain of heat in latitudes lower than about 35° and a net loss in higher latitudes. Leaving aside the possibility of very long-term climatic change there is a long-term equilibrium in the distribution of heat over the earth. Atmospheric and oceanic circulations must play a vital part in redistributing and exchanging heat. The direct contribution by ocean currents is smaller than that of the atmosphere but is not negligible. The circulations of the earth's atmosphere at levels above the lower stratosphere are imperfectly understood but their direct contribution to exchanges of heat are most unlikely to be significant for day-to-day forecasting (their importance, if any, for longer-period forecasting has yet to be demonstrated). Knowledge of the contribution due to air movements at tropospheric and lower stratospheric levels is somewhat greater but there is still much to be learnt. These are the levels with which the practising forecaster has to deal. In a search for techniques for forecasting the development, decay and motion of atmospheric systems in these levels it would be natural to look to the distribution of temperature in the horizontal and vertical.

It was shown in Chapter 2 that the mean virtual temperature between two pressure levels p_1 and p_2 was constant along each isopleth of thickness for the layer p_1 to p_2, that is, the thickness pattern is also the pattern of mean virtual temperature. For many forecasting purposes it is permissible to replace virtual temperature by temperature without significant loss of accuracy and for practical consideration of upper air charts the thickness pattern may be regarded as identical with the pattern of mean temperature between the pressure levels concerned.

Figures 5.9*(a)* to *(e)* show contours for the 1000-, 500- and 300-millibar levels and thicknesses for the layers 1000–500 millibars and 500–300 millibars. It will be seen that the major troughs, ridges and closed centres of the upper contours bear a marked similarity to corresponding features in the thickness patterns. Also the concentration of contours is generally similar to the concentration of thicknesses up to 300 millibars (that is, throughout much of the troposphere) and a closed thickness pattern in one layer lies almost vertically over a similar closed pattern of a lower layer. Further, in regions well removed from the concentration of thickness lines, extensive regions are occupied by warm (or cold) tropospheric air masses in which there is little horizontal gradient of temperature. If the pattern is viewed on a broad scale the concentration of thicknesses and contours extend throughout a section which is almost vertical. The deviations from the vertical are important in detailed forecasting but they are nevertheless small and, taking a broad view, there exists throughout the troposphere and over substantial distances around the hemisphere an almost vertical zone in which is concentrated a belt of strong winds and temperature contrast. Figure 5.9 shows only one occasion but that occasion was selected more or less at random and the general truth of the preceding sentence can be readily checked from an examination of a number of daily aerological reports. This zone of temperature contrast is located in temperate or lower temperate latitudes. In areas away from this zone of contrast the thickness lines are more widely spaced, that is, there is little isobaric (horizontal) gradient of temperature. It is thus clear that the troposphere may be regarded, on a broad scale, as being composed of extensive domes of warm air and pools of cold air in which there is little horizontal variation of temperature. These areas of warm and cold

Some Dynamical Aspects of Atmospheric Systems

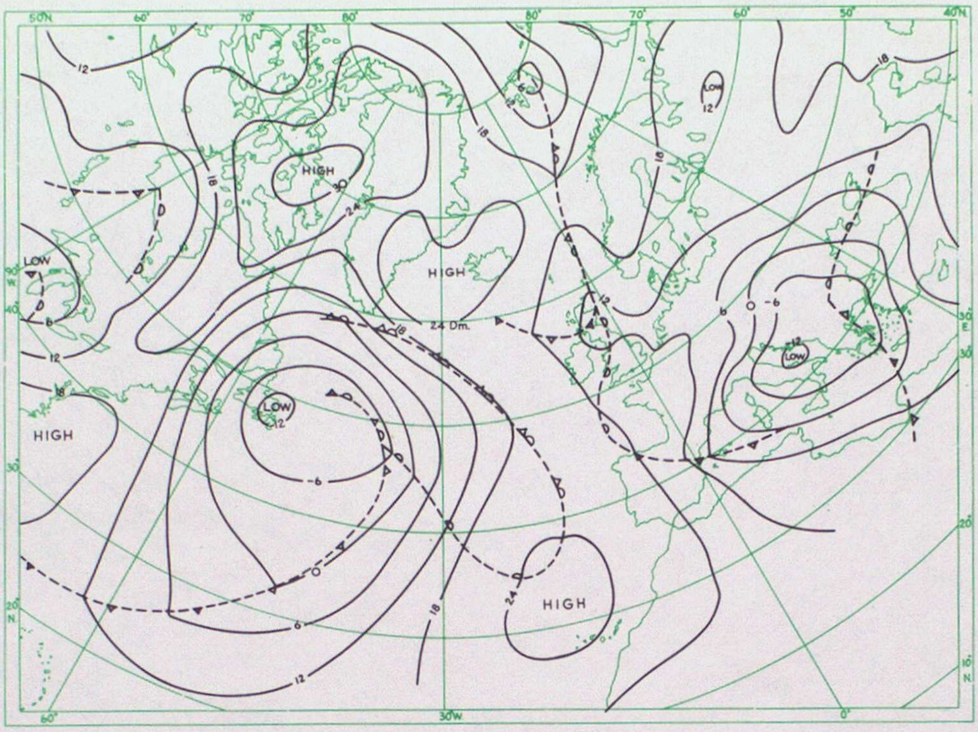

FIGURE 5.9(*a*) *1000-millibar contours in decametres, 0000 G.M.T., 13 January 1960*

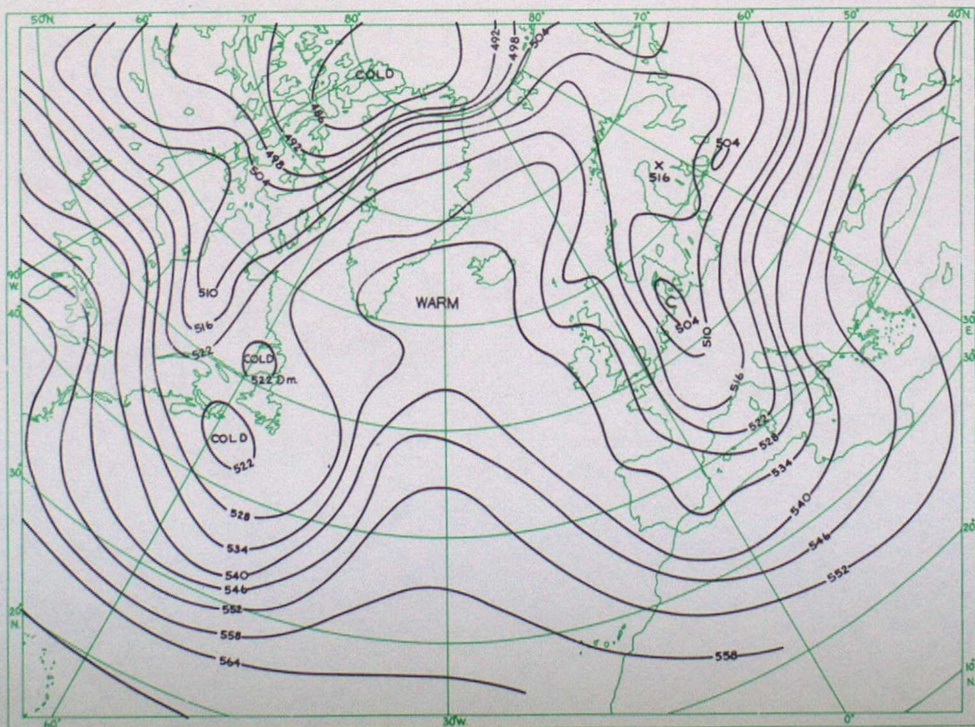

FIGURE 5.9(*b*) *1000–500-millibar thickness in decametres, 0000 G.M.T., 13 January 1960*

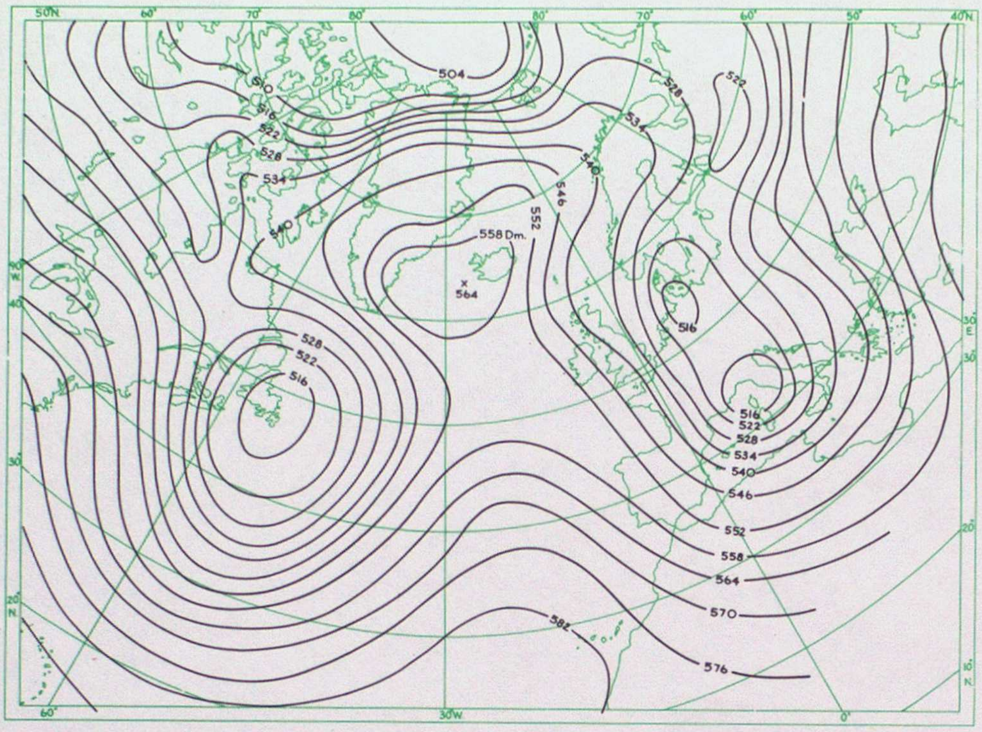

FIGURE 5.9(c) *500-millibar contours in decametres, 0000 G.M.T., 13 January 1960*

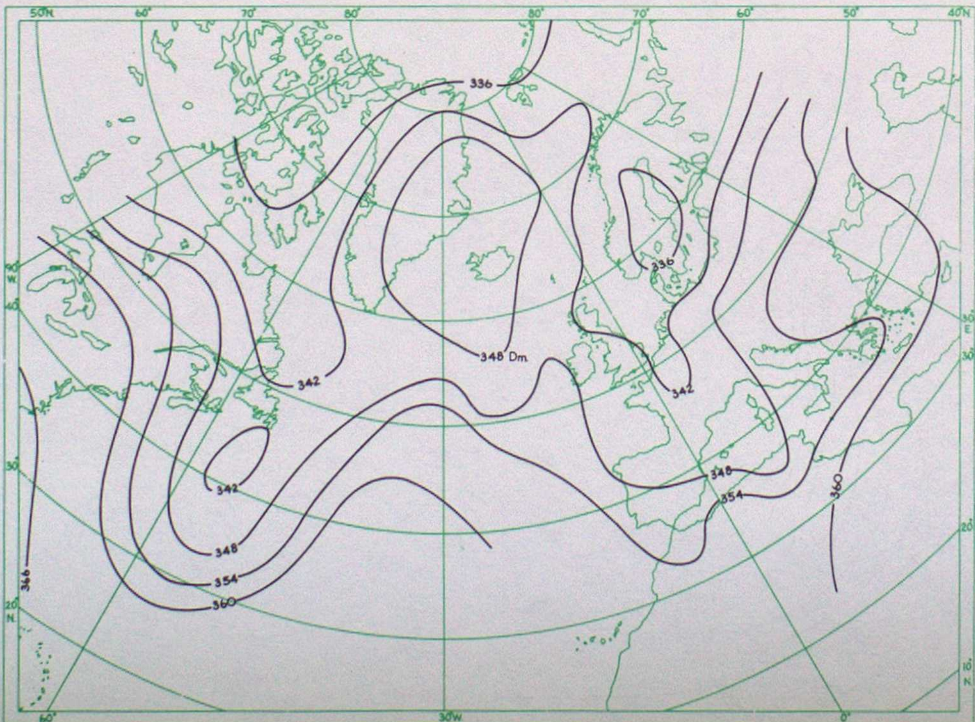

FIGURE 5.9(d) *500–300-millibar thickness in decametres, 0000 G.M.T., 13 January 1960*

Some Dynamical Aspects of Atmospheric Systems

BASE MAP (B)

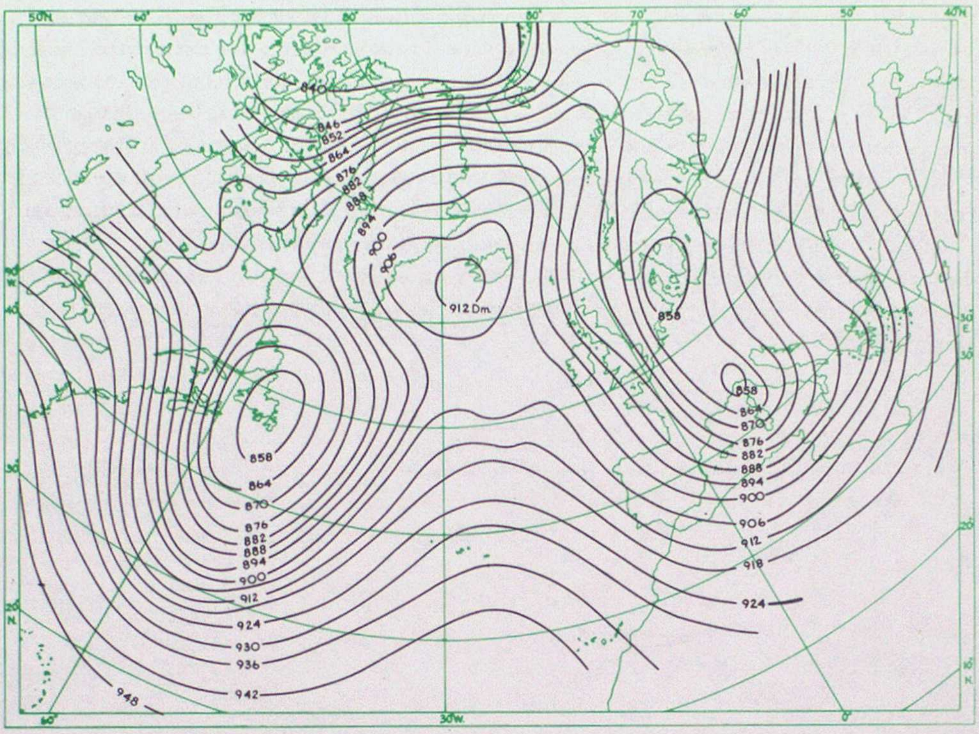

FIGURE 5.9(*e*) *300-millibar contours in decametres,*
0000 G.M.T., 13 January 1960

air are separated by an almost vertical zone of transition in which there is a substantial temperature gradient. This distribution bears a striking similarity to frontal concepts but the idea of a very limited frontal zone is replaced by the concept of a much broader zone – of the order of 300–500 miles in width – in which exists a temperature gradient which is broadly uniform and parallel in direction throughout the troposphere.

The relative simplicity in the broad-scale atmospheric structure of the troposphere makes it possible for the main features of the distribution of temperature to be displayed by a chart for a single atmospheric layer. The chart of 1000–500-millibar thickness is particularly convenient for this purpose and shows all the principle tropospheric regions of horizontal temperature contrast which are likely to be important in determining the behaviour of the large-scale atmospheric systems.

Although the inter-relation of cause and effect between changes in the troposphere and in the lower stratosphere is imperfectly understood, there is some coupling between these atmospheric layers. Therefore it is appropriate in this section to make a few remarks on temperature distribution in the lower stratosphere above the tropopause. (More complete discussions of the tropopause and stratosphere are contained in Chapter 7, Sections 7.4 and 7.5.) On the hemispheric scale the tropopause and lower stratosphere are high and cold in low latitudes and warm and low in high latitudes. If there are well marked long waves with substantial meridional components of flow extending through much of the troposphere into the lower stratosphere then the southerly component of wind will carry northwards the high and cold tropopause and lower stratosphere from lower latitudes and the southerly component will carry southwards the low and warm tropopause and lower stratosphere from higher latitudes. Thus the long-wave ridges which are associated with a warm troposphere have a high tropopause and cold lower stratosphere. Conversely the long-wave troughs which are associated with a cold troposphere have a low tropopause and a warm lower stratosphere. As early as 1919 Dines[5] showed statistically that a cold troposphere is associated with a low tropopause and relatively warm lower stratosphere. Conversely a warm troposphere is associated with a high tropopause and relatively cold lower stratosphere. Dines' work, based on very limited data, was remarkably accurate and Bannon and Gilchrist,[6] using much more extensive upper air data, have produced more complete results which confirm most of Dines' work at least for the seasons and areas affected by travelling depressions and anticyclones, that is, our temperate latitudes.

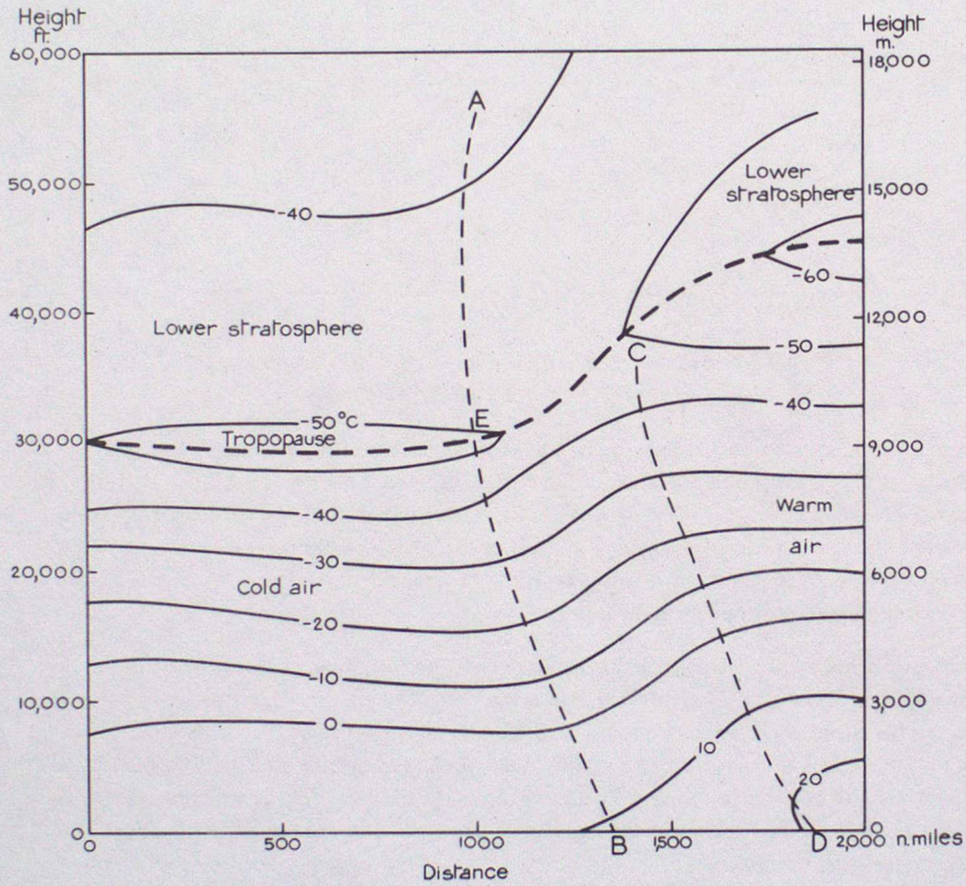

FIGURE 5.10 ***Schematic vertical cross-section across the zone of temperature contrast***

Figure 5.10 is a schematic diagram of a vertical cross-section of the troposphere and lower stratosphere along a line at right-angles to the main zone of temperature contrast which is generally located in temperate latitudes.

Along the horizontal axis in Figure 5.10 is an indication of distance to set the scale of the temperature fields. To the left of AB and the right of CD there is very little variation of temperature in the horizontal. The tropospheric zone in which the greater part of the temperature variation is concentrated is clearly shown by the area EBDC and it will be observed that temperatures in the warm air are some 10°–15°C. above those at the same level in the cold air. To the left of AB the lowest temperature is about −50°C. around the tropopause level but to the right of CD the temperature decreases to about −60°C. around the warm air tropopause which is higher than the cold air tropopause. It is thus clear that the temperature difference is reversed to the right of AE above a level somewhat above the tropopause and in the lower stratosphere. Further, this temperature difference is of the same order of magnitude as in the troposphere. The horizontal scale in Figure 5.10 shows that these distributions refer to synoptic systems of major dimensions. Minor variations in the temperature field, which are nearly always present, have been excluded from the diagram and the tropopause has been shown as a continuous surface but, as will be indicated in Chapter 7, the tropopause sometimes appears to be discontinuous – particularly in such a well marked system as depicted in Figure 5.10.

5.5. BAROTROPY AND BAROCLINITY

The adjectives barotropic and baroclinic are in common use and a few remarks on barotropy and baroclinity are made.

The acceleration of any part of a fluid such as the atmosphere depends upon its mass and upon the forces acting upon it, an important contribution to which comes from the pressure exerted by neighbouring parts of the fluid. Thus, fundamental to an understanding of the movements of a fluid is a recognition of the distributions of mass and pressure. The former is conveniently represented by surfaces of equal specific volume (specific volume = 1/density) and these are known as isosteric surfaces. The pressure distribution is also conveniently represented by surfaces of equal pressure (or isobaric surfaces).

In a fluid subject to gravity but to no other external forces, the gravity forces can only be balanced by the internal pressure forces if the isobaric and isosteric surfaces coincide. The fluid is then said to be "barotropic" and there are no buoyancy forces tending to change the motion of the fluid.

Any other fluid, that is, one in which isobaric and isosteric surfaces intersect, is said to be "baroclinic" and these two sets of surfaces give an important indication of the acceleration to which the fluid is subject. In many meteorological textbooks it is shown that the number of isobaric–isosteric solenoids in a cross-section is a measure of the baroclinity of the fluid and also of the rate of generation of circulation. This material is not reproduced in this handbook partly because of its inclusion in many textbooks (see Haurwitz[7] for a very clear derivation) but partly also because the idea of circulation directly generated by isobaric–isosteric solenoids does not enter directly into practical forecasting methods mainly because baroclinity is almost always balanced by the thermal wind. It is, however, worthy of note that Petterssen[8] shows in his textbook that the degree of baroclinity in a vertical section of the atmosphere is given by the product of the thermal wind speed and the Coriolis parameter. Consequently the thickness pattern gives a representation of the baroclinity of the atmosphere in the vertical. Closely packed thickness lines indicate a strongly baroclinic atmosphere and very widely spaced thickness lines indicate a quasi-barotropic atmosphere.

5.6. THE CONCEPT OF VORTICITY

Before the mathematical derivation of some expressions concerning the dynamics of synoptic systems is given it is desirable to introduce the concept of vorticity. In this section the treatment is restricted to a description of vorticity in simple terms in the hope that forecasters will appreciate that vorticity is of basic importance in understanding current techniques and is not an artificial concept arising from the mathematical manipulations of the equations of motion.

Vorticity is a measure of the spin of the fluid. Consider a rectangular laminar portion of a fluid such as ABCD shown in Figure 5.11*(a)* and suppose that the fluid is deformed (but without bodily transport of the mass of the fluid) so that it takes the shape $A_1B_1C_1D_1$ where BC is parallel to B_1C_1 and AD is parallel to A_1D_1. Then, in moving to their new positions, lines of particles such as AD and BC are not rotated but lines of particles such as AB and CD undergo a rotation in taking up their new positions. Suppose now that $A_1B_1C_1D_1$ is further deformed without bodily transport to assume the new position $A_2B_2C_2D_2$ so that A_1B_1 and C_1D_1 are parallel to A_2B_2 and C_2D_2 respectively, as is shown in Figure 5.11*(b)*. (Figure 5.11*(b)* is displaced from 5.11*(a)* for clarity but bodily transport of the fluid lamina is not necessary.) It will be seen that, in this deformation from $A_1B_1C_1D_1$ to $A_2B_2C_2D_2$, lines of fluid particles such as A_1B_1 and C_1D_1 are not further rotated but lines of particles B_1C_1 and D_1A_1 are rotated to assume their new positions B_2C_2 and D_2A_2. Thus if the laminar portion of fluid is deformed from ABCD to $A_2B_2C_2D_2$ the parcel of fluid undergoes a rotation and this can be conveniently measured by the turning of the lines of fluid elements along AB and AD (or axes parallel to them). The sum of the rates of rotation of AB and AD is a measure of the vorticity in the plane ABCD. Although this was demonstrated for a rectangular lamina of fluid it is generally true for fluids in motion that the sum of the rates of rotation of any two rectangular axes in the fluid is a measure of the vorticity in the plane of the axes. (It should be noted that in Figure 5.11 the fluid undergoes a deformation, that is a dilatation or contraction but this deformation is of no concern in this present context.) It is of course possible for fluids to possess vorticity without undergoing deformation. Suppose a fluid is spinning as if it were a solid body with the same angular velocity (ω) everywhere as indicated in Figure 5.12. Then the sum of the rates of rotation of any two lines at right-angles in a plane perpendicular to the axis of the spin is clearly twice the angular velocity = 2ω (since each line rotates with angular velocity ω).

If the plane of rotation is known then the vorticity can be regarded as a rotation in the plane or a spin about an axis perpendicular to that plane and vorticity can be represented by a vector at right-angles to the plane of rotation.

Vorticity is a property of all scales of atmospheric motion. In this section atmospheric motion on the scale of synoptic systems, recognizable on working charts, is being considered and the rest of this section will deal with the vorticity of motion on such scales only. Let us consider now the motion in a horizontal plane. It will be assumed for simplicity that the air is a purely westerly current and that wind speeds are greater near the centre of the current than to the north or the south. Then it is clear from Figure 5.13 that such a motion has a vorticity about a vertical axis and, furthermore, that the vorticity to the north of the maximum westerly wind is of opposite sense to that to the south. By convention the vorticity depicted to the north of the axis of maximum wind is termed cyclonic, being the same as in a cyclone, and that to the south anticyclonic.

It is appropriate now to mention the effect of the earth's rotation. In the example shown in Figure 5.13 the vorticity of the atmospheric motion is shown relative to the earth. Such vorticity is often termed relative vorticity. However the earth is itself rotating about its axis once per day so that any mass or system of axes fixed on the earth is itself rotating with the earth. For example a mass of air which was wholly at rest on the earth would have no vorticity relative to the earth but would possess vorticity relative to axes fixed in space because the mass of air was

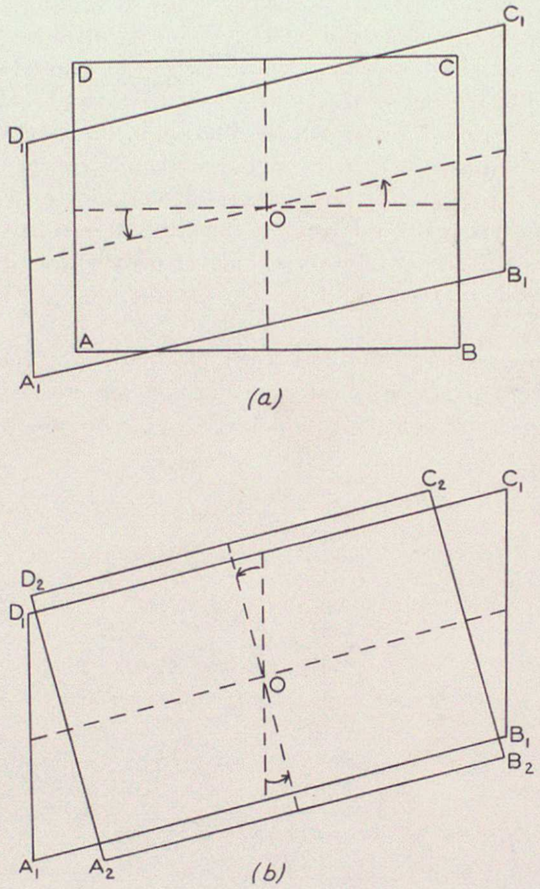

FIGURE 5.11

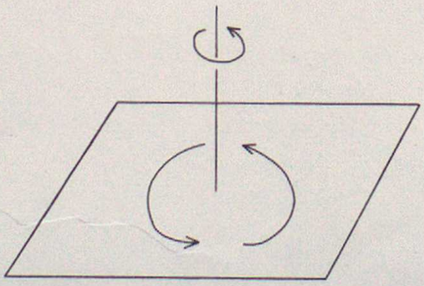

FIGURE 5.12

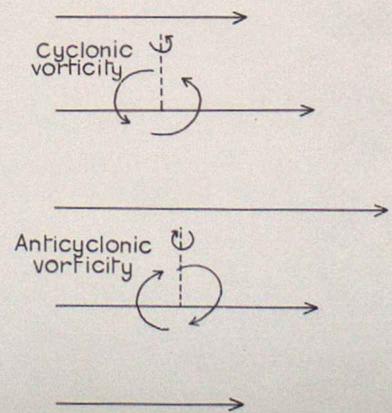

FIGURE 5.13

rotating with the earth. Vorticity relative to axes fixed in space is known as absolute vorticity. To obtain absolute vorticity the vorticity relative to the earth must be compounded with the earth's own vorticity. Much of the material in the rest of this chapter is concerned explicitly or implicitly with the vertical component of vorticity and we shall now determine the vertical component of the earth's vorticity. The earth rotates as a solid body on its axis with angular velocity Ω so that its vorticity about its axis is 2Ω. It is readily seen from Figure 5.14 that the component of this vorticity about the local vertical in latitude ϕ is $2\Omega \sin \phi = l$, the Coriolis parameter. By convention, vorticity in the sense indicated is regarded as positive and hence the vertical component of absolute vorticity of a mass of air, with vertical component of vorticity relative to the earth of ζ, is then $\zeta + l$. Now the earth rotates once per day but substantial meteorological systems on the synoptic scale rotate at a considerably slower rate (for example once in a few days). Thus the vertical component of the earth's vorticity generally contributes the greater part to the absolute vertical vorticity of the air involved in the circulation of synoptic systems.

Let us consider now the motion in a vertical plane. For simplicity it will be assumed that the wind direction is constant but that the speed increases with height. This is shown schematically in Figure 5.15. Air which was initially in

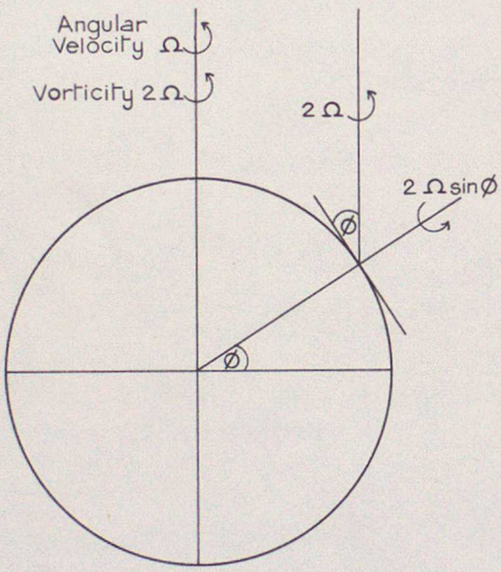

FIGURE 5.14 *Vertical component of vorticity at latitude ϕ due to the rotation of the earth*

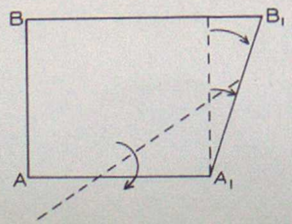

FIGURE 5.15 *Motion in a vertical plane*

the vertical column AB reaches a position A_1B_1 after a time t and it is clear that the air has undergone a rotation in a vertical plane, that is it has a spin about a horizontal axis. The concept of vorticity about horizontal axes does not appear in meteorological literature as frequently as that of vorticity about a vertical axis. The change of wind with height is usually dealt with in terms of other concepts but it should be remembered that, in synoptic systems, the vorticity about horizontal axes is usually much greater than that about a vertical axis.

The preceding subsections have been made descriptive in the hope that they will convey to forecasters that vorticity is a property of all atmospheric systems important on the synoptic scale. The mathematical expressions for vorticity (which are derived in many meteorological textbooks) are quoted below:

Vorticity about the z axis (or in the xy plane) ζ is given by $\dfrac{\partial v}{\partial x} - \dfrac{\partial u}{\partial y}$

Vorticity about the x axis (or in the yz plane) ξ is given by $\dfrac{\partial w}{\partial y} - \dfrac{\partial v}{\partial z}$

Vorticity about the y axis (or in the zx plane) η is given by $\dfrac{\partial u}{\partial z} - \dfrac{\partial w}{\partial x}$

where u, v and w are the velocities along the x, y and z axes.

It is readily seen from these expressions that vorticity has the dimensions of velocity/length = $LT^{-1}/L = T^{-1}$. A suitable time scale for use in meteorological work is the hour, and vorticity is often expressed in hour^{-1} units. The Coriolis parameter l has the same dimensions and in latitude 50°N. l is about 0·4 hour^{-1}.

Now that the general concept of vorticity has been described the basic vorticity equation which is widely applied in meteorological work will be derived.

5.7. BASIC VORTICITY EQUATION IN METEOROLOGY

In practical upper air analysis and forecasting it is more convenient to use pressure as the vertical co-ordinate rather than height. Thus the contours of fixed pressure surfaces are drawn in preference to the isobars of fixed heights. Using pressure as the vertical co-ordinate the mathematical expressions for geostrophic wind are independent of density so that one geostrophic wind scale can be used at all pressure levels.

In the following derivation of the basic vorticity equation, pressure will be used as the vertical co-ordinate so that the results are directly applicable to the working chart. Using pressure as the vertical co-ordinate the slope of the pressure surface enters into the equations of motion through such terms as $\partial h/\partial x$ where h is the height of the pressure surface above mean sea level. The approximate equations of motion in a pressure surface are:

$$\frac{du}{dt} - lv + g\frac{\partial h}{\partial x} = 0 \qquad \ldots (1)$$

$$\frac{dv}{dt} + lu + g\frac{\partial h}{\partial y} = 0 \qquad \ldots (2)$$

where u and v are the component velocities, d/dt represents total differentiation following the motion of the fluid, l is the Coriolis parameter, g is the acceleration due to gravity, h is the height of the pressure surface above mean sea level and $\dfrac{\partial}{\partial x}$ and $\dfrac{\partial}{\partial y}$ represent partial differentiation with respect to x and y respectively.

The geostrophic wind (components u_g, v_g) is obtained from equations (1) and (2) by putting:

$$\frac{du}{dt} = \frac{dv}{dt} = 0.$$

Thus
$$u_g = -\frac{g}{l}\frac{\partial h}{\partial y} \qquad \ldots (3)$$

and
$$v_g = \frac{g}{l}\frac{\partial h}{\partial x}. \qquad \ldots (4)$$

Equations (3) and (4) do not explicitly involve the density so that the geostrophic wind scale used in upper air work with contours on pressure surfaces may be used at all levels.

In two-dimensional flow:

$$\frac{d}{dt} \equiv \frac{\partial}{\partial t} + u\frac{\partial}{\partial x} + v\frac{\partial}{\partial y} \qquad \ldots (5)$$

and equations (1) and (2) may therefore be written in the following extended form:

$$\frac{\partial u}{\partial t} + u\frac{\partial u}{\partial x} + v\frac{\partial u}{\partial y} - lv + g\frac{\partial h}{\partial x} = 0 \qquad \ldots (6)$$

$$\frac{\partial v}{\partial t} + u\frac{\partial v}{\partial x} + v\frac{\partial v}{\partial y} + lu + g\frac{\partial h}{\partial y} = 0 \qquad \ldots (7)$$

Terms containing h can be eliminated by differentiating equation (6) with respect to y and equation (7) with respect to x and subtracting. By rearranging terms and changing the order of differentiation in some terms the following equation is obtained (for the details of the algebra see Appendix I):

$$\frac{\partial}{\partial t}\left\{\frac{\partial v}{\partial x} - \frac{\partial u}{\partial y}\right\} + u\frac{\partial}{\partial x}\left\{\frac{\partial v}{\partial x} - \frac{\partial u}{\partial y} + l\right\} + v\frac{\partial}{\partial y}\left\{\frac{\partial v}{\partial x} - \frac{\partial u}{\partial y} + l\right\} +$$
$$+\left\{\frac{\partial v}{\partial x} - \frac{\partial u}{\partial y} + l\right\}\left\{\frac{\partial u}{\partial x} + \frac{\partial v}{\partial y}\right\} = 0 \qquad \ldots (8)$$

Let us now write
$$\left.\begin{aligned} \frac{\partial u}{\partial x} + \frac{\partial v}{\partial y} &= \operatorname{div} V \\ \text{and} \quad \frac{\partial v}{\partial x} - \frac{\partial u}{\partial y} &= \operatorname{curl} V = \zeta, \end{aligned}\right\} \qquad \ldots (9)$$

where V is the velocity which has components u, v. Then equation (8) may be written

$$\frac{\partial \zeta}{\partial t} + u\frac{\partial}{\partial x}(\zeta + l) + v\frac{\partial}{\partial y}(\zeta + l) + (\zeta + l)\operatorname{div} V = 0 \qquad \ldots (10)$$

and this is the practical form in which the equation is used. Equation (10) is known as the vorticity equation and it may be written in several ways. For example, by making use of the identity (5) it is clear that equation (10) may be re-written

$$\frac{d}{dt}(\zeta + l) + (\zeta + l)\operatorname{div} V = 0. \qquad \ldots (11)$$

Equation (11) shows that the changes in the absolute vorticity of a parcel of air (followed along its path) arise because of the divergence div V and that if the divergence is zero, the absolute vorticity remains constant.

When equation (10) is used in computation it is often sufficiently accurate to replace u and v by their geostrophic values in the computation of the vorticity ζ and of the advection terms

$$u\frac{\partial \zeta}{\partial x} + v\frac{\partial \zeta}{\partial y} \quad \text{and} \quad u\frac{\partial l}{\partial x} + v\frac{\partial l}{\partial y}.$$

Thus from equations (3), (4) and (9) we have

$$\begin{aligned} \zeta &= \frac{\partial v_g}{\partial x} - \frac{\partial u_g}{\partial y} \\ &= \frac{g}{l}\frac{\partial^2 h}{\partial x^2} + \frac{g}{l}\frac{\partial^2 h}{\partial y^2} \qquad \text{if variations of } l \text{ are neglected as being small} \\ &= \frac{g}{l}\left(\frac{\partial^2 h}{\partial x^2} + \frac{\partial^2 h}{\partial y^2}\right) \\ &= \frac{g}{l}\nabla^2 h, \qquad \qquad \ldots (12) \end{aligned}$$

where $\nabla^2 \equiv \dfrac{\partial^2}{\partial x^2} + \dfrac{\partial^2}{\partial y^2}$, the two-dimensional Laplacian operator.

It should be noted, however, that u and v cannot be replaced by their geostrophic values in the computation of divergence because from (3), (4) and (9) we have

$$\begin{aligned} \text{div } V_g = \frac{\partial u_g}{\partial x} + \frac{\partial v_g}{\partial y} &= -\frac{g}{l}\frac{\partial^2 h}{\partial x \partial y} + \frac{g}{l}\frac{\partial^2 h}{\partial x \partial y} \qquad \text{if variations of } l \text{ are neglected as being small} \\ &= 0. \end{aligned}$$

Thus geostrophic values of u and v cannot be used to compute divergence. If the variation of l with latitude is taken into account, non-zero values of divergence are obtained from geostrophic winds but these values are small compared with the actual convergence and divergence in depressions and anticyclones, and satisfactory values of div V could be computed from $(\partial u/\partial x + \partial v/\partial y)$ only if actual wind components u and v were known.

The vorticity equation given in equation (10) is not exact; in the exact equation there are other terms which involve the vertical velocity but these are often small compared with those retained in equation (10). The vorticity ζ is normally small compared with l except in intense frontal regions or near the centre of deep depressions, and in the latter case ζ is positive anyhow. Thus $(\zeta + l)$ is normally positive in atmospheric systems on the synoptic scale and equation (11) shows that isobaric divergence, that is div $V > 0$, leads to decreasing $(\zeta + l)$ or increasing anticyclonic circulation; and horizontal convergence leads to increasing vorticity or more cyclonic circulation.

If variations in density and frictional forces are ignored it can be shown that the circulation with respect to fixed axes around a closed curve moving with a fluid is conserved. The circulation can be represented by the average absolute vorticity multiplied by the area enclosed by the curve. Thus when the circulation is conserved an increase in absolute vorticity must be accompanied by a decrease in area. This leads to the same conclusion as the preceding paragraph, namely that convergence which leads to a decrease in area is accompanied by increasing vorticity or more cyclonic circulation. In other words cyclogenesis requires the creation of vorticity and convergence; anticyclogenesis the destruction of vorticity and divergence.

Consider the development of a depression from air which has zero relative vorticity initially, that is $\zeta = 0$. In our latitudes, l has a value of about 0·4 hour^{-1}, so that the initial absolute vorticity of the air is 0·4 hour^{-1}. In a well marked depression ζ has a value of about 0·4 hour^{-1}, so that the absolute vorticity will have increased to 0·8 hour^{-1}. Assuming it is valid to apply the conservation of circulation it follows that the area covered by the cyclone must have shrunk to one-half of its initial value, that is there must have been much convergence. The accumulation of air accompanying such convergence would have led to a marked rise of surface pressure unless it was compensated by divergence occurring at higher levels. Instead of there being a rise of pressure when depressions form there is usually a net fall of pressure. It is reasonable therefore to look for a vertical distribution of convergence and divergence such that the divergence at upper levels is of the same order of magnitude as at lower levels but, because for the formation of a depression pressure must fall, the upper divergence just exceeds the lower-level convergence. Conversely, during the development of an anticyclone it is reasonable to expect lower-level divergence to be overlain by upper convergence of slightly greater integrated magnitude to account for rising pressures. Thus the local pressure tendency at the surface must be regarded as a result of a small residual convergence or divergence between two much larger quantities of opposing signs.

The upper and lower areas of convergence and divergence are connected by the vertical currents over extensive areas of depressions and anticyclones. The various systems are represented schematically in Figure 5.16.

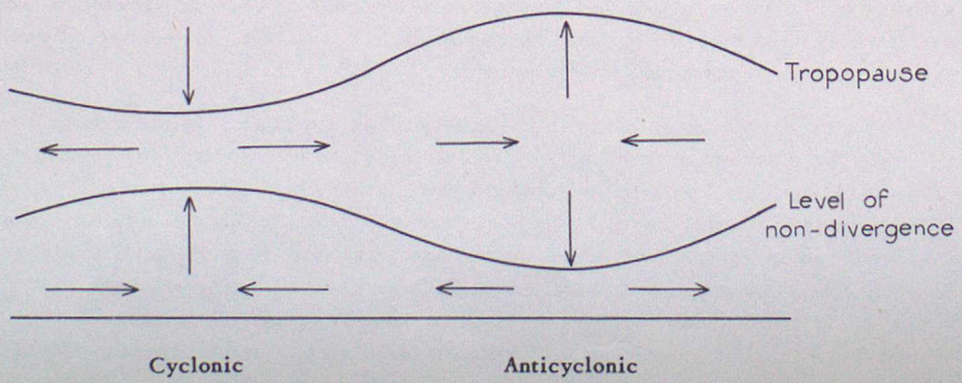

FIGURE 5.16 *Schematic illustration of cyclonic and anticyclonic development*

Figure 5.16 shows the typical features of major atmospheric systems; that is, in anticyclonic areas high-level convergence, subsiding motion and low-level divergence and the reverse in cyclonic areas.

5.8. NON-DIVERGENT FLOW AND CONSTANT ABSOLUTE VORTICITY

Since low-level convergence (divergence) is often overlain by high-level divergence (convergence) it is reasonable to assume that at some level convergence/divergence will be zero. There may be more than one such level and any surface of non-divergence may not be horizontal. Nevertheless we may expect to find a level of generally small divergence in mid-troposphere. If equation (11) is applied to a level of non-divergence then

$$\frac{d}{dt}(\zeta + l) = -(\zeta + l)\ \mathrm{div}\ V = 0$$

or $(\zeta + l)$ is constant. The motion is one of constant absolute vorticity (C.A.V.). At the level of non-divergence the air will move so that its absolute vorticity is conserved. Several techniques have been developed, notably in the United States, for practical application of the idea of C.A.V. to forecasting. The level of non-divergence is often taken as about 500 millibars.

5.8.1. *Rossby long waves*

Rossby[9] showed that waves could exist in a broad zonal non-divergent current of uniform velocity U. The appropriate formulae can be derived quite simply from the basic vorticity equation (11).

Choose the x-axis towards the east and the y-axis to the north and superimpose a small perturbation with velocity components u' and v' on the zonal flow U. Let ζ be the vorticity of the motion as a whole. Then

$$u = U + u' \text{ and } v = v'$$

and $$\zeta = \frac{\partial v}{\partial x} - \frac{\partial u}{\partial y} = \frac{\partial v'}{\partial x} - \frac{\partial u'}{\partial y} \quad \text{since } U \text{ is constant.}$$

If now the motion is horizontal and non-divergent then from equation (11)

$$\frac{d}{dt}(\zeta + l) = 0 \quad \text{or} \quad \frac{d\zeta}{dt} = -\frac{dl}{dt}.$$

But $$\frac{d}{dt} \equiv \frac{\partial}{\partial t} + u\frac{\partial}{\partial x} + v\frac{\partial}{\partial y} \quad \text{and so we have:}$$

$$\frac{\partial \zeta}{\partial t} + u\frac{\partial \zeta}{\partial x} + v\frac{\partial \zeta}{\partial y} = -v\frac{\partial l}{\partial y} \quad \left(\text{since} \quad \frac{\partial l}{\partial t} = \frac{\partial l}{\partial x} = 0\right).$$

But $l = 2\Omega \sin\phi$, therefore:

$$\frac{\partial l}{\partial y} = \frac{2\Omega\cos\phi}{R}, \text{ since } \frac{\partial \phi}{\partial y} = \frac{1}{R} \text{ where } R \text{ is the radius of the earth,}$$

$$= \beta \text{ (say).}$$

Therefore $$\frac{\partial \zeta}{\partial t} + u\frac{\partial \zeta}{\partial x} + v\frac{\partial \zeta}{\partial y} = -\beta v'.$$

Neglecting second order terms of the type $u'\frac{\partial \zeta}{\partial x}$ and $v'\frac{\partial \zeta}{\partial y}$ the equation becomes

$$\frac{\partial \zeta}{\partial t} + U\frac{\partial \zeta}{\partial x} = -\beta v'. \qquad \ldots (13)$$

Now if we assume that the wave disturbances specified by u' and v' travel without change of shape and at constant speed (c) then

$$\frac{\partial \zeta}{\partial t} = -c\frac{\partial \zeta}{\partial x},$$

since the local rate of change of vorticity must just balance the advection of vorticity. Also if the perturbations vary only in the direction of the main stream, that is, they are independent of y, then

$$\frac{\partial u'}{\partial y} = 0$$

and therefore $\zeta = \dfrac{\partial v'}{\partial x}$

and so $\dfrac{\partial \zeta}{\partial x} = \dfrac{\partial^2 v'}{\partial x^2}$.

Then equation (13) takes the form

$$-c\frac{\partial \zeta}{\partial x} + U\frac{\partial \zeta}{\partial x} = -\beta v'$$

or

$$(U - c)\frac{\partial \zeta}{\partial x} = -\beta v'$$

or

$$(U - c)\frac{\partial^2 v'}{\partial x^2} = -\beta v'. \qquad \ldots (14)$$

Putting $v' = \sin\dfrac{2\pi}{L}(x - ct)$ then $\dfrac{\partial v'}{\partial x} = \dfrac{2\pi}{L}\cos\dfrac{2\pi}{L}(x - ct)$

and $\dfrac{\partial^2 v'}{\partial x^2} = -\dfrac{4\pi^2}{L^2}\sin\dfrac{2\pi}{L}(x - ct)$.

Equation (14) will be satisfied provided that:

$$\frac{4\pi^2}{L^2}(U - c) = \beta$$

or

$$c = U - \frac{\beta L^2}{4\pi^2}. \qquad \ldots (15)$$

Suppose the wave pattern is stationary, that is, $c = 0$, then the stationary wavelength L_s is:

$$L_s = 2\pi\sqrt{\frac{U}{\beta}}.$$

Thus equation (15) may be written:

$$c = U\left(1 - \frac{L^2}{L_s^2}\right). \qquad \ldots (16)$$

This last form shows that if the actual wavelength L is less than the stationary wavelength L_s then c is positive and the wave pattern is progressive towards the east. If the wavelength L is longer than L_s then c is negative and the wave pattern tends to be retrogressive, that is, it moves towards the west against the general zonal flow. At 50°N. and with a zonal wind speed U of 40 knots $L_s \approx 3{,}000$ nautical miles. It is thus clear that these waves are of the same order of magnitude as those observed over substantial areas of the hemisphere in meteorological analysis.

It would seem that the equation could have considerable prognostic value but there are a number of difficulties. Firstly the assumptions leading up to its derivation were a uniform west wind, horizontal motion and perturbations on the zonal flow which could be regarded as small. Such conditions are seldom observed over extensive portions of the globe yet the wave-like solutions of the formula bear a fairly close resemblance to the waves actually observed, that is, in spite of the restrictive nature of the assumptions, the formula accounts for a substantial part of the motion of the waves when the actual conditions bear a general similarity to zonal flow. Extensive work has been carried out, primarily in the United States, to devise quantitative techniques for practical application. In the United Kingdom the techniques have been applied with rather less fervour – possibly due to an investigation by Sumner[10] who found the results of limited value for short- and medium-range forecasting. The quantitative application of long-wave techniques in forecasting necessitates upper air charts being drawn over substantial portions of the northern hemisphere (about one-half) and numerical computations can only be applied at the larger forecasting centres. Details of some techniques based on the Rossby wave equation will be found in papers by Sumner[10] or Riehl[2] and in several original papers listed by the latter. Although the calculation of wave speeds from equation (16) has had little quantitative success nevertheless comparison of the actual wavelength with the stationary wavelength has been found useful as indicating whether or not a trough or ridge will progress eastward. Waves with wavelength less than the stationary wavelength by 15° longitude or more can usually be relied on to progress eastward. The behaviour of waves longer than the stationary wavelength by 15° longitude or more is often complicated by the formation of a new trough which effectively shortens the wavelength and allows eastward progression of the original downstream trough. For the purpose of such application of equation (16) the stationary wavelength is often calculated by assessing the zonal wind U from the average difference in 500-millibar height over a long band of latitude 20° in width. A set of instructions for carrying out such a computation, together with Figure 5.17 for obtaining the stationary wavelength from the mean height difference as given by Smith,[4] is reproduced below.

5.8.1.1. *Computation of stationary wavelengths.* The step-by-step procedure is as follows:

(i) Estimate a "central" latitude to the flow pattern (the nearest 5° is probably all that is warranted).

(ii) Obtain the appropriate zonal parameter by averaging the zonal component of the 500-millibar flow for a 20° band width (10° on either side of the selected latitude) and for a sector just including the trough (or ridge) in question and the one immediately upwind of it (ridges are usually less sharply defined than troughs and, because of the sharper features of troughs, calculations for troughs are usually to be preferred to those for ridges). Differences of contour height should be read off at intervals of 10° longitude commencing with the 10° meridian just to the west of the axis of the upwind member of the trough (ridge) pair. The average contour height difference for this zone should then be obtained.

(iii) The corresponding stationary wavelength is read off directly from Figure 5.17. The units of length are degrees of longitude measured along the appropriate (central) latitude circle. Interpolation between the isopleths is not linear, but the spacing is close enough to give the required value to within one or two degrees.

(iv) If desired the zonal index in degrees of longitude per day (that is, the geostrophic equivalent of the average contour difference) may also be read off directly (dashed lines). In this case interpolation is linear. The expected displacement of the downstream trough during the next 24 hours is given by the difference between the zonal indices appropriate to L and L_s (degrees of longitude per day).

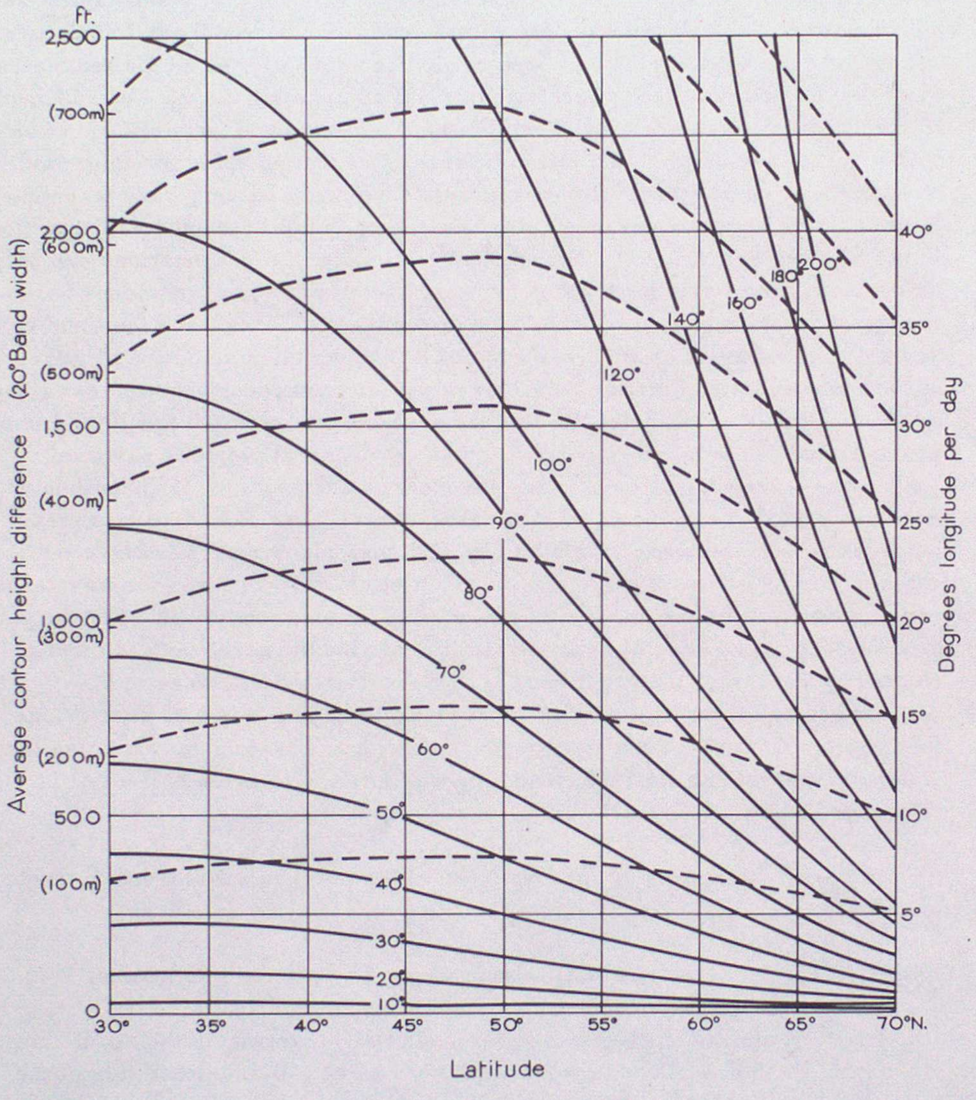

FIGURE 5.17 *Computation of stationary wavelengths* ($L_s = 2\pi\sqrt{\frac{u}{\beta}}$)

The continuous curves represent lines of equal stationary wavelength expressed in degrees of longitude measured along the appropriate latitude circle and the dashed curves represent the zonal velocity in degrees of longitude per day.

5.9. SUTCLIFFE DEVELOPMENT EQUATION

In Section 5.7 it was shown that in cyclonic (anticyclonic) systems there was divergence (convergence) in the upper troposphere and convergence (divergence) in the lower troposphere. Using these concepts Sutcliffe[11] showed in an early paper that the patterns of upper and lower divergence can be inferred from a study of their difference. In a later paper Sutcliffe[12] showed that a measure of the development occurring between two levels was given by the difference between the divergence at the two levels and that this quantity could be approximated in terms which could be derived from routine analysed charts. A derivation of the Sutcliffe development equation is given below.

In Section 5.7 the simplified form of the vorticity equation was derived; namely

$$\frac{\partial \zeta}{\partial t} + u\frac{\partial}{\partial x}(\zeta + l) + v\frac{\partial}{\partial y}(\zeta + l) = -(\zeta + l)\,\mathrm{div}\, V. \quad \ldots (10)$$

This is often approximated by using the geostrophic wind values on the left-hand side of this equation but not on the right. Further, over much of the synoptic chart ζ is small compared with l so that, on the right-hand side of equation (10), $(\zeta + l)$ may be replaced by l with fair approximation. Thus equation (10) then becomes

$$\frac{\partial \zeta}{\partial t} + u\frac{\partial}{\partial x}(\zeta + l) + v\frac{\partial}{\partial y}(\zeta + l) = -l\,\mathrm{div}\, V. \quad \ldots (17)$$

Consider equation (17) at two pressure levels p_1 and p_0 whose heights above mean sea level are h_1 and h_0, where the wind velocities are V_1 and V_0 with components $(u_1 v_1)$ and $(u_0 v_0)$ and where the relative vorticities are ζ_1 and ζ_0. The thickness between the pressure surfaces is $h' = h_1 - h_0$ and the thermal wind is $V' = V_1 - V_0$ with components $(u'v')$ where $u' = u_1 - u_0$ and $v' = v_1 - v_0$. Equation (17) applied to the two levels p_1 and p_0 gives

$$\frac{\partial \zeta_1}{\partial t} + u_1\frac{\partial}{\partial x}(\zeta_1 + l) + v_1\frac{\partial}{\partial y}(\zeta_1 + l) = -l\,\mathrm{div}\, V_1 \quad \ldots (18)$$

and

$$\frac{\partial \zeta_0}{\partial t} + u_0\frac{\partial}{\partial x}(\zeta_0 + l) + v_0\frac{\partial}{\partial y}(\zeta_0 + l) = -l\,\mathrm{div}\, V_0. \quad \ldots (19)$$

Subtracting equation (19) from (18) and substituting $u_0 + u'$ for u_1 and $v_0 + v'$ for v_1 in equation (18) gives

$$\frac{\partial}{\partial t}(\zeta_1 - \zeta_0) + (u_0 + u')\frac{\partial}{\partial x}(\zeta_1 + l) + (v_0 + v')\frac{\partial}{\partial y}(\zeta_1 + l) -$$

$$- u_0\frac{\partial}{\partial x}(\zeta_0 + l) - v_0\frac{\partial}{\partial y}(\zeta_0 + l) = -l\,(\mathrm{div}\, V_1 - \mathrm{div}\, V_0). \quad \ldots (20)$$

All terms on the left-hand side of equation (20) with the exception of the first can be approximated in terms of quantities available from analysed charts. The first term is the time-derivative of $\zeta_1 - \zeta_0$ and

$$\zeta' = \zeta_1 - \zeta_0 \text{ and, using equation (12),}$$

$$= \frac{g}{l}\nabla^2 (h_1 - h_0)$$

$$= \frac{g}{l}\nabla^2 h'. \quad \ldots (21)$$

So far only the dynamical equations have been used and it is unlikely that any equation which does not account in some way for the thermodynamical properties of the atmosphere will be directly useful in forecasting. The simplest thermodynamical assumption applicable to a layer is that the mean temperature of the air column between the pressure surfaces p_1 and p_0 moves with the mean wind speed between these pressure surfaces and it is observed that a major part of the thickness change is accounted for by advection of the mean temperature by the geostrophic wind. If, additionally, it is assumed that the thermal wind of any layer from p_1 to p_0 is parallel to the thickness lines for the layer p_1 to p_0 and so does not transport them, then the mean transporting wind may be taken as that at the level p_0, or at level p_1, which is that at p_0 augmented by the thermal wind. These assumptions, whose approximate validity is supported by observations and practical experience, may be expressed in the form of the equation

$$\frac{\partial h'}{\partial t} + u_0 \frac{\partial h'}{\partial x} + v_0 \frac{\partial h'}{\partial y} = 0 . \qquad \ldots (22)$$

Equation (22) asserts that the thickness patterns move with the wind at the lower level p_0.

Equation (22) will now be used to eliminate the time-derivative from the left-hand side of equation (20). This time-derivative is

$$\frac{\partial}{\partial t} (\zeta_1 - \zeta_0)$$

which, by using equation (21), is

$$\frac{\partial}{\partial t}\left(\frac{g}{l} \nabla^2 h' \right).$$

To obtain such an expression we shall operate on equation (22) with

$$\nabla^2 = \left(\frac{\partial^2}{\partial x^2} + \frac{\partial^2}{\partial y^2} \right).$$

The detailed algebra is given in Appendix II. After some manipulation equation (22) then becomes

$$\nabla^2 \frac{\partial h'}{\partial t} + u_0 \frac{\partial}{\partial x} \nabla^2 h' + v_0 \frac{\partial}{\partial y} \nabla^2 h' - u' \frac{\partial}{\partial x} \nabla^2 h_0 - v' \frac{\partial}{\partial y} \nabla^2 h_0 + D = 0 , \qquad \ldots (23)$$

where D represents some terms which are small enough to be neglected in comparison with those retained. Using the geostrophic approximations of equation (12), that is,

$$\zeta_0 = \frac{g}{l} \nabla^2 h_0 \quad \text{and} \quad \zeta' = \frac{g}{l} \nabla^2 h'$$

and neglecting D and the variation of l equation (23) becomes

$$\begin{aligned}
\frac{l}{g}\left(u_0 \frac{\partial \zeta'}{\partial x} + v_0 \frac{\partial \zeta'}{\partial y} - u' \frac{\partial \zeta_0}{\partial x} - v' \frac{\partial \zeta_0}{\partial y} \right) &= - \nabla^2 \frac{\partial h'}{\partial t} \\
&= - \frac{\partial}{\partial t} \nabla^2 h' \qquad \text{(changing the order of differentiation)} \\
&= - \frac{l}{g} \frac{\partial \zeta'}{\partial t} \\
&= - \frac{l}{g} \frac{\partial}{\partial t} (\zeta_1 - \zeta_0) . \qquad \ldots (24)
\end{aligned}$$

Substituting the expression for $\frac{\partial}{\partial t} (\zeta_1 - \zeta_0)$ from equation (24) in equation (20) gives

$$- u_0 \frac{\partial \zeta'}{\partial x} - v_0 \frac{\partial \zeta'}{\partial y} + u' \frac{\partial \zeta_0}{\partial x} + v' \frac{\partial \zeta_0}{\partial y} + (u_0 + u') \frac{\partial}{\partial x} (\zeta_1 + l) + (v_0 + v') \frac{\partial}{\partial y} (\zeta_1 + l) -$$

$$- u_0 \frac{\partial}{\partial x} (\zeta_0 + l) - v_0 \frac{\partial}{\partial y} (\zeta_0 + l) = - l \; (\text{div } V_1 - \text{div } V_0) \,. \qquad . \; . \; . \; (25)$$

Collecting terms:

$$- u_0 \frac{\partial}{\partial x} \; (\zeta' - \zeta_1 - l + \zeta_0 + l) - v_0 \frac{\partial}{\partial y} \; (\zeta' - \zeta_1 - l + \zeta_0 + l) +$$

$$+ u' \frac{\partial}{\partial x} (\zeta_0 + \zeta_1 + l) + v' \frac{\partial}{\partial y} (\zeta_0 + \zeta_1 + l) = - l \; (\text{div } V_1 - \text{div } V_0).$$

Remembering that $\zeta_1 = \zeta_0 + \zeta'$, the terms in u_0 and v_0 vanish. Thus equation (25) becomes

$$l \; (\text{div } V_1 - \text{div } V_0) = - u' \frac{\partial}{\partial x} (\zeta_0 + \zeta_1 + l) - v' \frac{\partial}{\partial y} (\zeta_0 + \zeta_1 + l) \,. \qquad . \; . \; . \; (26)$$

If now we introduce the co-ordinate s, measured along the local direction of the thickness lines, and remembering that V' is the thermal wind with components u' and v' the right-hand side of equation (26) becomes:

$$- V' \frac{\partial}{\partial s} \; (\zeta_0 + \zeta_1 + l)$$

$$= - V' \frac{\partial}{\partial s} \, (2 \zeta_0 + \zeta' + l) \quad \text{since} \quad \zeta_1 = \zeta_0 + \zeta' \,.$$

The development equation, in the form given by Sutcliffe,[12] is then

$$l \; (\text{div } V_1 - \text{div } V_0) \; = \; - V' \frac{\partial}{\partial s} (l + 2 \zeta_0 + \zeta') \,. \qquad . \; . \; . \; (27)$$

Equation (27) could be applied to each stratum of the troposphere between the various isobaric levels for which thickness and contour charts are constructed. Although such procedures might increase the forecaster's understanding of the atmospheric processes taking place, the routine operational application of such procedures is precluded by the amount of computation involved which cannot normally be carried out with the manpower or within the time available on the forecast bench. In practice it is necessary to apply the Sutcliffe development equation to one stratum, generally 1000–500 millibars, and use models as a guide to practical forecasting. Such a restriction may render the expression of little value when the situations are very complex, but in most cases where the shear increases fairly steadily with height throughout the troposphere very useful indications of development are obtained.

It should be noted that relative divergence indicates ascent and cyclogenesis, and relative convergence indicates descent and anticyclogenesis. Thus from equation (27) it is seen that the development is of cyclonic or anticyclonic type according as:

$$V' \frac{\partial}{\partial s} (l + 2 \zeta_0 + \zeta') < 0 \quad \text{(cyclonic development)}$$

$$\text{or} \quad > 0 \quad \text{(anticyclonic development)}. \qquad . \; . \; . \; (28)$$

The terms in the inequality (28) will now be considered in detail. Firstly it should be noted that the development depends on V', the vertical shear. The stronger the shear the greater is the development but if there is no shear, that is $V' = 0$, then there is no development.

Let us now consider each term separately.

(i) $V' \partial l/\partial s$, the latitudinal term.
$\partial l/\partial s$ is the variation of the Coriolis parameter with s and is clearly a maximum when V is meridional. Thus the greatest effect will be with southerly or northerly thermal winds. Since

$$\frac{\partial l}{\partial s} = \frac{2\,\Omega\cos\phi}{R}\;\frac{\partial \phi}{\partial s},$$

$\partial l/\partial s$ is positive for increasing ϕ and consequently a wind shear with a northward component makes

$$V'\frac{\partial l}{\partial s} > 0$$

so that the term $V' \partial l/\partial s$ contributes to anticyclonic development. Conversely a wind shear with a southward component is one of cyclonic development. The magnitude of contributions due to this term is usually small and generally masked by the other two terms, particularly where variations in the horizontal shear of wind and the curvature of the flow are large.

Since $\partial l/\partial s$ depends only on latitude, $V' \partial l/\partial s$ is often called the latitudinal term.

(ii) $2\,V' \partial\zeta_0/\partial s$, the thermal steering term.
$\partial\zeta_0/\partial s$ is the variation in vorticity of the lower-level circulation (usually 1000 millibars) in the direction of s. Let us consider a simple schematic circular cyclonic circulation (see Figure 5.18). The centre of the depression is a region of maximum cyclonic vorticity. For simplicity the thermal wind is assumed straight and uniform.

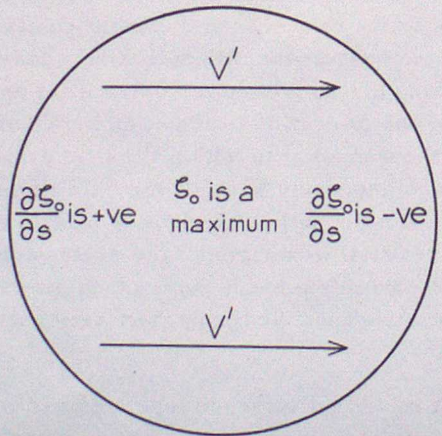

FIGURE 5.18 *Circular depression and straight thermal wind*

Then in advance of the centre in the direction of V', $\partial\zeta_0/\partial s$ is negative so that $V' \partial\zeta_0/\partial s$ is negative, that is, the development ahead of the depression is cyclonic. To the rear of the centre, $\partial\zeta_0/\partial s$ is positive in the direction of V' so that the development to the rear is anticyclonic.

It is thus apparent that the contribution of $2\,V' \partial\zeta_0/\partial s$ will be to a translation of the depression in the direction of the thermal wind. This translation should not be regarded as a simple bodily movement of the depression but rather as a movement due to the creation of vorticity ahead of the depression and the destruction of vorticity in its rear.

An anticyclone is a region of negative vorticity with a minimum value near the centre. Applying arguments similar to those above it is readily seen that this term also contributes to a movement of the anticyclone in the direction of the thermal wind.

Troughs and ridges are, broadly speaking, areas of maximum and minimum vorticity and the same rule applies: namely, that the term $2V'\partial\zeta_0/\partial s$ contributes to the displacement of such pressure systems in the direction of the thermal wind by a process of development; or pressure systems tend to be steered in the direction of the thermal wind. Hence the term $2V'\partial\zeta_0/\partial s$ is often called the thermal steering term.

It should be noted that where $\partial\zeta_0/\partial s$ is zero this term does not contribute to development. Now centres of high or low pressure are usually minima or maxima of vorticity so that at these centres $\partial\zeta_0/\partial s$ is zero. Thus $2V'\partial\zeta_0/\partial s$ does not contribute to intensification at the centre of the system but only to its displacement.

(iii) $V'\partial\zeta'/\partial s$, the thermal vorticity effect.
This term depends entirely on the thickness pattern and the distribution of thermal winds. Broadly speaking it indicates cyclonic development where the thermal vorticity decreases in the direction of the shear (that is $\partial\zeta'/\partial s$ is negative) so that $V'\partial\zeta'/\partial s$ is negative and therefore contributes to cyclonic development and ascent of air. Conversely, anticyclonic development (and descent) is indicated where the thermal vorticity increases in the direction of the vertical shear.

It is seen that development, as defined by the Sutcliffe term, can be obtained from the thermal wind, the vorticity of the surface (1000-millibar) flow and the vorticity of the 1000–500-millibar thermal wind. Contours of the 1000-millibar surface and thicknesses of the 1000–500-millibar layer are readily available at most outstations so that the practical application of this theory is a possibility provided procedures can be devised for the quantitative or qualitative assessment of vorticity patterns.

5.10. THE CALCULATION AND RECOGNITION OF VORTICITY FROM SYNOPTIC CHARTS

5.10.1. *The calculation of vorticity*

If h is the height of a contour on an isobaric surface and u_g and v_g are the components of geostrophic wind then

$$u_g = -\frac{g}{l}\frac{\partial h}{\partial y} \quad \text{and} \quad v_g = \frac{g}{l}\frac{\partial h}{\partial x}.$$

So that geostrophic vorticity $= \dfrac{\partial v_g}{\partial x} - \dfrac{\partial u_g}{\partial y}$

$$= \frac{g}{l}\left(\frac{\partial^2 h}{\partial x^2} + \frac{\partial^2 h}{\partial y^2}\right)$$ provided variations of l with latitude are neglected as being small

$$= \frac{g}{l}\nabla^2 h,$$

where $\nabla^2 \equiv \dfrac{\partial^2}{\partial x^2} + \dfrac{\partial^2}{\partial y^2}$, the two-dimensional Laplacian operator.

Thus the field of geostrophic vorticity may be obtained by calculating the Laplacian of the contour surface. This can be obtained approximately using finite differences. Consider a rectangular grid of points as shown in Figure 5.19.

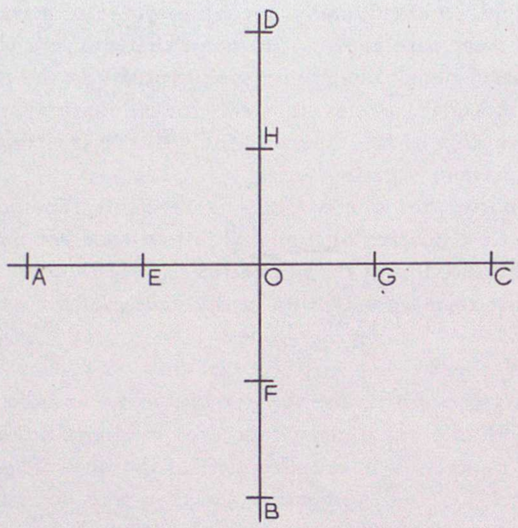

FIGURE 5.19 *Rectangular grid for estimating the Laplacian of a contour field*
AO = BO = CO = DO
EO = FO = GO = HO = ½AO

Then $\left(\dfrac{\partial h}{\partial x}\right)_E \approx \dfrac{h_O - h_A}{AO}$

and $\left(\dfrac{\partial h}{\partial x}\right)_G \approx \dfrac{h_C - h_O}{OC} = \dfrac{h_C - h_O}{AO}$

Also
$$\left(\frac{\partial^2 h}{\partial x^2}\right)_O \approx \frac{\left(\dfrac{\partial h}{\partial x}\right)_G - \left(\dfrac{\partial h}{\partial x}\right)_E}{EG}$$
$$\approx \frac{\left(\dfrac{\partial h}{\partial x}\right)_G - \left(\dfrac{\partial h}{\partial x}\right)_E}{AO}$$
$$\approx \frac{h_C - h_O - h_O + h_A}{AO^2}$$
$$\approx \frac{h_C - 2h_O + h_A}{AO^2}\,.$$

Similarly $\left(\dfrac{\partial^2 h}{\partial y^2}\right)_O \approx \dfrac{h_D - 2h_O + h_B}{AO^2}\,.$

$$\text{So } \left(\nabla^2 h\right)_O = \left(\frac{\partial^2 h}{\partial x^2}\right)_O + \left(\frac{\partial^2 h}{\partial y^2}\right)_O \approx \frac{h_A + h_B + h_C + h_D - 4h_O}{AO^2}\,. \qquad \ldots (29)$$

Some Dynamical Aspects of Atmospheric Systems

For the calculation of vorticity Sawyer[13] has described a scale similar to that illustrated in Figure 5.20. By estimating height in units of tens of metres, choosing AO = BO = CO = DO = 166·7 nautical miles, applying the finite difference formula (29) and dividing by three, vorticity is given in units of 0·1 hour^{-1} in latitude 50°.

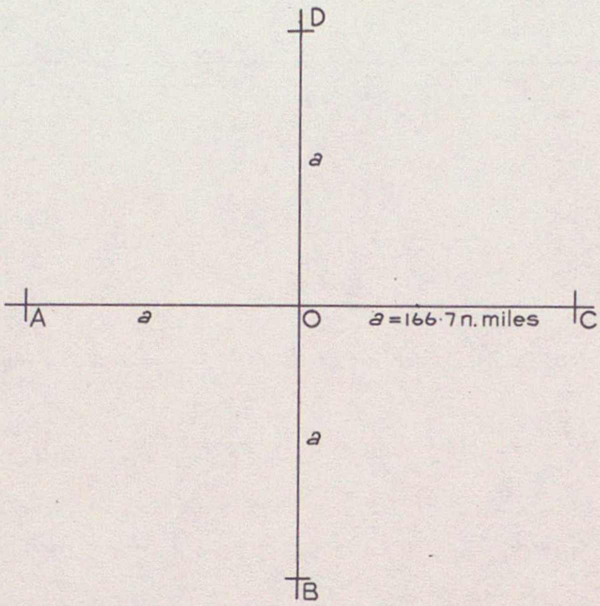

FIGURE 5.20 *Scale for measuring vorticity on an isobaric chart*

The use of this scale would permit of the calculation of vorticity at a finite number of points, but before the Sutcliffe development terms could be assessed it would be necessary to construct isopleths of vorticity of the 1000-millibar contour and 1000–500-millibar thickness fields so that the gradients of vorticity ($\partial\zeta_0/\partial s$ and $\partial\zeta'/\partial s$) might be measured or calculated. This is a tedious operation and outstation staffs do not have either the labour or time to use such a procedure. Computations have shown that the thermal steering term $2V'\,\partial\zeta_0/\partial s$ is often the numerically larger term in the inequality (28). However, the development term $V'\,\partial\zeta'/\partial s$, although often smaller, is more important in some ways since it gives rise to new synoptic systems. Computation of terms such as $V'\,\partial\zeta_0/\partial s$ and $V'\,\partial\zeta'/\partial s$ can be carried out, using finite differences, from contour/thickness charts in a single operation by using a scale of the type described by Sawyer. Figure 5.21 shows a suitable scale.

On the forecast bench the operational time-table usually precludes such calculations at more than a few key points. The scale has been included, however, so that forecasters can evaluate approximately terms such as $2V'\,\partial\zeta_0/\partial s$ and $V'\,\partial\zeta'/\partial s$ when desired. Even if this is only done after the event, forecasters should obtain an indication of magnitudes which should lead to useful experience when estimating probable magnitudes on charts on future occasions.

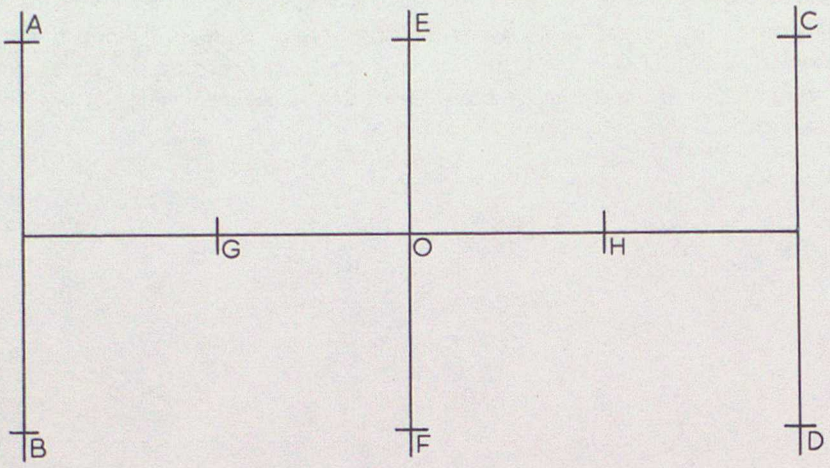

FIGURE 5.21 *Scale for evaluating* $V'\dfrac{\partial\zeta_0}{\partial s}$ *and* $V'\dfrac{\partial\zeta'}{\partial s}$

$$\left(V'\frac{\partial\zeta_0}{\partial s}\right)_{\text{At O}} \propto (h'_F - h'_E)\ \{h_C + h_D - h_A - h_B + 4\ (h_G - h_H)\}$$

$$\left(V'\frac{\partial\zeta'}{\partial s}\right)_{\text{At O}} \propto (h'_F - h'_E)\ \{h'_C + h'_D - h'_A - h'_B + 4\ (h'_G - h'_H)\}\ .$$

When h and h' are read off in tens of metres the expressions give results in units of 10^{-3} hr.$^{-2}$ in latitude 50° when the unit of length (OG = OE etc.) represents 104 n. miles on the chart in use.

The axis GOH is aligned tangential to the thickness at O, the point where the terms are to be evaluated.

5.10.2. *The recognition of vorticity*

It is seen that the calculation of vorticity fields and gradients over substantial areas is beyond the resources of most outstations. Development in the use of electronic computers may, at some future date, make possible the transmission of isopleths of vorticities (or some other suitable quantity) to outstations as a matter of routine. This time has not yet come and techniques for applying the Sutcliffe expression on a day-to-day basis rest on the use of simplified models.

It is not particularly difficult to recognize the thermal steering term $2V'\,\partial\zeta_0/\partial s$ from a chart containing 1000-millibar contours and the 1000–500-millibar thicknesses and, although this term is often numerically larger than the thermal vorticity term $V'\,\partial\zeta'/\partial s$, it is an important part of present forecasting techniques that the development to be expected from the thermal vorticity term with various schematic configurations of thicknesses should be recognized and used – at least qualitatively – in the preparation of prebaratic/prontour charts and of forecasts.

These configurations (or models) of thicknesses are rather more easily understood if the expression for vorticity is transformed to a system of orthogonal axes determined by the stream-lines of the flow and their normals.

In such axes the vertical component of relative vorticity is given by

$$\zeta = \frac{\partial v}{\partial n} + \frac{v}{r},$$

where v is the velocity of flow, r is the radius of curvature of the stream-line, cyclonic curvature being regarded as positive and anticyclonic as negative, and $\partial v/\partial n$ is the horizontal shear along the normal to the stream-line, the positive direction of the normal being taken to the right of the flow.

If curvature $k = 1/r$ is substituted, then the expression for vorticity becomes

$$\zeta = \frac{\partial v}{\partial n} + kv \qquad \ldots (30)$$

and is seen clearly to separate into two parts.

The term $\partial v/\partial n$ arises from the shear of wind along the normal to the stream-line. It is important to keep the sign of the contribution clear. The positive normal is drawn to the right of the flow, standing with one's back to the flow. Thus in a wind system where the wind increases to the right of the flow $\partial v/\partial n$ is positive and contributes to positive vorticity or cyclonic circulation. Conversely, where the wind decreases to the right of the flow the contribution is to negative vorticity or anticyclonic circulation.

The term kv arises from the curvature of the stream-lines. The curvature k is regarded by convention as positive for cyclonic flow, so that cyclonic curvature of the stream-line yields a positive contribution and anticyclonic curvature a negative contribution.

The thermal vorticity term $V'\,\partial\zeta'/\partial s$ means that we have to assess a term

$$V'\frac{\partial}{\partial s}\left(\frac{\partial V'}{\partial n} + k'V'\right)$$

obtained by putting in equation (30) the thermal wind V' and the curvature k' of the stream-line of the thermal wind. Performing the differentiation shows that there are three terms to consider, that is,

$$V'\left\{\frac{\partial}{\partial s}\left(\frac{\partial V'}{\partial n}\right) + k'\frac{\partial V'}{\partial s} + V'\frac{\partial k'}{\partial s}\right\}.$$

The three terms are: (i) the variation in horizontal shear of the thermal wind in the direction of s; (ii) the product of the curvature and the variation of the thermal wind in the direction of s; and (iii) the product of the thermal wind and the change in curvature of the thermal wind in the direction of s, respectively. Each term will be considered separately and we shall regard the curvature of the thickness lines as an approximation to the curvature of the stream-lines of the thermal wind.

(i) The term $V'\dfrac{\partial}{\partial s}\left(\dfrac{\partial V'}{\partial n}\right)$.

For simplicity consider a pure confluence with straight thickness lines, shown in Figure 5.22, about an axis of maximum thermal wind, ST. Then the horizontal shear increases numerically down the thermal wind. By convention $\partial V'/\partial n$ is known as cyclonic shear, positive to the left of ST so that $\dfrac{\partial}{\partial s}\left(\dfrac{\partial V'}{\partial n}\right)$ is positive. Hence the term $V'\dfrac{\partial}{\partial s}\left(\dfrac{\partial V'}{\partial n}\right)$ is positive and so by equation (28) contributes to low-level anticyclonic development –

marked as A in Figure 5.22. Conversely, to the right of ST, $\partial V'/\partial n$ is negative so that $\dfrac{\partial}{\partial s}\left(\dfrac{\partial V'}{\partial n}\right)$ is negative. Hence the term $V'\dfrac{\partial}{\partial s}\left(\dfrac{\partial V'}{\partial n}\right)$ is negative and so contributes to low-level cyclonic development – marked as C in Figure 5.22. By quite similar arguments it is readily seen that the term contributes to development as shown in the pure thermal diffluence illustrated in Figure 5.23.

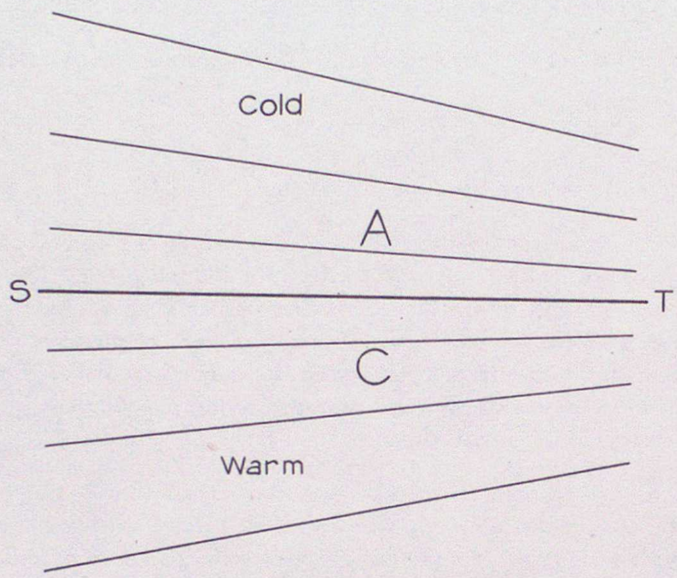

FIGURE 5.22 *Schematic thermal confluence*

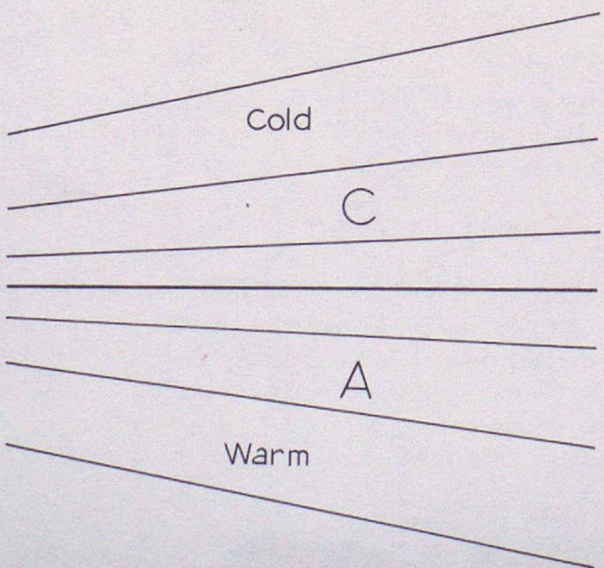

FIGURE 5.23 *Schematic thermal diffluence*

(ii) The term $V'k'\dfrac{\partial V'}{\partial s}$.

This term depends on the curvature and the rate of change of thermal wind along the thermal field. Thus if the thermal wind increases downstream $\partial V'/\partial s$ is positive and, when associated with cyclonic curvature, (that is k'

is positive) $k' \partial V'/\partial s$ is positive and it therefore contributes to low-level anticyclonic development. Conversely for anticyclonic curvature the contribution is to cyclonic development.

If the thermal wind decreases downstream the signs are reversed and the contribution from cyclonic curvature is to cyclonic development and from anticyclonic curvature to anticyclonic development.

(iii) The term $(V')^2 \dfrac{\partial k'}{\partial s}$.

This term depends on the change of curvature downstream. The value of k' is positive for cyclonic curvature and if the curvature becomes more cyclonic then $(V')^2 \partial k'/\partial s$ is positive and contributes to low-level anticyclonic development. If the curvature becomes less cyclonic the term contributes to cyclonic development. Conversely, for increasing anticyclonic curvature the contribution is to cyclonic development and for decreasing anticyclonic curvature to anticyclonic development.

It is convenient to summarize the contributions from the three terms (see Table 5.1). The contributions from each term are indicated by letters C and A for cyclonic and anticyclonic development respectively and each C and A is given a suffix to distinguish from which feature of the thermal pattern the contribution arises:

suffix s refers to a contribution from the change of shear,
suffix v' refers to a contribution from the change of thermal wind,
suffix k' refers to a contribution from the change of curvature.

TABLE 5.1

Contribution from $\dfrac{\partial V'}{\partial n}$ *(indicated by* A_s *or* C_s*)*

Increasing shear	*Decreasing shear*
A_s for cyclonic shear	C_s for cyclonic shear
C_s for anticyclonic shear	A_s for anticyclonic shear

Contribution from $k' \dfrac{\partial V'}{\partial s}$ *(indicated by* $A_{v'}$ *or* $C_{v'}$*)*

Increasing thermal wind	*Decreasing thermal wind*
$A_{v'}$ for cyclonic curvature	$C_{v'}$ for cyclonic curvature
$C_{v'}$ for anticyclonic curvature	$A_{v'}$ for anticyclonic curvature

Contribution from $V' \dfrac{\partial k'}{\partial s}$ *(indicated by* $A_{k'}$ *or* $C_{k'}$*)*

$A_{k'}$ for increasing cyclonic curvature	$C_{k'}$ for increasing anticyclonic curvature
$C_{k'}$ for decreasing cyclonic curvature	$A_{k'}$ for decreasing anticyclonic curvature

5.10.3. *Some thickness patterns and their contribution to development*

It is now possible to assess qualitatively the contribution of the thermal vorticity term to the Sutcliffe development expression for some simple configurations of thicknesses.

5.10.3.1. *The simple sinusoidal pattern with uniformly spaced and parallel thickness lines.* Figure 5.24 shows schematically a simple sinusoidal thickness pattern. For simplicity it will be assumed that AB and EF are the ridge lines, CD the trough line and each is perpendicular to the thermal field at the ridge and trough lines. Since the thickness lines are uniformly spaced and parallel then

$$\frac{\partial V'}{\partial n} = \frac{\partial V'}{\partial s} = 0$$

and the contribution of thermal vorticity to development is contained solely in the term $V' \partial k'/\partial s$.

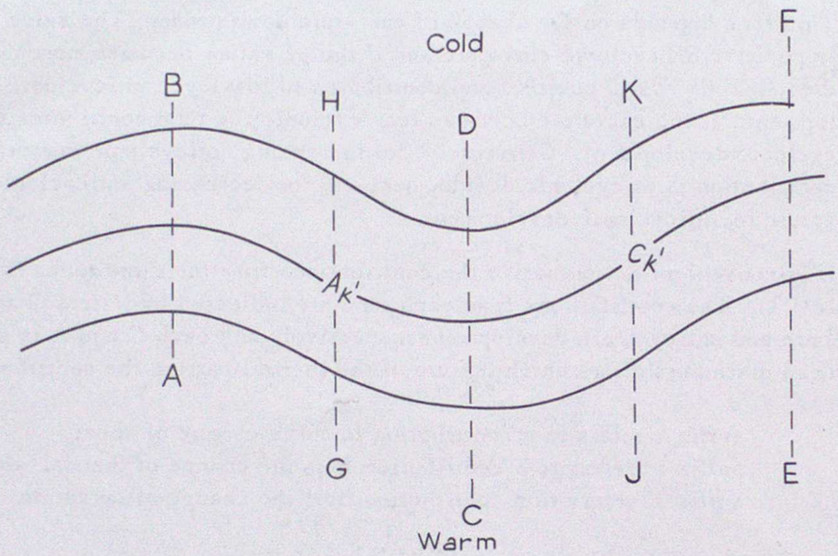

FIGURE 5.24 *Simple sinusoidal thickness pattern*

Along AB curvature k' is anticyclonic and curvature decreases between AB and GH up to the inflexion points lying along GH. Thus from Table 5.1 the contribution is to anticyclonic development. From GH to CD cyclonic curvature increases and again the contribution is to anticyclonic development. Thus from AB to CD (that is, thermal ridge to trough) thermal vorticity leads to anticyclonic development. Further, since $\partial k'/\partial s$ is a maximum (numerically) where $\partial^2 k'/\partial s^2 = 0$ (that is, at the inflexion points) the maximum anticyclogenetic area is centred on the inflexion of the thickness pattern.

Similarly, by considering the pattern from CD to EF, the maximum cyclogenetic area is centred around JK.

It is also readily seen, by considering half-wavelengths from inflexion to inflexion points, that for a simple thermal trough with a uniform thickness pattern thermal vorticity contributes to anticyclonic development in its rear portion and cyclonic development in its forward portion; and for ridges, cyclonic development in the rear and anticyclonic ahead.

In naturally occurring thermal troughs and ridges the curvature often changes more rapidly near the trough and ridge lines than near the inflexion points. This sometimes has the effect of displacing the areas of maximum development towards the trough or ridge line.

5.10.3.2. *A simple thermal jet with a straight central axis.* Figure 5.25 shows schematically such a thermal distribution. Everywhere to the left of PQR the term $\partial V'/\partial n$ is positive and the shear is cyclonic; to the right $\partial V'/\partial n$ is negative and the shear is anticyclonic. In the left-hand quadrant from P to Q the term $\partial V'/\partial n$

is positive and increasing so that the contribution is to anticyclonic development A_s. The curvature k' is cyclonic and increasing in this quadrant also, so that from Table 5.1 there is anticyclonic development $A_{k'}$. The thermal wind also increases and this contributes to anticyclonic development $A_{V'}$. Thus thermal vorticity leads to anticyclonic development in the rear left-hand quadrant.

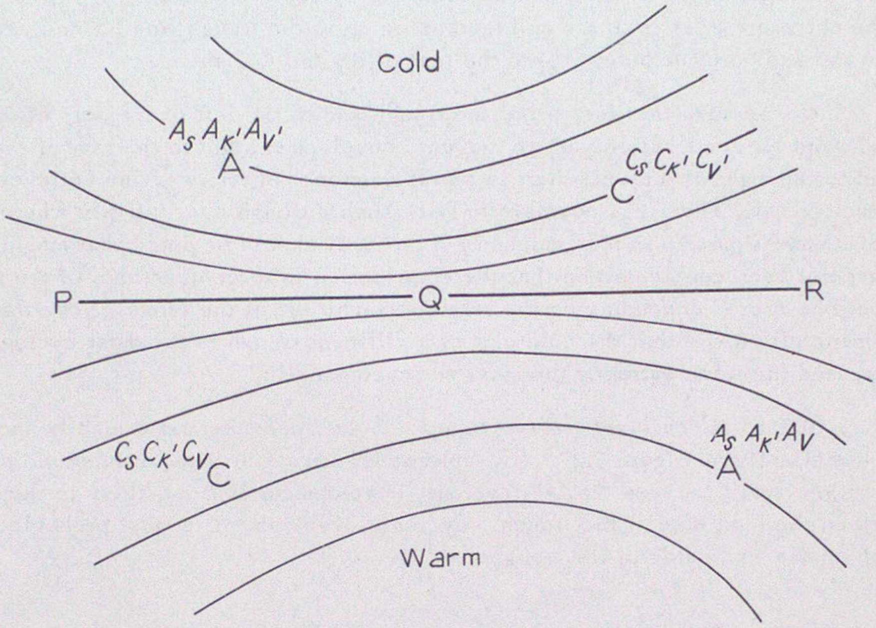

FIGURE 5.25 *Thermal jet*

The application of similar arguments to the other quadrants readily shows that:

The forward right quadrant is also one of anticyclonic development.

The rear right-hand and forward left-hand quadrants are areas prone to cyclonic development.

5.10.3.3. *A diffluent thermal trough.* Figure 5.26 shows a schematic diffluent thermal trough in which PQ is the axis of strongest thermal wind and RS is the axis of the thermal trough. Considering the contribution of each term to thermal

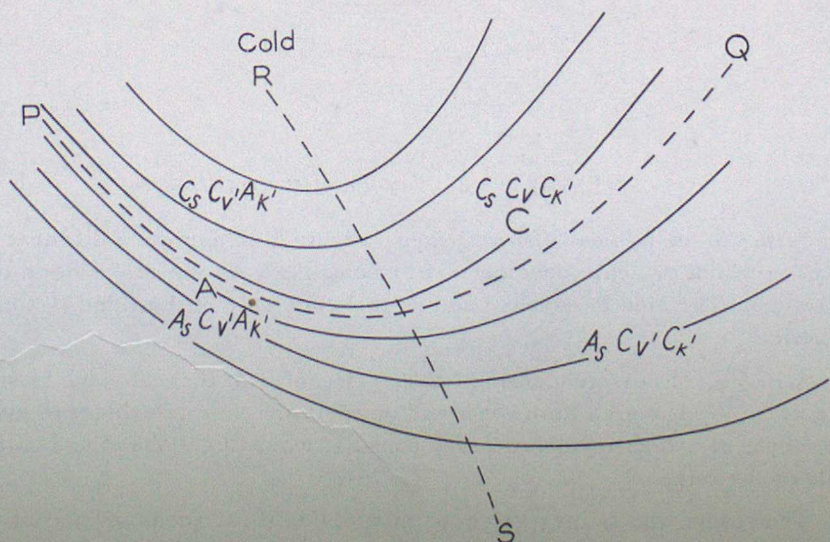

FIGURE 5.26 *Diffluent thermal trough*

vorticity it is readily seen from Table 5.1 and the geometry of Figure 5.25 that $\partial V'/\partial n$ is positive and decreasing with s to the left of PQ and so contributes C_s as shown. To the right of PQ, the term $\partial V'/\partial n$ is negative and decreasing and so contributes to anticyclonic development A_s. The thermal wind decreases generally with increasing s and since curvature is cyclonic contributes $C_{V'}$ everywhere. The curvature k' is cyclonic and increasing up to the trough line RS and decreasing beyond and so contributes $A_{k'}$ to the rear of RS and $C_{k'}$ ahead.

Now it is seen that forward of the trough and to the left of the axis of the thermal wind all contributions are to cyclonic development and to the rear of the trough and to the right of the axis there is a preponderance of terms giving anticyclonic development. Thus it is possible to mark such a trough qualitatively where the development pattern is predominantly A or C. It should be noted that magnitudes have not been considered so that the contribution in three quadrants of the trough could be A or C depending on the relative magnitude of the terms. Nevertheless it is generally found that the cold exit of a diffluent trough is the most cyclogenetic area and the warm entrance the most anticyclogenetic.

5.10.3.4. *A confluent thermal trough.* A confluent thermal trough is shown schematically in Figure 5.27. By applying arguments similar to those in Section 5.10.3.3 it will be seen that anticyclonic development is most likely to the rear and on the cold side of the trough. Cyclonic development is most probable ahead and on the warm side of the trough.

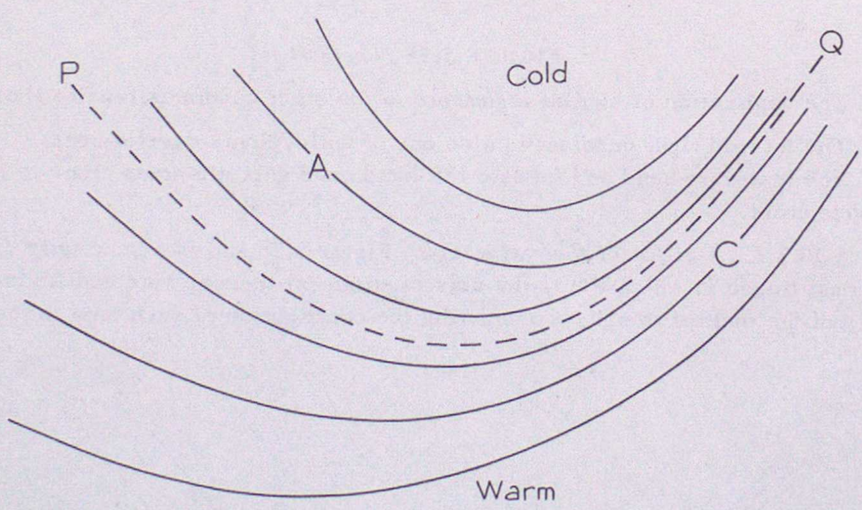

FIGURE 5.27 *Confluent thermal trough*

5.10.3.5. *A diffluent thermal ridge.* Figure 5.28 depicts a diffluent thermal ridge in which cyclonic development is most likely on the cold side to the rear of the ridge. The area in advance and on the warm side of the ridge is anticyclogenetic.

5.10.3.6. *A confluent thermal ridge.* A confluent thermal ridge is shown in Figure 5.29. The area to the rear and on the warm side is subject to cyclonic development and anticyclonic development is most likely ahead and on the cold side of the ridge.

The reader who is inexperienced in applying these ideas of thermal vorticity will find it useful to determine on Figures 5.26 to 5.28 at least the sign of the contribution due to each of the three terms listed in Table 5.1. The arguments are very simple and can be modelled on those used to describe Figure 5.25.

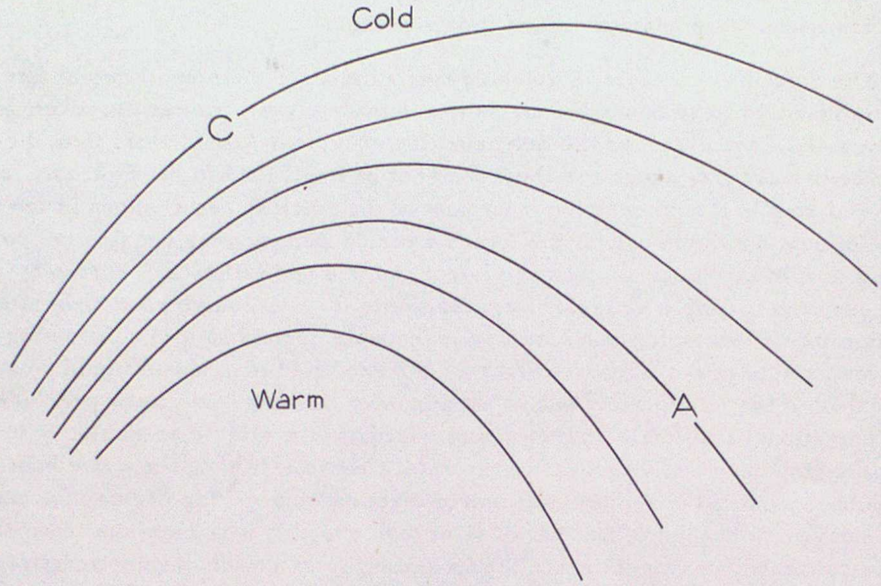

FIGURE 5.28 *Diffluent thermal ridge*

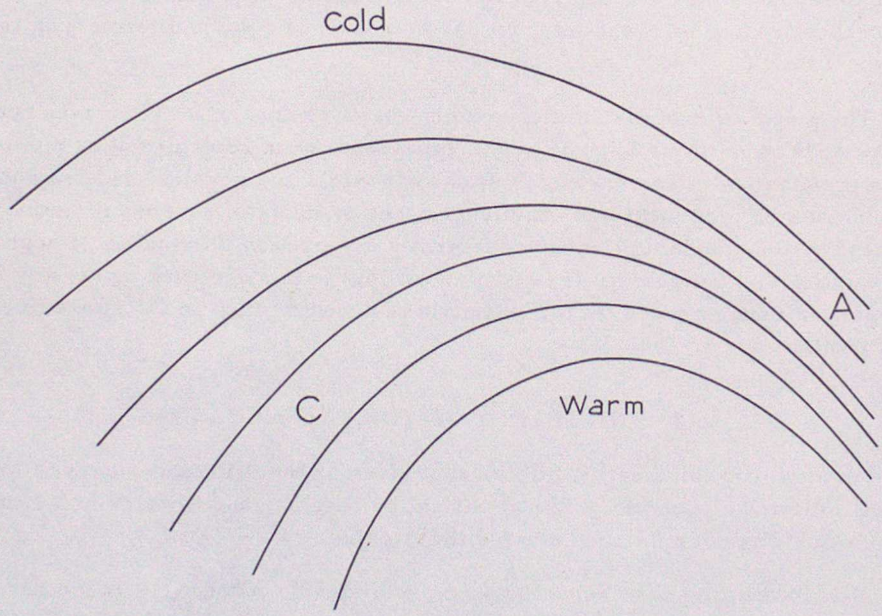

FIGURE 5.29 *Confluent thermal ridge*

Before proceeding further it is useful to summarize the stage reached in the arguments of this chapter. Development has been related to relative divergence which, in turn, is shown to be given with fair approximation by the Sutcliffe development term

$$V' \frac{\partial}{\partial s} \ (l + 2\zeta_0 + \zeta') \, .$$

The latitudinal term $V' \partial l / \partial s$ is normally small and can often be neglected – particularly when the thickness pattern shows a reasonably well marked configuration. The thermal steering term $2V' \partial \zeta_0 / \partial s$ is usually fairly large – particularly with marked cyclones, anticyclones, troughs and ridges and with strong thermal gradients. Thermal vorticity $V' \partial \zeta' / \partial s$ is also important and areas prone to cyclonic (C) or anticyclonic (A) development for a number of simplified thermal configurations have been described in this Section.

The Sutcliffe technique is valuable particularly for the preparation of forecast charts about 24 to 48 hours ahead of the current analysed charts. However, forecasters should realize that the determination of typical A or C areas from the thickness pattern on the latest chart does not of itself lead to the forecast. It is a useful step in the process but movement of the patterns and changes in the development areas throughout the forecast period must also be considered, so that a simple extrapolation from the latest chart is not sufficient. A step-by-step process of preparing a series of forecast charts for successive short time intervals (within which extrapolation might be a reasonable approximation) culminating in the preparation of the forecast charts for the specified time ahead would probably be valuable but, in practice, such a step-by-step process is normally precluded by the operational time-table and the limited manpower available at outstations. (A step-by-step quantitative process over small time intervals of about one hour is possible by using the capacity of modern electronic computing devices for carrying out a great number of computations at high speed.) It is clear that current practical techniques must enable the forecaster to visualize developments over the forecast period, assess the values of the various development processes and so proceed qualitatively to a judgement of the development and movement at the time of the forecast. The forecast is usually expressed quantitatively but the processes leading up to the forecast can be assessed only qualitatively on the forecast bench.

The preparation of prebaratic/prontour charts is thus an intricate task but, for periods up to about 24 to 36 hours, fair success can be achieved as routine by a combination of careful analysis, use of models and physical understanding combined with judgement and experience. The standard of success is demonstrated by the standard of accuracy currently achieved in the routine 24-hour prebaratic/prontour charts. It is quite clear that to produce such forecasts working rules are needed for the movement and modification to thickness lines and patterns.

5.11. THE THEORY OF THICKNESS CHANGES

The treatment in this section follows that given by Sutcliffe and Forsdyke[14] which itself followed closely an earlier treatment by Sutcliffe and Godart[15] in a memorandum which was not published outside the Air Ministry.

If h' is the thickness between two pressure levels p and p_0, R is the gas constant, g is the acceleration due to gravity, x and y are horizontal Cartesian co-ordinates and p is the vertical co-ordinate, then

$$h' = \int_p^{p_0} \frac{RT}{gp}\, dp = \frac{R}{g}\int_p^{p_0} T\, d(\log p) .$$

Thus $$\frac{\partial h'}{\partial t} = \frac{R}{g}\int_p^{p_0} \frac{\partial T}{\partial t}\, d\,(\log p) . \qquad \ldots (31)$$

Strictly T is the virtual temperature which is usually only slightly different from the actual temperature. In practical forecasting the difference is usually of small account and T will be taken as the actual temperature.

The total variation in temperature following the moving particle is

$$\frac{dT}{dt} = \frac{\partial T}{\partial t} + \frac{dx}{dt}\frac{\partial T}{\partial x} + \frac{dy}{dt}\frac{\partial T}{\partial y} + \frac{dp}{dt}\frac{\partial T}{\partial p} ,$$

that is, $$\frac{\partial T}{\partial t} = \frac{dT}{dt} - u\frac{\partial T}{\partial x} - v\frac{\partial T}{\partial y} - \frac{dp}{dt}\frac{\partial T}{\partial p} . \qquad \ldots (32)$$

Now Brunt[16] shows that $$\frac{dT}{dt} = \frac{1}{C_p}\frac{dq}{dt} + \frac{\gamma}{g\rho}\frac{dp}{dt} , \qquad \ldots (33)$$

where q is the amount of heat supplied per unit mass of gas, C_p is the specific heat at constant pressure, γ is the dry-adiabatic lapse rate, ρ is the density and g the acceleration due to gravity.

Then substituting for dT/dt from equation (33) in (32) and subsequently for $\partial T/\partial t$ in (31) and rearranging terms we have:

$$\frac{\partial h'}{\partial t} = \frac{R}{g}\int_p^{p_0} \left\{ -\left(u\frac{\partial T}{\partial x} + v\frac{\partial T}{\partial y}\right) + \left(\frac{\gamma}{g\rho} - \frac{\partial T}{\partial p}\right)\frac{dp}{dt} + \frac{1}{C_p}\frac{dq}{dt}\right\} d\,(\log p) . \qquad \ldots (34)$$

If the air is saturated the case can be dealt with by substituting the wet-adiabatic lapse rate (γ_s) for γ.

The long expression under the integral in equation (34) has been split into three components which can be regarded as advective (A), dynamical (D) and non-adiabatic (N) processes.

Symbolically, equation (34) becomes $$\frac{\partial h'}{\partial t} = A + D + N .$$

5.11.1. *The advective term*

The advective term is $$A = -\frac{R}{g}\int_p^{p_0}\left(u\frac{\partial T}{\partial x} + v\frac{\partial T}{\partial y}\right) d\,(\log p)$$

which may be written $$-\left(u_m\frac{\partial}{\partial x} + v_m\frac{\partial}{\partial y}\right) h'$$

where u_m and v_m are some mean values of the component velocities over the height range between p and p_0.

If p_0 and p are regarded as referring to the base and top of the troposphere, it is reasonable to suppose that component velocities at 500 millibars will approximate to a suitable mean. The wind at 500 millibars may be represented by the vectorial equation:

$$\mathbf{V}_{500} = \mathbf{V}_{g(0)} + \mathbf{V}'_g + \mathbf{V}_a ,$$

where $\mathbf{V}_{g(0)}$ is the geostrophic wind at 1000 millibars, $\mathbf{V}'_g$ is the geostrophic thermal wind between 1000 and 500 millibars and $\mathbf{V}_a$ is the ageostrophic wind. The advective term may then be written vectorially:

$$A = -\mathbf{V}_{g(0)} \cdot \nabla h' - \mathbf{V}'_g \cdot \nabla h' - \mathbf{V}_a \cdot \nabla h' ,$$

that is, as the sum of three scalar products. The term $(-\mathbf{V}_{g(0)} \cdot \nabla h')$ indicates that the thickness lines are advected by the 1000-millibar geostrophic wind.

The second term $(-V'_g \cdot \nabla h')$ is the contribution due to the thermal field. One of the assumptions in deriving the Sutcliffe development expression was that the direction of the vertical shear of the thermal wind did not vary with height. Under such circumstances V'_g the thermal wind, is perpendicular to $\nabla h'$, that is, their scalar product is zero. There is thus some justification for neglecting this term where the thermal wind direction is reasonably constant with height but, if there is a marked change in direction, thermal advection may be important and some qualitative allowance can be made.

The third term involves the product of the ageostrophic motion and this is usually small compared with the first term, that is, geostrophic advection. Existing techniques of analysis and observations do not permit routine assessments of this term and so it is usually ignored but it may be important at times.

It is seen that the first approximation to the advection of thickness is given by the 1000-millibar geostrophic advection.

5.11.2. *The dynamical term*

The dynamical term is $D = \dfrac{R}{g}\displaystyle\int_p^{p_0}\left(\frac{\gamma}{g\rho} - \frac{\partial T}{\partial p}\right)\frac{dp}{dt}\, d(\log p)$.

Except over very limited depths (usually near the surface) the lapse rate does not exceed the dry adiabatic so that, for adiabatic compression or expansion:

$$\left(\frac{\gamma}{g\rho} - \frac{\partial T}{\partial p}\right) \text{ is positive}$$

and so the contribution takes the sign of dp/dt. If dp/dt is positive – which corresponds to subsidence – then clearly the thickness increases. With ascent dp/dt is negative and we must distinguish between unsaturated and saturated ascent. For unsaturated ascent with a lapse less than the dry adiabatic, ascent produces a decrease in thickness. For saturated ascent with a lapse less than the wet adiabatic:

$$\left(\frac{\gamma}{g\rho} - \frac{\partial T}{\partial p}\right) \text{ is positive}$$

and so ascent contributes to decreasing thicknesses. If the air is conditionally unstable, that is, the lapse exceeds the saturated adiabatic, then:

$$\left(\frac{\gamma}{g\rho} - \frac{\partial T}{\partial p}\right) \text{ becomes negative}$$

and ascent contributes to an increase of thickness. This can usually be disregarded on the broad synoptic scale since, to be effective, it requires general ascent over an extensive area and it is clear that any such general ascent will soon degenerate into convection cells with limited regions of active ascent and other areas of descending motion. It is thus unlikely that ascent of unstable saturated air will contribute materially to an increase of thickness over substantial areas. Accordingly over any region of general ascent the thickness up to 500 millibars is likely to be reduced by the ascent, although the cooling and reduction of thickness may be slight in rain areas where the lapse rate is near the saturated adiabatic.

5.11.3. *The non-adiabatic term*

The non-adiabatic term is $N = \dfrac{R}{g}\displaystyle\int_p^{p_0}\frac{1}{C_p}\frac{dq}{dt}\, d(\log p)$.

Some Dynamical Aspects of Atmospheric Systems

At the commencement of this chapter, reference was made to the part played by the day-to-day atmospheric motions in the redistribution of the heat energy received by the earth and its atmosphere from the sun. This redistribution ultimately results in a balance between the radiation received from and emitted to space. Consequently it is not justifiable to neglect the non-adiabatic terms completely. Nevertheless for the forecasting problem for one or two days ahead numerical allowances based on theoretical considerations are almost impossible to make on the forecast bench. For forecasts a few hours ahead it is probably best to ignore non-adiabatic changes, but for periods from about 24 hours the non-adiabatic term can become important and some allowances described in Section 5.12 can be made.

Some idea of the magnitude of the combined effects of subsidence (or ascent), heating or cooling by the underlying surface and radiation effects on some air masses as they move from their source regions towards the British Isles can be obtained from Chapter 14, Figures 15 to 17, and Tables 14 and 15.

5.12. THE PRACTICAL APPROACH TO THICKNESS CHANGES

It is unfortunately true that numerical estimates of the dynamical and non-adiabatic terms in equation (34) cannot currently be made during practical forecasting, since current techniques of analysis do not permit the evaluation of these terms nor have empirical rules so far been propounded. The estimation of thickness changes remains subjective.

5.12.1. *Geostrophic advection*

The best technique is to start with simple advection by the 1000-millibar geostrophic wind field. For periods of a few hours (about six) simple extrapolation will give a reasonable estimate, but for longer periods some account must be taken of the expected changes in the 1000-millibar winds. Assessments based on geostrophic advection nearly always overestimate the movement of thickness lines. The known exceptions are the advection of cold air from sea to a colder land mass in winter and the advection of warm air which is subsiding strongly. Notwithstanding the exceptions, the simple advection should always be made as a starting point since this is the only calculation which can be done in all synoptic situations. Another reason is that, because the movement is usually an overestimate, this process will tend to throw into high relief the possible formation of thermal troughs and ridges and those areas of the chart where thermal contrasts are becoming more intense (that is, areas prone to frontogenesis) or less intense (frontolytic regions).

The adjustments to these thickness changes are then made by judgement and experience. The following points give some guidance.

5.12.2. *Thermal advection*

It was explained in Section 5.11.1 that where the direction of the vertical shear of the thermal wind did not vary with height, thermal advection would be zero. In practice the thermal wind direction is often fairly constant over substantial layers in the troposphere and, in such cases, it is probably best to ignore the effect of thermal advection. Where the variation of thermal wind direction with height is substantial some allowance may be justified. An assessment of thermal advection may be obtained from the hodograph of the wind.

5.12.3. *Ageostrophic advection*

So little is known on a day-to-day basis about the magnitudes of ageostrophic winds that this term must nearly always be neglected.

5.12.4. *The dynamical term*

Numerical estimates cannot yet be made in practical forecasting and it is necessary to make a judgement. Subsidence contributes to increasing thickness and ascent generally to decreasing thickness. In this context we are only concerned with prolonged and reasonably steady vertical motion over substantial areas.

A rough estimate of the probable magnitude of the effect of subsidence may be made from work by Petterssen, Sheppard, Priestley and Johannessen.[17] Regarding the vertical extent through which subsidence occurs they found that there was a distinct tendency for the lower limit of warming due to subsidence to occur in the layer between 900 and 800 millibars. The upper limit of subsidence showed rather more variation but only in a minority of cases did the upper limit occur below the 500-millibar level. In the majority of cases the upper limit was at higher levels and Petterssen *et alii*[17] concluded that in the majority of cases subsidence affected the major part of the troposphere above the 900–800-millibar level.

The amount and rate of subsidence showed wide variations but they were able to deduce the following average values for changes in thickness for the 750–500-millibar and 500–300-millibar layers:

750–500-millibar layer: 6 feet (1·8 metres) per 6 hours
500–300-millibar layer: 17 feet (5·2 metres) per 6 hours.

If it is assumed that subsidence extends down to about 900 millibars it would be reasonable to assume a change of about 40 feet (12 metres) for the 1000–500-millibar and 70 feet (21 metres) for the 500–300-millibar thicknesses for 24 hours.

Well marked cases of subsidence have vertical velocities of about 3 centimetres per second (3 centimetres per second is equivalent to about 5 millibars per hour at 300 millibars and about 7 millibars per hour at 500 millibars) over substantial depths in the troposphere. If these vertical velocities are continued throughout 24 hours there would be an increase of thickness (1000–500-millibar) of the order of 300 feet (90 metres). This increase is several times greater than the average which occurs, so that the correct value to assign to a forecast change of thickness on any one occasion is a matter for personal judgement.

Typical values of the vertical velocity for ascent in frontal regions or other active rain areas would be around 10 centimetres per second (10 centimetres per second is equivalent to about 17 millibars per hour at 300 millibars and to about 23 millibars per hour at 500 millibars). Vertical velocities tend to be greatest where the lapse rate is near the adiabatic and are less when the air is very stable. Large-scale ascent in dry stably stratified regions is probably of the order of 3 to 5 centimetres per second, but the effect on the thickness pattern may be as great as more rapid ascent under less stable conditions. Bushby[18] calculated decreases of 1000–500-millibar thickness of 40 feet (12 metres) per hour due to vertical ascent. There seems little doubt that vertical velocities exert a vital modifying effect on the change of thickness. Techniques available on the forecast bench do not provide quantitative estimates and the best that can be done is for the forecaster to infer the areas of vertical ascent and make some reduction in thicknesses advected to that area.

5.12.5. *Non-adiabatic effects*

When warm air streams over a cooler surface the lower layers of the air are cooled and a stable lapse rate is established in the lower layer. This stable lapse diminishes turbulence and effectively restricts the transport of heat from the underlying warm surface to lowest layers – the cooling does not usually extend above 850 millibars. (This is confirmed by Belasco[19] for air masses approaching the British Isles – see also Chapter 14, Figures 15 and 16.) The effect of cooling on the 1000–500-millibar thickness is normally restricted to a magnitude of a few tens of feet (perhaps 10 to 20 metres) per 24 hours and is probably best neglected for such periods.

The movement of cold air over a warm surface is much more important. Vigorous convection transports the heat supplied by the surface through the convective layer and the modification to thicknesses is considerable. Craddock[20] has examined the changes in thickness when a broad cold airstream moved from the Iceland–Jan Mayen region to the British Isles. He was able to show that the rate of transfer of heat was closely associated with the difference between the sea surface temperature and the surface temperature of the air mass. He suggests the following rule for practical use:

If the boundary lapse is n°F. and the convective limit not above 700 millibars then the thickness of the layer from 1000 to 700 millibars will increase by n feet per hour.

The boundary lapse is obtained by subtracting the mean of the actual initial and estimated final air surface temperature from the mean sea surface temperature along the track. A rule for estimating the surface temperature of cold air after a sea track is given in Chapter 14. If the convective limit is above 700 millibars the heating extends above the 700-millibar level and the increase in thickness should be divided between the layers concerned. Where only the 1000–500-millibar thickness is required, the values given by this rule should be increased by an arbitrary ten per cent.

Current techniques do not permit of quantitative allowances for radiative effects. For 24-hour forecasts diurnal effects are nil and for shorter-period forecasting any attempt at refinement to take them into account is almost valueless owing to the greater uncertainties in allowing for the dynamical effects and warming or cooling by surface contact.

Work by Houghton and Brewer[21] indicates that the cooling of a cloud-free atmosphere by radiation is about 1° to 2°C. per 24 hours. This corresponds to a decrease of the 1000–500-millibar thickness of about 75 to 150 feet (23 to 46 metres) per 24 hours. On one occasion in July 1954 outgoing radiation from 8/8 stratocumulus from 2000 to 4000 feet was measured and if the heat had been lost by the cloud alone it would have cooled by 9°C. in a day. Such large cooling is not observed because heat is supplied from adjacent layers of the atmosphere and from the ground, but this is an indication of the strong cooling effect of outgoing radiation.

In the absence of any more precise rules it would seem that the best average value for the radiational cooling effect is about 100 feet (30 metres) per 24 hours for the 1000–500-millibar thickness. This loss is roughly made good by incoming radiation in summer, but represents a real decrease in thickness in winter when the incoming radiation in our latitudes is much smaller.

5.12.6. *The final adjustment*

It is quite clear from the preceding sub-sections that the practical estimation of thickness changes is highly subjective. In spite of the complexity of the problem, forecasters can acquire the ability to make reasonably satisfactory estimates on most occasions. Practical experience of the way in which thickness patterns do change often provides a valuable guide and useful background knowledge against which to assess the probable changes from the current charts. Forecasters are recommended to make determined and sustained efforts to acquire such knowledge in the course of their day-to-day work with thickness charts.

Care should be taken that seasonal extreme positions of thickness lines are not unwittingly exceeded and, to this end, forecasters should find the charts in *Meteorological Report No. 13*[22] and in Chapter 12, Section 12.8 valuable for reference.

5.13. CHARACTERISTICS OF SOME COMMON THICKNESS PATTERNS

Sutcliffe and Forsdyke[14] have described some selected thickness patterns and their characteristic features, and the following is an extract from that paper.

5.13.1. "*The cold thermal trough* [Figure 30*(a)*]

The cold trough is a common feature. It is associated with upper divergence and surface convergence (cyclogenesis marked C in the diagrams) ahead of the trough and upper convergence with surface divergence (anticyclogenesis marked A in the diagrams) behind. Apart from the tendency for new features to develop in accord with the rules, travelling pressure features tend to intensify or decline as would be inferred. That is, a depression travelling through the pattern (by thermal steering) will run readily across the trough to intensify at C while a travelling anticyclone or ridge will not readily pass the trough line and is liable to intensify at A. The mutual interaction of pre-existing cold trough and travelling pressure perturbation is of course important. An anticyclone at A and/or a cyclone at C produce circulations which by advection maintain or accentuate the thermal trough and the situation has a self-maintaining or self-aggravating character. Out-of-phase associations, by contrast, are quickly resolved and cannot long persist.

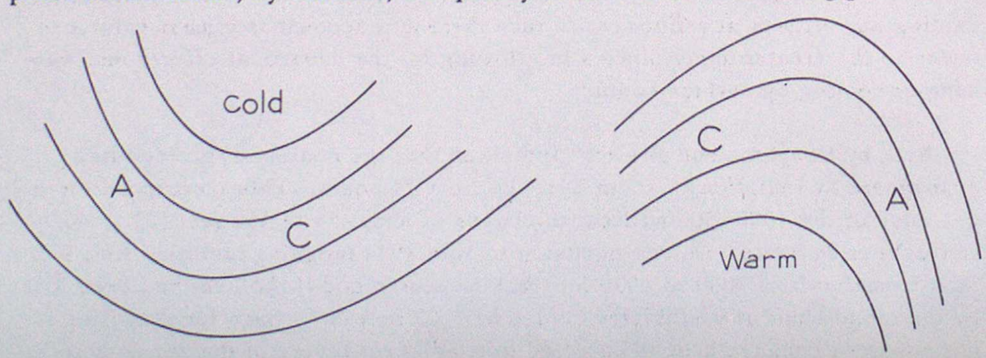

FIGURE 30*(a)* *The cold thermal trough;* *(b)* *The warm thermal ridge*

Cyclonic development, C, occurs forward of the thermal trough, behind the thermal ridge; anticyclonic development, A, on the opposite sides.

5.13.2. "*The warm thermal ridge* [Figure 30*(b)*]

As the complement of the trough pattern, the development features may be inferred without further discussion. Probably the cyclogenetic post-ridge situation is less well known than the pre-trough situation but it is important. The pre-ridge anticyclogenesis corresponds with the building and maintenance of the warm anticyclone whereas the post-trough A of Figure 30*(a)* typifies the subsiding cold air mass.

5.13.3. "*The sinusoidal thermal pattern* [Figure 5.31]

The sinusoidal pattern is essentially a combination of trough and ridge. It is the pattern of the classical warm-sector depression and cold anticyclone and the C and A regions are immediately inferred from the above. Thermal steering is usually dominant and the situation travels in a wave-like manner.

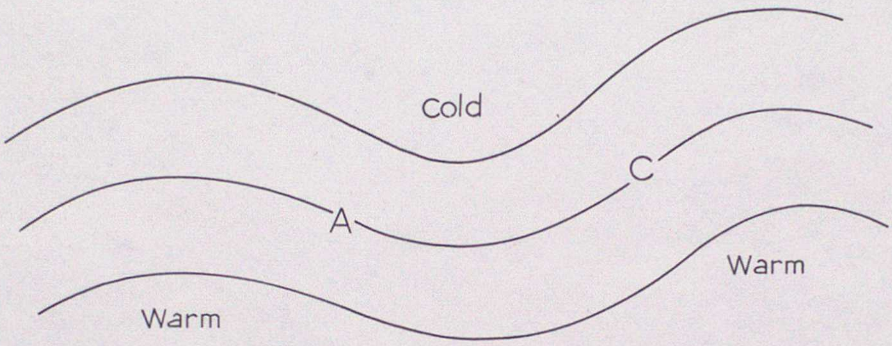

FIGURE 5.31 *The sinusoidal thermal pattern*

Cyclonic development is centred at the pre-trough inflexion, anticyclonic at the pre-ridge inflexion. With small amplitude wave-form, thermal steering is dominant and the situation travels in a wave-like manner.

5.13.4. "*The cyclonic thermal involution* [Figure 5.32*(a)*]

The cyclonic thermal involution is an exaggerated form of the sinusoidal and develops therefrom in the earlier stages of cyclonic occlusion. The reversed thermal gradient over the cyclonic region is, however, not in harmony with wave-like thermal steering and the situation is liable to evolve further with little movement.

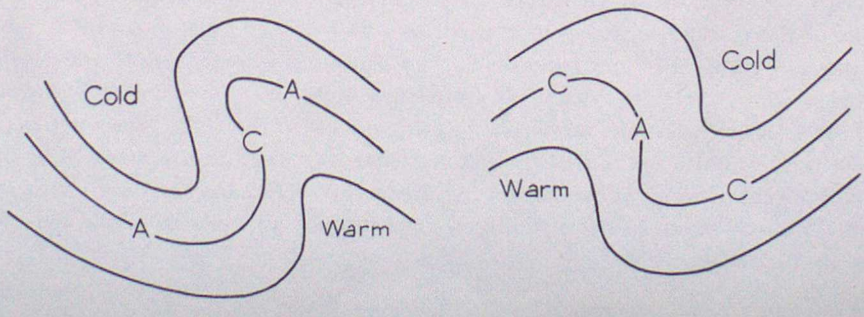

FIGURE 5.32*(a)* *The cyclonic involution;* *(b)* *The anticyclonic involution*

These patterns are distortions of the sinusoidal perturbations usually produced by depressions or anticyclones in the appropriate development regions. They are self-developing.

5.13.5. "*The anticyclonic thermal involution* [Figure 5.32*(b)*]

This complementary sinusoidal involution is similarly the pattern of the well-developed and slow moving anticyclonic cell.

5.13.6. "*The diffluent thermal jet* [Figure 5.33*(a)*]

Thermal diffluence and confluence are of necessity associated with more or less well marked regions of concentrated gradient and it is convenient to use the term "jet" without implying any specially strong gradient. In the region of strong gradient the vorticity (due to shear) is cyclonic on the cold side, anticyclonic on the warm side and, as with the opening gradient the vorticity falls off, the anticyclonic A and cyclonic C regions are tolerably easily picked out. Again it is remarked that pressure systems travelling as they so often do in the strong thermal are so affected that cyclones swing out of the jet to the left, anticyclones to the right, and with little shear to carry them out of the region they may then slow down markedly.

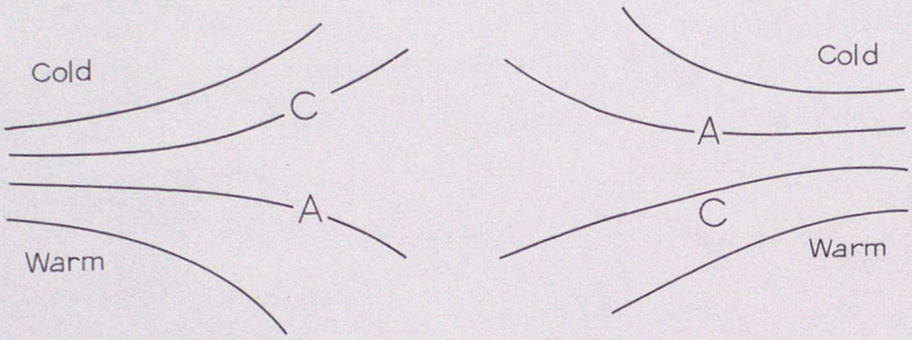

FIGURE 5.33*(a) The diffluent thermal jet;* *(b) The confluent thermal jet*

Cyclonic development is a feature of the left exit and right entrance of the thermal jet, anticyclonic development on the opposite sides.

5.13.7. "*The confluent thermal jet* [Figure 5.33*(b)*]

The A and C regions are shown in the diagrams to the left and right of the entrance to the jet. Travelling pressure features are however highly liable to break away from the jet entrance and run through the strong gradient to be replaced by new developments.

5.13.8. "*The diffluent thermal ridge* [Figure 5.34*(a)*]

The combinations of curvature and shear variations are numerous but the four cases of thermal ridge and trough situations with either confluence or diffluence are often recognizable and important. The situation is represented ideally in Figure 5.34*(a)* where the essential points are that the pre-ridge anticyclogenesis is thrown to the right, the post-ridge cyclogenesis to the left. Thus anticyclones do not tend to build up across the upper stream but keep to the warm side and the surface circulation so set up tends to extend the diffluence forward. With weak thermals ahead there is little tendency for pressure systems to break and run through the pattern.

5.13.9. "*The confluent thermal ridge* [Figure 5.34*(b)*]

Here the pre-ridge anticyclogenesis is to the cold side with the post-ridge cyclogenesis to the warm side. The surface circulation so set up tends to prevent the forward movement of the thermal ridge and even to cause it to become retrograde. The strong thermal ahead is however favourable for pressure features to break away and run through the thermal pattern rapidly. This is a notoriously difficult pattern to deal with in forecasting. Anticyclogenesis to the north and cyclogenesis to the south are symptoms of "blocking" in the westerlies, while the break-away features through the strong gradient are often critical points in short-period forecasting. The thermal field may be associated with break-away secondary depressions on warm fronts and warm occlusions. [For further consideration of these aspects see Section 5.14.]

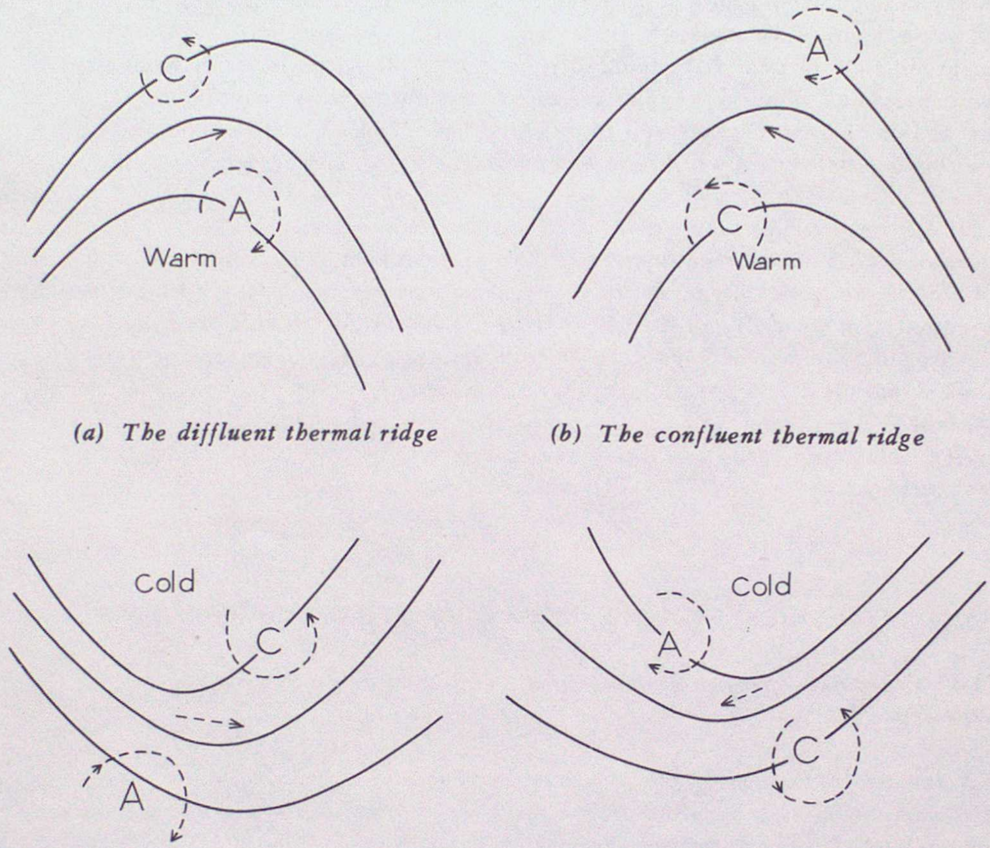

(a) The diffluent thermal ridge *(b) The confluent thermal ridge*

(c) The diffluent thermal trough *(d) The confluent thermal trough*

FIGURE 5.34 *Combinations of thermal ridge and trough with diffluence and confluence*
See text for descriptive comment

5.13.10. "*The diffluent thermal trough* [Figure 5.34(*c*)]

The combination of thermal diffluence with the trough is probably the most certain indication of cyclogenesis on the cold side, at C in the figure. Anticyclonic development is most likely behind the trough on the warm side. The advection set up by such pressure features tends to carry the cold trough forwards but, with light thermals ahead, the pressure systems do not readily break away from the thermal feature and the depression may deepen greatly with slow movement. It is to be noted that while the situation often evolves to a slow-moving cold occluded depression this is to the cold side of the main thermal gradient. Neither blocking of the westerlies nor a large cold outbreak into low latitudes readily evolves from this situation.

5.13.11. "*The confluent thermal trough* [Figure 5.34(*d*)]

With the strong thermal gradient ahead of the thermal trough cyclonic development is favoured on the warm side ahead of the trough with anticyclonic development to the cold side. The blocking tendency due to surface easterlies is important and the thermal trough moves slowly or becomes retrograde. Breakaway depressions running in the strong thermals from the C-region are common but the situation is, like 5.13.9 above, difficult to deal with. Cold air is liable to break through behind the cyclonic region into low latitudes and a cold cut-off depression south of the main westerlies may result. The anticyclonic development in the cold air near and behind the confluent cold trough is liable to be of much importance. There is regularly a dilemma in forecasting, whether a cold ridge will or will not develop well into the cold air behind a cold trough, and the difference between the diffluent and confluent trough can be decisive.

"If a thermal trough is markedly confluent cyclonic activity is most pronounced on the warm side forward of the trough line and anticyclonic on the cold side to the rear. The tendency for cyclonic activity, which is so frequently associated with the diffluent thermal trough, to pass to the warm side of the confluent trough so permitting anticyclonic development to the colder side, usually to higher latitudes, is a possible explanation of certain cases of unpredicted ridge building well into the cold air even across the cold trough. As in other complex cases confluence and diffluence effects may be overlooked in the trough · ridge patterns."

5.14. SOME THICKNESS PATTERNS ASSOCIATED WITH DEPRESSIONS

5.14.1. *Classical warm-sector depression which develops into a major depression*

A descriptive account of the idealized life cycle of a classical open warm-sector depression as it develops from a short-wave synoptic feature into a long-wave cyclone of major dimensions (diameter about 1000–1500 nautical miles or so) and the associated changes in thickness patterns should prove useful particularly for the inexperienced forecaster.

Figures 5.35 to 5.39 show the idealized surface fronts, contours of the 1000 and 500-millibar surfaces and the 1000–500-millibar thickness patterns of a wave depression during its development to a major depression. For simplicity the development is shown as taking place on a purely zonal flow pattern. A typical period for such a sequence would be three to five days. Figure 5.35 shows the initial conditions with a stationary front lying parallel to the isobars, contours and thickness pattern. Most of the thickness gradient is concentrated just to the north of the front. Figure 5.36 shows the early stages of the development of a typical wave depression and it is seen that the thickness and 500-millibar contour show only a slight sinuosity. The sinusoidal thickness pattern favours cyclonic development between the thermal trough and ridge and anticyclonic development to the rear. Advection and continued development favours the continued distortion of the thickness pattern and a more advanced stage of development is shown in Figure 5.37. There are closed contours on the 1000-millibar chart and the fronts have now acquired the typical curvature due to the developing pressure gradients across them. The thickness pattern is more noticeably deformed. A tongue of warm air is being advected northwards ahead of the depression and to its rear cooler air is moving southwards. The thickness pattern is being modified and takes a form mainly similar to the surface fronts but of a somewhat more diffuse and smooth shape. The 500-millibar contour shows a slight trough lying to the rear of the 1000-millibar centre and a noticeable diminution of gradient to the north and west of that centre. Ahead of the depression there is a slight but noticeable ridge at 500 millibars.

Figure 5.38 shows the depression very well developed with several closed contours at the 1000-millibar level. The thickness lines have been further deformed but still resemble the frontal pattern and the pattern is now clearly wave-like with a trough to the south-west and a ridge to the east or south-east of the 1000-millibar centre. The tightest thickness gradient is often just to the north of the cold front. At the 500-millibar level there is a distinct trough whose axis is situated to the rear of the surface centre. A ridge is also developing ahead of the centre.

Figure 5.39 shows the latter stages of the depression when the movement has slowed down and the process of occlusion is well advanced. The thickness pattern shows a very well marked thermal trough and ridge, both of considerable amplitude, and the 500-millibar contour shows similar features.

It is seen that during the development of this major depression both the thermal and wind fields have been considerably modified and deformed from those depicted in Figure 5.35. The depression is now associated with its own circulation and can be regarded as a feature of the long-wave pattern.

It is instructive to examine the changes of phase between the three families of isopleths in Figures 5.36 to 5.39. In the early stages (Figures 5.36 and 5.37) the thermal ridge is associated with the 1000- and 500-millibar troughs. As development proceeds (Figures 5.38 and 5.39) it is seen that the phase relationships change and in the final stages the thermal trough is associated with the 1000- and 500-millibar troughs. The thermal ridge has moved ahead and is linked with the 1000- and 500-millibar ridges ahead of the depression. At the beginning the depression was a short-wave mobile feature and at the end it was a slow-moving system forming part of a long-wave pattern. The change in phase relationships seen during this development typifies the difference in thermal patterns between long and short waves. In the long-wave pattern, ridges in the upper contours are closely associated with (warm) ridges in the thermal pattern – and troughs with (cold) troughs. For the short-wave, mobile, transient systems, ridges in the upper contours are more closely associated with thermal (cold) troughs and troughs in the upper contours with thermal (warm) ridges.

In some cases the cold trough to the rear of the major depression is further developed and distorted and a cold pool with closed thickness lines appears in the trough. Cold pools were described briefly in Section 5.3.4. They are more fully discussed in Chapter 12, Section 12.5.3.

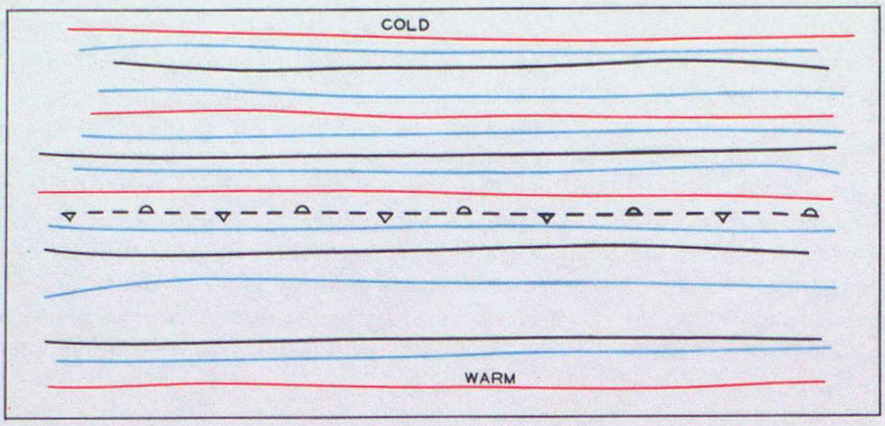

FIGURE 5.35

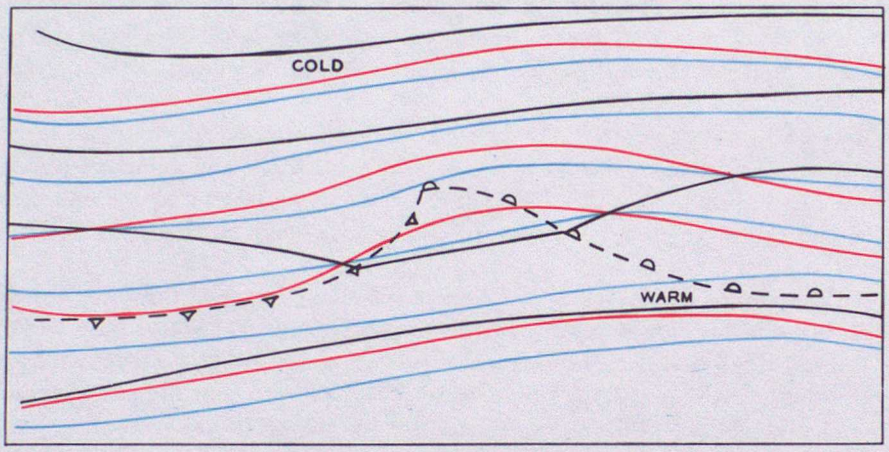

FIGURE 5.36

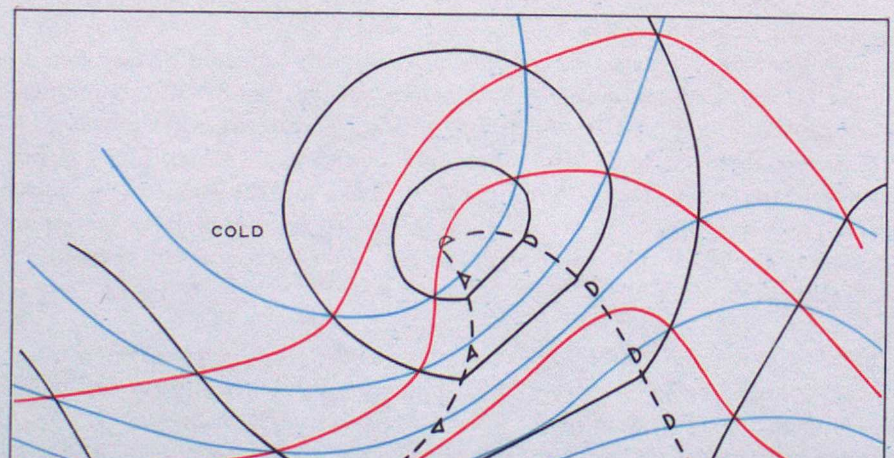

FIGURE 5.37

Development of a warm-sector depression into a major depression

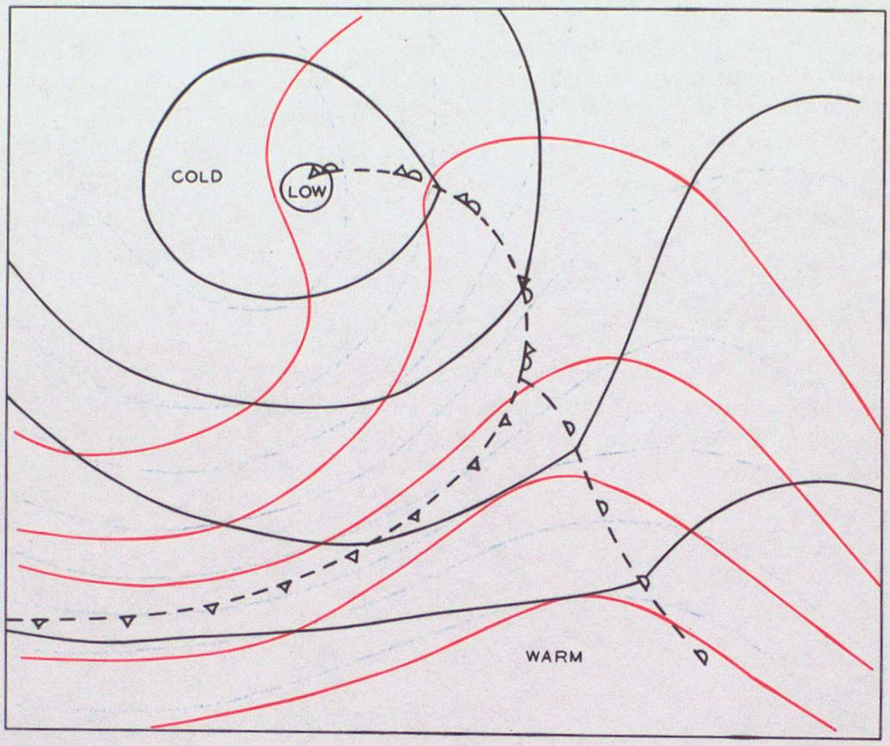

FIGURE 5.38

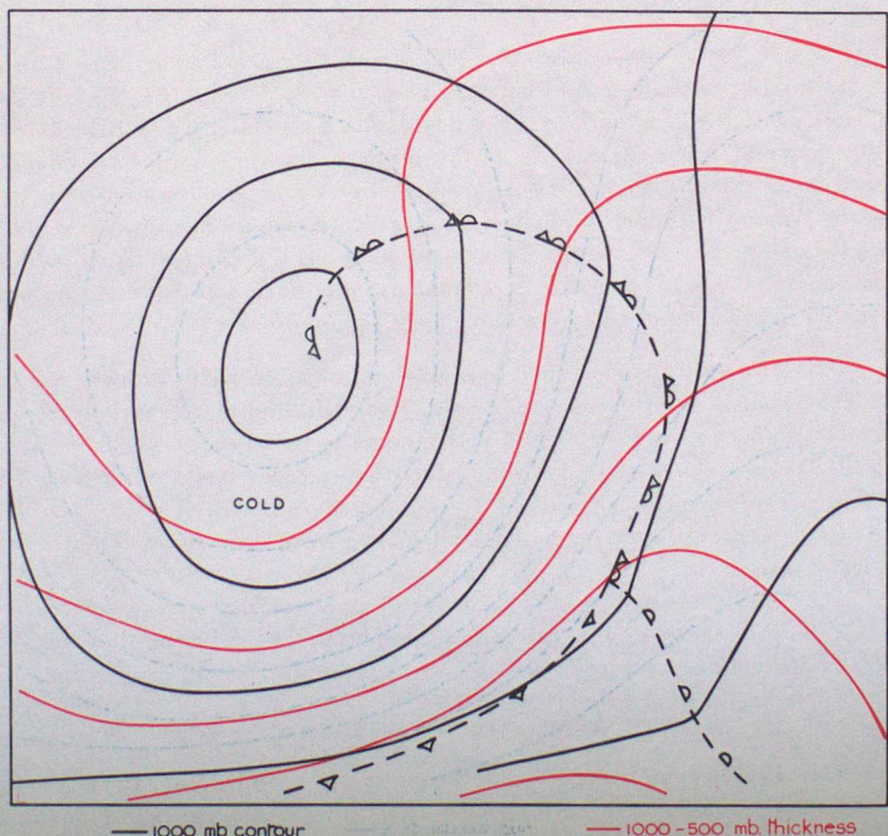

FIGURE 5.39

Development of a warm-sector depression into a major depression

5.14.2. *Secondary depressions*

5.14.2.1. *Waves on warm fronts.* Sawyer[23] has examined these waves. These are rather unusual formations but, when they do form, they have characteristic isobaric and thickness patterns as shown in Figure 5.40. Their behaviour is described in Section 5.14.2.3. below.

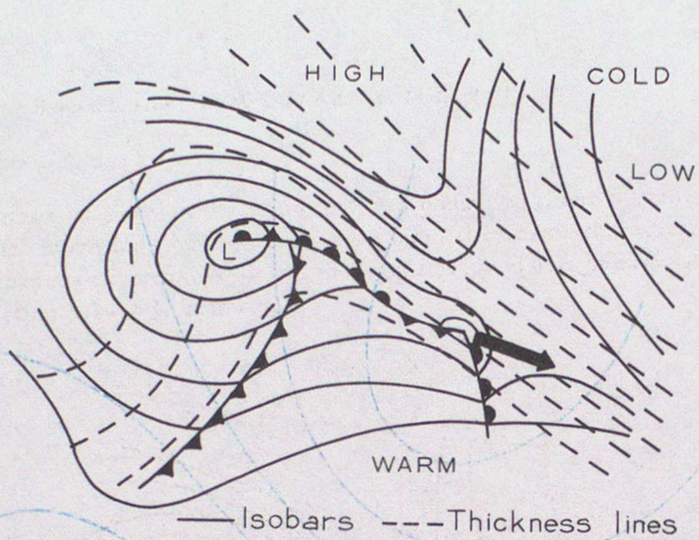

FIGURE 5.40 *Characteristic isobaric and thickness pattern accompanying the formation of a warm-front wave*

5.14.2.2. *Waves on cold fronts.* The thickness pattern associated with waves on cold fronts is usually somewhat similar to that depicted in Figure 5.36 (but not all wave cyclones develop into major depressions as indicated in Figures 5.37 to 5.39). Sawyer[24] has made a study of these fairly common waves. All waves which formed in the eastern half of the Atlantic and over Europe during the year February 1948 to January 1949 were examined. A number of results useful in forecasting were obtained. The following results deal specifically with waves on cold fronts and associated thickness patterns. (Some aspects of weather associated with waves on fronts are considered in Chapter 8.)

(i) If a cold front extends over a length of 1,200 miles or more and is associated with a thermal wind (1000–500 millibars) of 25 knots or more over this length, a new wave should be expected on it.

(ii) New waves should not be inserted on shorter fronts or fronts not fulfilling condition (i).

(iii) On fronts satisfying condition (i) the wave may be expected to develop either:

(a) where the front is subject to orographic distortion,

(b) where a bulge in the front can be produced by the flow round adjacent pressure systems

or *(c)* where the thermal vorticity term $V' \dfrac{\partial \zeta'}{\partial s}$ is a maximum.

(iv) If a direct estimate of the thermal vorticity advection is not possible the most probable position for a new wave to form is between 200 and 600 miles east of a thermal trough-line.

(v) Both the thermal wind and the direction of the warm-sector isobars are a good guide to the direction of motion of a newly formed wave.

(vi) The speed of the newly formed wave is not closely related with the thermal wind speed and probably the most useful initial estimate is obtained by taking about four-fifths of the geostrophic wind speed in the warm sector.

(vii) Waves associated with a markedly diffluent thermal pattern move slowly.

Waves which form under conditions satisfying iii *(a)* and *(b)* may be regarded as "induced" and those forming according to iii *(c)* may be considered as "non-induced". Sawyer[24] found no common thickness patterns associated with either "induced" or "non-induced" waves. Indeed for "non-induced" waves the existence of negative values of the thermal vorticity term $V' \frac{\partial \zeta'}{\partial s}$ showed that this is not a major factor in the formation of these waves. On the other hand there was such a strong preponderance of negative values of $V' \frac{\partial \zeta'}{\partial s}$ in association with induced waves as to suggest that an area of negative values of $V' \frac{\partial \zeta'}{\partial s}$ is needed for the spontaneous development of a wave. New waves tend to appear first towards that edge of the area of positive thermal vorticity towards which the thermal wind is directed.

5.14.2.3. *Secondary depressions at the triple point of a warm occlusion.* For the formation of a secondary depression at the triple point of a warm occlusion there must be, according to Sawyer:[23]

(i) a slow-moving primary depression,

(ii) a notably strong thermal gradient of warm-front type ahead of the primary (somewhere to the east) with the maximum gradient displaced some distance from the centre of the primary. The thermal wind (1000–500 millibars) is usually 40–80 knots.

A characteristic isobaric and thickness pattern is shown in Figure 5.41.

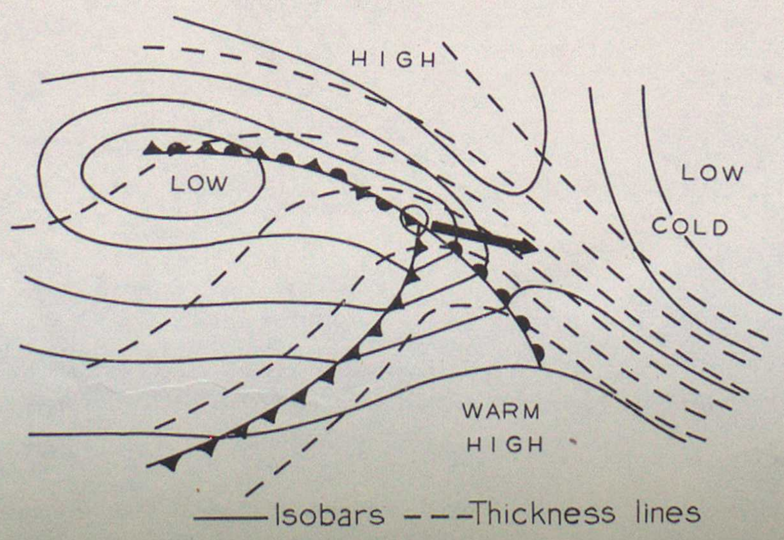

FIGURE 5.41 *Characteristic isobaric and thickness pattern leading to the formation of a warm-occlusion secondary*

Once formed, the behaviour of warm-occlusion secondaries and warm-front waves is very similar. They move quickly away from the primary at a speed usually between 30 and 50 knots and for this reason are often called break-away depressions. The direction of motion follows closely the thickness line over the centre but, due to the distortion caused by the secondary itself, it tends to be inclined slightly towards the cold side of the strong thermal belt which existed before the secondary appeared; the average inclination is about 30 degrees for warm-occlusion secondaries and 10 degrees for warm-front waves. Forecasters can usually infer the time at which such a thermal field is likely to be established and there is usually a lag of up to or somewhat more than 24 hours between the first appearance of the pattern and the formation of a secondary at the point of occlusion.

5.14.2.4. *Secondary depressions at the triple point of a cold occlusion.* Sawyer's[23] investigation shows that for the formation of a secondary at the triple point of a cold occlusion there must be:

(i) a strong thermal gradient several hundred miles from the centre of the primary – the thermal gradient over the centre of the primary is relatively weak and the primary is usually slow-moving,

(ii) a marked diffluence of the thickness lines ahead of the point of occlusion from the region of strong thermal gradient behind it (that is, usually to the west).

Characteristic isobaric and thickness patterns are shown in Figure 5.42.

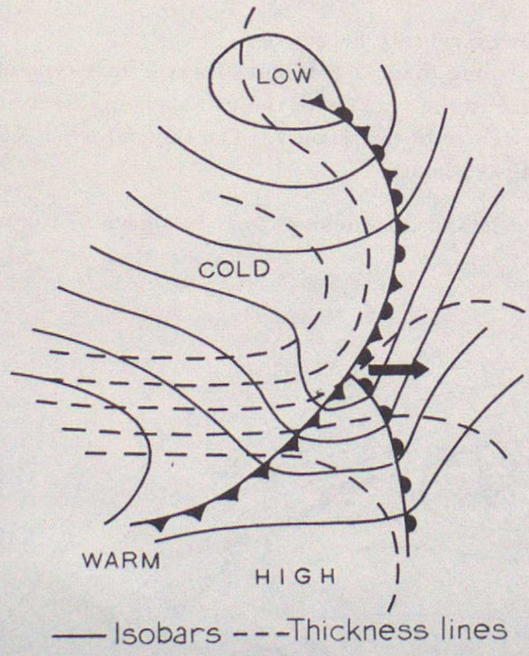

FIGURE 5.42 *Characteristic isobaric and thickness pattern accompanying the formation of a secondary on a cold occlusion*

Sawyer further comments that:

"The behaviour of secondaries on cold occlusions is less regular than that of those on warm occlusions, and it seems to be more dependent on the details of the thickness pattern around them. If the diffluence of the thickness lines is broadly symmetrical as indicated in Figure 5.42 a rather slow motion is usual in the general direction of the strong thermal winds. A speed of 10–20 kt. can be expected. However, if the thermal gradient is stronger in the left-hand or right-hand branch of the diffluence corresponding motion towards the left or right is probable and the speed is somewhat greater than in the symmetrical case. Although these secondaries often go through a short-lived phase of rapid deepening very few become major features of the synoptic chart.

"There is an important association between secondaries on cold occlusions and the "jet stream" . . . A jet stream will usually be found above the strong thermal belt behind the point of occlusion at which a secondary forms. The secondary forms beneath the left exit from the jet, and the changes in the flow which accompany the development of the secondary result in the extension of the jet in the direction of the stream."

As with warm-front waves and secondaries forecasters can normally recognize in advance occasions when the characteristic thickness pattern will appear and there is usually a lag of up to 24 hours between the first appearance of the pattern and the formation of a secondary.

5.14.2.5. *Application of* 5.14.2.3 *and* 5.14.2.4 *to forecasting.* An indication of the success which may be achieved in using the criteria in 5.14.2.3 and 5.14.2.4 to forecast the formation of secondaries at points of occlusion may be obtained from the test which Sawyer[23] made during the period October 1947 to September 1948. Each occlusion was considered and counted once only and the results are shown in Table 5.2.

TABLE 5.2. *Summary of results of test of criteria for the formation of a secondary depression at the point of occlusion October 1947 to September 1948*

	No secondary expected	*Cold occlusion, secondary expected*	*Warm occlusion, secondary expected*
No secondary formed	137	14	9
Secondary formed	14	40	23

Total successes = 200; total failures = 37

5.15. SOME THICKNESS PATTERNS ASSOCIATED WITH ANTICYCLONES

Sawyer[25] has made a preliminary classification of the main types of thickness patterns which occur over anticyclones. The classification was made from an examination of anticyclones (identifiable by 4-millibar isobars over a 24-hour period) over the area between latitudes 40° and 60°N. and longitudes 0° and 50°W. during the period October 1946 to April 1948. It should be noted that the area is limited to the eastern North Atlantic Ocean and the seaboard of western Europe. The majority of anticyclones could be classified into three main types with distinct thickness patterns. A fourth type was suggested but the number of cases were insufficient to establish the fourth type with certainty. Sawyer describes the following types.

5.15.1. "*Type 1 – Open wave type* [*the classical mobile high*]

"The features of the thermal field are:

(a) Strong thermal wind over the centre (usually 40–50 kt. over the range 1000–500 mb.)

(b) Flat "wave" pattern of thickness lines with the anticyclonic centre between a "thermal ridge" and the next "thermal trough" in the direction of the thermal wind (for this purpose a "flat" wave pattern may be regarded as one in which the maximum inclination to the general stream is less than 45°).

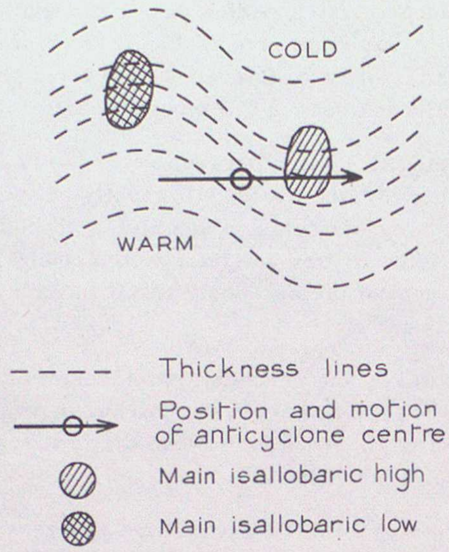

FIGURE 5.43 *Open wave type of anticyclone*

"The simultaneous behaviour of the centre is:

(i) Fast motion towards the "thermal trough". The average speed is about 25 kt. but varies over a wide range; motion is in a direction roughly perpendicular to the trough line but there appears to be a tendency to move toward the region where the thermal wind is strongest.

(ii) Central pressure may rise or fall slowly; possibly rising pressure is slightly more frequent.

5.15.2. "*Type 2 – Distorted wave type*

"The features of the thermal field are:

(a) Strong thermal wind over the centre; usually 40–50 kt. when taken over the range 1000–500 mb.

(b) A "wave" pattern of wide amplitude in the thickness lines with the anticyclonic centre between a "thermal ridge" and the next "thermal trough" in the direction of the thermal wind. The difference between this type and the preceding type is in the distortion of the wave pattern which should twist the thickness lines to an angle of more than 45° from the general stream, i.e. from the

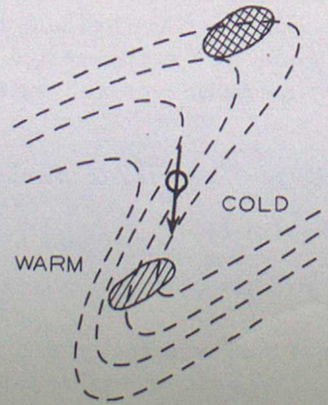

FIGURE 5.44 *Distorted wave type of anticyclone*

general direction of the thickness lines over a wide area over which the distortion in the region of the anticyclone can be ignored.

"The simultaneous behaviour of the pressure centre is:

(i) Slow motion (10–25 kt.) towards the "thermal trough". The direction is usually inclined to the right of the perpendicular to the trough line, but involves displacement across the thickness lines into the cold air.

(ii) Central pressure changing little or rising slowly.

5.15.3. "*Type 3 – Warm anticyclone*

"The features of the thermal field are:

(a) Very weak thermal gradients near the anticyclonic centre.

(b) Anticyclonic centre lies on or near the axis of the warm tongue.

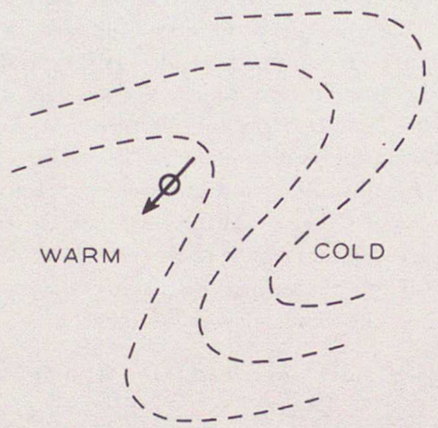

FIGURE 5.45 *Warm anticyclone*

"The characteristic behaviour is:

(i) Very slow motion (usually less than 10 kt.).

(ii) Direction of motion usually in a direction between the axis of the warm tongue towards the higher temperature and the direction from the anticyclone centre to the apex of the cold trough.

(iii) Little change in central pressure.

5.15.4. "*Type 4 – Diffluent ridge type* [*now termed occluding ridge type*]

"This type is not clearly defined because of lack of examples. Its main features are similar to Type 3 but it differs in that the next thermal trough is

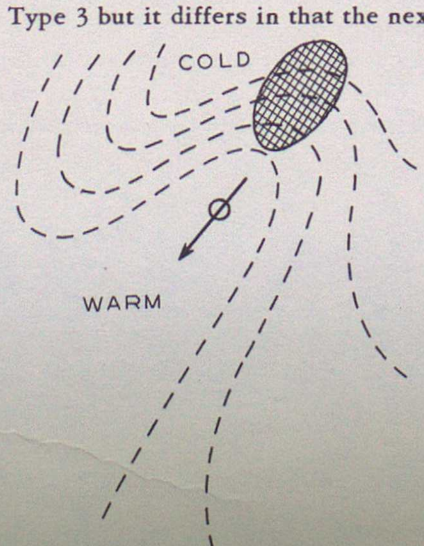

FIGURE 5.46 *Occluding ridge type of anticyclone*

advancing towards the anticyclone centre. [The short distance between the advancing thermal trough and the thermal ridge makes the cross-hatched area highly cyclogenetic leading to the rapid retreat and/or decline of the anticyclone.]

"The motion of the centre is in a similar direction to that of Type 3 but quicker (15–20 kt.); the central pressure decreases, sometimes rapidly."

5.16. SELF-MAINTAINING AND SELF-DESTROYING SYSTEMS

In using thickness techniques on the bench forecasters will soon realize that the relatively simple schematic patterns described in previous sections, although they occur quite frequently as types, are usually somewhat less smooth and more distorted in practice. Nevertheless, on a day-to-day basis, the forecasting problem – so far as the thickness technique is concerned – reduces to a qualitative assessment of thermal steering, thermal vorticity and the distortion of the temperature field. All three are interacting and a solution rests on a qualitative judgement. In spite of the complexities forecasters will, through experience based on careful forecasting and subsequent back-casting, come to recognize situations which are self-maintaining and therefore persistent. These are naturally common or typical. Other situations are self-destroying and therefore non-persistent. These are unusual but it is nevertheless desirable to recognize them since the successful forecaster hopes to achieve accuracy when unusual developments – as well as the more common – occur.

Sutcliffe and Forsdyke[14] have described three types of self-maintaining systems. They are:

(i) The classical warm-sector depression.

This was illustrated in Figures 5.36 to 5.38. It is readily seen that the circulation of the depression creates the sinusoidal thermal pattern by advection and so produces a thermal field which in turn requires cyclogenesis at the trough – ridge thermal inflexion.

(ii) The classical mobile anticyclone.

This was illustrated in Figure 5.43 and it is clear that the circulation and continued development of the anticyclone leads to the distortion of the thickness pattern to that illustrated in Figure 5.44 and finally to Figure 5.45. This is the transformation of the mobile cold anticyclone to the warm type. The processes are clearly analogous to that described in (i) above.

(iii) The jet-stream complex.

The thickness pattern associated with a thermal jet is shown schematically in Figure 5.47 which is, in effect, a combination of Figures 5.33*(a)* and *(b)*. Cyclonic (C) and anticyclonic (A) regions due to thermal vorticity are shown.

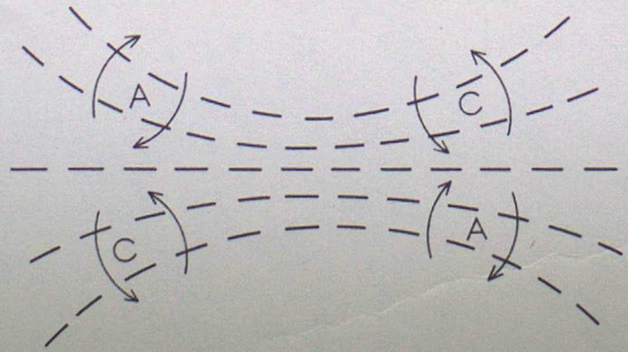

FIGURE 5.47 *The thermal jet*

If a depression and anticyclone appear at the exit with associated circulations as indicated by the arrows, advection tends to close the thickness lines together in the rear of the centres and to fan them out ahead. Thus the diffluence at the exit is maintained and, as the systems move forward, the circulations in their rear maintain the tight thermal gradient.

The systems marked at the entrance to the jet also lead to its maintenance. Thus the thermal jet is of a self-generating type in which the circulations often tend to produce and maintain frontogenesis along the axis of the jet.

(iv) Self-destroying systems.

Self-destroying systems are less common and have not been studied in detail. It does happen that circulations move into areas where the thermal pattern and its subsequent modification (due to the system) do not support the continued existence of the circulation. These situations are self-destroying and can usually be recognized by considering the future thickness pattern which is likely to arise from advection.

5.17. SYNOPTIC EXAMPLES

In this chapter there is a liberal number of schematic illustrations of features associated with various configurations of 1000–500-millibar thicknesses. The further benefit which forecasters would derive directly from the charts and descriptive text of a large number of actual synoptic examples would be relatively small since they would mainly duplicate the schematic illustrations. Practising forecasters will more readily derive valuable experience and develop expertise in applying the concepts by consistently and conscientiously interpreting the day-to-day charts in terms of the dynamical theories expounded in this chapter. Accordingly a series of synoptic examples is not included here.

It should, however, be instructive to include a set of charts indicating the magnitudes of the thermal steering and thermal vorticity terms in the Sutcliffe development equation. Figure 5.48 shows the surface fronts, the 1000-millibar contours and the 1000–500-millibar thicknesses for 1500 G.M.T., 4 October 1955. A wave depression in mid-Atlantic was moving east-north-east at about 40 knots and deepening at a rate of about 2 millibars per 3 hours. Figures 5.49*(a)* and *(b)* show the distribution of isopleths of the thermal steering and thermal vorticity terms. It will be seen that the magnitude of the steering term is greater and contributes toward forward translation. The smaller thermal vorticity gives an indication that troughing might be expected to develop to north-west of the tip of the wave.

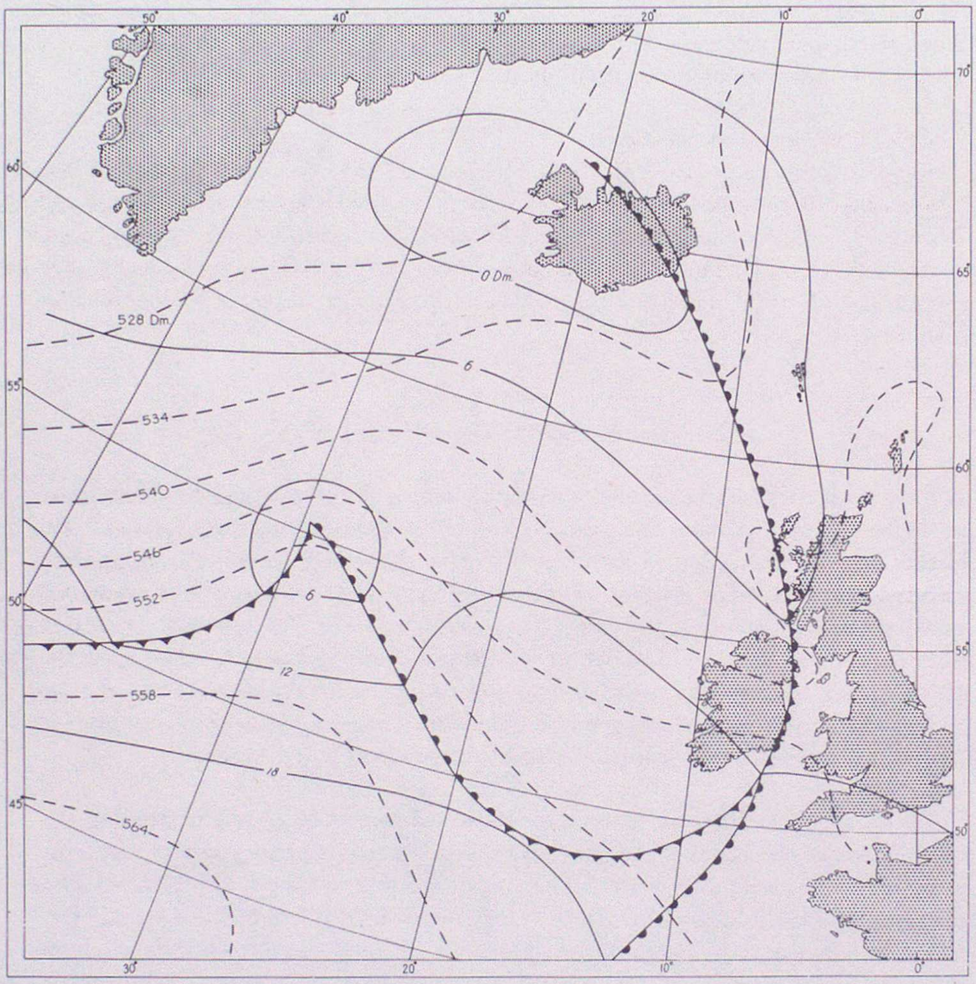

FIGURE 5.48 *Surface fronts, 1000-mb. contours (full lines) and 1000–500-mb. thicknesses (broken lines), 1500 G.M.T., 4 October 1955*

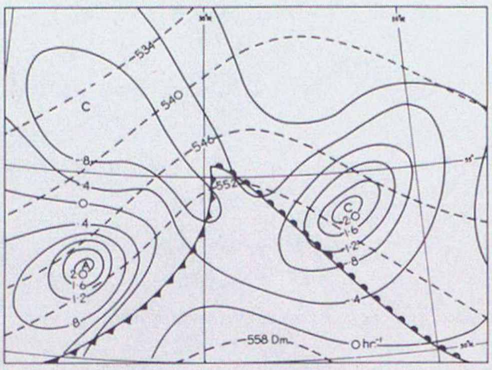

FIGURE 5.49(*a*) *1000–500-mb. thickness (broken lines) and isopleths of* $\dfrac{2V'}{l} \cdot \dfrac{\partial \zeta_o}{\partial s}$ *(thermal steering term), 1500 G.M.T., 4 October 1955*

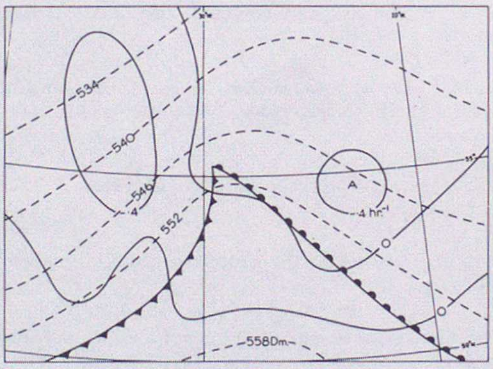

FIGURE 5.49(*b*) *1000–500mb. thickness (broken lines) and isopleths of* $\dfrac{V'}{l} \cdot \dfrac{\partial \zeta'}{\partial s}$ *(thermal vorticity term), 1500 G.M.T., 4 October 1955*

BIBLIOGRAPHY

1. DOUGLAS, C.K.M.; The evolution of 20th century forecasting in the British Isles. *Quart. J.R. met. Soc., London,* 78, 1952, p. 1.

2. RIEHL, H. *et alii;* Forecasting in middle latitudes. *Met. Monogr., Boston, Mass.,* 1, No. 5, 1952.

3. GLASER, A.H.; A possible sunspot influence on the general circulation. *J. Met., Boston, Mass.,* 14, 1957, p. 375.

4. SMITH, C.V.; Synoptic evolution of 500-millibar flow patterns. *Met. Rep., London,* 3, No. 21, 1959.

5. DINES, W.H.; The characteristics of the free atmosphere. *Geophys. Mem., London,* 2, No. 13, 1919.

6. BANNON, J.K. and GILCHRIST, A.; Variation of temperature in the troposphere and lower stratosphere. *Quart. J.R. met. Soc., London,* 82, 1956, p. 58.

7. HAURWITZ, B.; Dynamic meteorology. London, 1941, p. 138.

8. PETTERSSEN, S.; Weather analysis and forecasting. London, Vol. I, 1956, p.104.

9. ROSSBY, C.–G.; Relation between variations in the intensity of the zonal circulation of the atmosphere and the displacements of the semi-permanent centers of action. *J. Mar. Res., New Haven,* 2, 1939, p.38.

10. London, Meteorological Office; A test of the Rossby formula as applied to the movement of long atmospheric waves at the 500 mb. level. *Met. Res. Pap., London,* No. 605, 1951.

11. SUTCLIFFE, R.C.; Cyclonic and anticyclonic development. *Quart. J.R. met. Soc., London,* 65, 1939, p.518.

12. SUTCLIFFE, R.C.; A contribution to the problem of development. *Quart. J.R. met. Soc., London,* 73, 1947, p.370.

13. SAWYER, J.S.; The significance of vorticity in dynamical meteorology. 1951. Unpublished. Copy available in Meteorological Office Library.

14. SUTCLIFFE, R.C. and FORSDYKE, A.G.; Theory and use of upper air thickness patterns. *Quart. J.R. met. Soc., London,* 76, 1950, p.189.

15. SUTCLIFFE, R.C. and GODART, C.H.; Isobaric analysis. *S.D.T.M. No.* 50. Unpublished. Copy available in Meteorological Office Library.

16. BRUNT, D.; Physical and dynamical meteorology. Cambridge, 1939, pp.38, 40.

17. PETTERSSEN, S., SHEPPARD, P.A., PRIESTLEY, C.H.B. and JOHANNESSEN, K.R.; An investigation of subsidence in the free atmosphere. *Quart. J.R. met. Soc., London,* 73, 1947, p.43.

18. BUSHBY, F.H.; Vertical velocity and thickness tendency. *Quart. J.R. met. Soc., London,* 78, 1952, p.354.

19. BELASCO, J.E.; Characteristics of air masses over the British Isles. *Geophys. Mem., London,* 11, No. 87, 1954.

20. CRADDOCK, J.M.; The warming of arctic air masses over the eastern North Atlantic. *Quart. J.R. met. Soc., London,* 77, 1951, p.355.

21. HOUGHTON, J.T. and BREWER, A.W.; Measurements of the flux of long-wave radiation in the upper air, 1953–1954. *Met. Res. Pap., London,* No. 914. 1955.

22. London, Meteorological Office; 1000–500-millibar thickness, North America to Europe, 1946–51. Monthly means and extremes. *Met. Rep., London,* 2, No. 13, 1953.

23. SAWYER, J.S.; Formation of secondary depressions in relation to the thickness pattern. *Met. Mag., London,* 79, 1950, p. 1.

24. SAWYER, J.S.; The formation and behaviour of cold front waves. *Met. Res. Pap., London,* No. 553, 1950.

25. SAWYER, J.S.; A preliminary classification of anticyclones by means of the thickness pattern. *Met. Mag., London,* 78, 1949, p. 189.

BOOKS FOR FURTHER READING

BRUNT, D.; Physical and dynamical meteorology. Cambridge, 1939, Chapters 8, 9, 14, 15, 17 and 18.

PETTERSSEN, S.; Weather analysis and forecasting. New York, 1st. edn. 1940, Chapters 4, 5, 7, 9 and 10. 2nd. edn. 1956, Vol. I.

HEWSON, E.W. and LONGLEY, R.W.; Meteorology, theoretical and applied. London, 1951, Chapters 6 and 8.

SAUCIER, W.J.; Principles of meteorological analysis. Chicago, 1955, Chapters 6, 7, 9, 10 and 11.

PANOFSKY, H.; Introduction to dynamic meteorology. Pennsylvania, 1956, Chapters 1–5.

APPENDIX I

Detailed algebra to derive equation (8) from equations (6) and (7) (see page 36 of text)

$$\frac{\partial u}{\partial t} + u\frac{\partial u}{\partial x} + v\frac{\partial u}{\partial y} - lv + g\frac{\partial h}{\partial x} = 0 \qquad \ldots (6)$$

$$\frac{\partial v}{\partial t} + u\frac{\partial v}{\partial x} + v\frac{\partial v}{\partial y} + lu + g\frac{\partial h}{\partial y} = 0 \qquad \ldots (7)$$

Differentiate equation (6) with respect to y; then:

$$\frac{\partial}{\partial y}\frac{\partial u}{\partial t} + \frac{\partial u}{\partial y}\frac{\partial u}{\partial x} + u\frac{\partial^2 u}{\partial x \partial y} + \frac{\partial v}{\partial y}\frac{\partial u}{\partial y} +$$

$$+ v\frac{\partial^2 u}{\partial y^2} - l\frac{\partial v}{\partial y} - v\frac{\partial l}{\partial y} + g\frac{\partial^2 h}{\partial x \partial y} = 0 . \qquad \ldots (6A)$$

Differentiate equation (7) with respect to x; then:

$$\frac{\partial}{\partial x}\frac{\partial v}{\partial t} + \frac{\partial u}{\partial x}\frac{\partial v}{\partial x} + u\frac{\partial^2 v}{\partial x^2} + \frac{\partial v}{\partial x}\frac{\partial v}{\partial y} +$$

$$+ v\frac{\partial^2 v}{\partial x \partial y} + l\frac{\partial u}{\partial x} + u\frac{\partial l}{\partial x} + g\frac{\partial^2 h}{\partial x \partial y} = 0 . \qquad \ldots (7A)$$

Subtract equation (6A) from (7A) to obtain:

$$\frac{\partial}{\partial x}\frac{\partial v}{\partial t} - \frac{\partial}{\partial y}\frac{\partial u}{\partial t} + \frac{\partial u}{\partial x}\frac{\partial v}{\partial x} - \frac{\partial u}{\partial y}\frac{\partial u}{\partial x} + u\frac{\partial^2 v}{\partial x^2} - u\frac{\partial^2 u}{\partial x \partial y} + \frac{\partial v}{\partial x}\frac{\partial v}{\partial y} - \frac{\partial v}{\partial y}\frac{\partial u}{\partial y} +$$

$$+ v\frac{\partial^2 v}{\partial x \partial y} - v\frac{\partial^2 u}{\partial y^2} + l\frac{\partial u}{\partial x} + l\frac{\partial v}{\partial y} + u\frac{\partial l}{\partial x} + v\frac{\partial l}{\partial y} = 0 . \qquad \ldots (8A)$$

Collect terms containing u, v or l explicitly as factors to obtain:

$$\underset{(1)}{\frac{\partial}{\partial x}\frac{\partial v}{\partial t}} - \underset{(2)}{\frac{\partial}{\partial y}\frac{\partial u}{\partial t}} + u\underset{(3)}{\left(\frac{\partial^2 v}{\partial x^2} - \frac{\partial^2 u}{\partial x \partial y} + \frac{\partial l}{\partial x}\right)} + v\underset{(4)}{\left(\frac{\partial^2 v}{\partial x \partial y} - \frac{\partial^2 u}{\partial y^2} + \frac{\partial l}{\partial y}\right)} +$$

$$+ \underset{(5)}{\left(\frac{\partial u}{\partial x}\frac{\partial v}{\partial x} - \frac{\partial u}{\partial y}\frac{\partial u}{\partial x} + \frac{\partial v}{\partial x}\frac{\partial v}{\partial y} - \frac{\partial v}{\partial y}\frac{\partial u}{\partial y}\right)} + l\underset{(6)}{\left(\frac{\partial u}{\partial x} + \frac{\partial v}{\partial y}\right)} = 0 . \qquad \ldots (8B)$$

The terms in equation (8B) are given subscript numbers for ease of identification.

Terms (1) and (2) are $\dfrac{\partial}{\partial x}\dfrac{\partial v}{\partial t} - \dfrac{\partial}{\partial y}\dfrac{\partial u}{\partial t}$

$= \dfrac{\partial}{\partial t}\dfrac{\partial v}{\partial x} - \dfrac{\partial}{\partial t}\dfrac{\partial u}{\partial y}$ (by changing the order of differentiation)

$$= \frac{\partial}{\partial t}\left(\frac{\partial v}{\partial x} - \frac{\partial u}{\partial y}\right) .$$

Term (3) is $\dfrac{\partial^2 v}{\partial x^2} - \dfrac{\partial^2 u}{\partial x \partial y} + \dfrac{\partial l}{\partial x}$

$$= \frac{\partial}{\partial x}\left(\frac{\partial v}{\partial x} - \frac{\partial u}{\partial y} + l\right) .$$

Term (4) is
$$\frac{\partial^2 v}{\partial x \partial y} - \frac{\partial^2 u}{\partial y^2} + \frac{\partial l}{\partial y}$$
$$= \frac{\partial}{\partial y}\left(\frac{\partial v}{\partial x} - \frac{\partial u}{\partial y} + l\right).$$

Term (5) is
$$\frac{\partial u}{\partial x}\frac{\partial v}{\partial x} - \frac{\partial u}{\partial y}\frac{\partial u}{\partial x} + \frac{\partial v}{\partial x}\frac{\partial v}{\partial y} - \frac{\partial v}{\partial y}\frac{\partial u}{\partial y}$$
$$= \frac{\partial u}{\partial x}\left(\frac{\partial v}{\partial x} - \frac{\partial u}{\partial y}\right) + \frac{\partial v}{\partial y}\left(\frac{\partial v}{\partial x} - \frac{\partial u}{\partial y}\right)$$
$$= \left(\frac{\partial u}{\partial x} + \frac{\partial v}{\partial y}\right)\left(\frac{\partial v}{\partial x} - \frac{\partial u}{\partial y}\right).$$

Thus term (5) plus term (6) is
$$\left(\frac{\partial u}{\partial x} + \frac{\partial v}{\partial y}\right)\left(\frac{\partial v}{\partial x} - \frac{\partial u}{\partial y}\right) + l\left(\frac{\partial u}{\partial x} + \frac{\partial v}{\partial y}\right)$$
$$= \left(\frac{\partial u}{\partial x} + \frac{\partial v}{\partial y}\right)\left(\frac{\partial v}{\partial x} - \frac{\partial u}{\partial y} + l\right).$$

Making use of these expressions for terms (1) to (6) it is seen that equation (8B) becomes:

$$\frac{\partial}{\partial t}\left(\frac{\partial v}{\partial x} - \frac{\partial u}{\partial y}\right) + u\frac{\partial}{\partial x}\left(\frac{\partial v}{\partial x} - \frac{\partial u}{\partial y} + l\right) + v\frac{\partial}{\partial y}\left(\frac{\partial v}{\partial x} - \frac{\partial u}{\partial y} + l\right) +$$
$$+ \left(\frac{\partial v}{\partial x} - \frac{\partial u}{\partial y} + l\right)\left(\frac{\partial u}{\partial x} + \frac{\partial v}{\partial y}\right) = 0$$

and this is identical with equation (8) on page 36.

APPENDIX 2

Detailed algebra to derive equation (23) from equation (22) (see page 44 of text)

The operator $\nabla^2 = \dfrac{\partial^2}{\partial x^2} + \dfrac{\partial^2}{\partial y^2}$ is used and the general form of $\nabla^2 (fg)$, where f and g are both functions of x and y, is established:

$$\frac{\partial (fg)}{\partial x} = f\frac{\partial g}{\partial x} + g\frac{\partial f}{\partial x}$$

$$\frac{\partial^2 (fg)}{\partial x^2} = f\frac{\partial^2 g}{\partial x^2} + \frac{\partial f}{\partial x}\frac{\partial g}{\partial x} + g\frac{\partial^2 f}{\partial x^2} + \frac{\partial g}{\partial x}\frac{\partial f}{\partial x}$$

$$= f\frac{\partial^2 g}{\partial x^2} + 2\frac{\partial f}{\partial x}\frac{\partial g}{\partial x} + g\frac{\partial^2 f}{\partial x^2}.$$

Similarly $$\frac{\partial^2 (fg)}{\partial y^2} = f\frac{\partial^2 g}{\partial y^2} + 2\frac{\partial f}{\partial y}\frac{\partial g}{\partial y} + g\frac{\partial^2 f}{\partial y^2}$$

therefore $$\nabla^2 (fg) = \frac{\partial^2 (fg)}{\partial x^2} + \frac{\partial^2 (fg)}{\partial y^2}$$

$$= f\left(\frac{\partial^2 g}{\partial x^2} + \frac{\partial^2 g}{\partial y^2}\right) + 2\frac{\partial f}{\partial x}\frac{\partial g}{\partial x} + 2\frac{\partial f}{\partial y}\frac{\partial g}{\partial y} + g\left(\frac{\partial^2 f}{\partial x^2} + \frac{\partial^2 f}{\partial y^2}\right)$$

$$= f\,\nabla^2 g + 2\frac{\partial f}{\partial x}\frac{\partial g}{\partial x} + 2\frac{\partial f}{\partial y}\frac{\partial g}{\partial y} + g\,\nabla^2 f.$$

This general expression can now be used to write down the result of operating on equation (22) with ∇^2.

Equation (22) is $$\frac{\partial h'}{\partial t} + u_o\frac{\partial h'}{\partial x} + v_o\frac{\partial h'}{\partial y} = 0. \qquad \ldots \quad (22)$$

Operating with ∇^2 gives:

$$\nabla^2\frac{\partial h'}{\partial t} + u_o\nabla^2\frac{\partial h'}{\partial x} + 2\frac{\partial u_o}{\partial x}\frac{\partial^2 h'}{\partial x^2} + 2\frac{\partial u_o}{\partial y}\frac{\partial^2 h'}{\partial x\,\partial y} + \frac{\partial h'}{\partial x}\nabla^2 u_o + v_o\nabla^2\frac{\partial h'}{\partial y} +$$

$$+ 2\frac{\partial v_o}{\partial x}\frac{\partial^2 h'}{\partial x\,\partial y} + 2\frac{\partial v_o}{\partial y}\frac{\partial^2 h'}{\partial y^2} + \frac{\partial h'}{\partial y}\nabla^2 v_o = 0. \qquad \ldots \quad (22A)$$

Rearranging the terms this becomes:

$$\underset{(1)}{\nabla^2\frac{\partial h'}{\partial t} + u_o\nabla^2\frac{\partial h'}{\partial x}} + \underset{(2)}{v_o\nabla^2\frac{\partial h'}{\partial y}} + \underset{(3)}{\frac{\partial h'}{\partial x}\nabla^2 u_o} + \underset{(4)}{\frac{\partial h'}{\partial y}\nabla^2 v_o} + \underset{(5)}{2\frac{\partial^2 h'}{\partial x\,\partial y}\left(\frac{\partial u_o}{\partial y} + \frac{\partial v_o}{\partial x}\right)} +$$

$$+ \underset{(6)}{2\left(\frac{\partial u_o}{\partial x}\frac{\partial^2 h'}{\partial x^2} + \frac{\partial v_o}{\partial y}\frac{\partial^2 h'}{\partial y^2}\right)} = 0. \qquad \ldots \quad (23B)$$

Some terms in the above equation are given subscript numbers for ease of identification. In terms (1) and (2) we shall change the order of differentiation so that they become $u_o\dfrac{\partial}{\partial x}\nabla^2 h'$ and $v_o\dfrac{\partial}{\partial y}\nabla^2 h'$ respectively.

We shall now make use of the geostrophic relations:

$$u_o = -\frac{g}{l}\frac{\partial h_o}{\partial y} \qquad v_o = \frac{g}{l}\frac{\partial h_o}{\partial x} \qquad u' = -\frac{g}{l}\frac{\partial h'}{\partial y} \qquad v' = \frac{g}{l}\frac{\partial h'}{\partial x}$$

Term (3) is $\frac{\partial h'}{\partial x}\nabla^2 u_o = \frac{l}{g} v'\nabla^2\left(-\frac{g}{l}\frac{\partial h_o}{\partial y}\right)$

$$= \frac{l}{g}\left(-\frac{g}{l}\right)v'\nabla^2\frac{\partial h_o}{\partial y}, \quad \text{provided that variations of } l \text{ are neglected,}$$

$$= -v'\nabla^2\left(\frac{\partial h_o}{\partial y}\right)$$

$$= -v'\frac{\partial}{\partial y}\nabla^2 h_o, \quad \text{by changing the order of differentiation.}$$

Similarly term (4) is $\frac{\partial h'}{\partial y}\nabla^2 v_o = -\frac{l}{g}u'\nabla^2\left(\frac{g}{l}\frac{\partial h_o}{\partial x}\right)$

$$= -u'\nabla^2\left(\frac{\partial h_o}{\partial x}\right)$$

$$= -u'\frac{\partial}{\partial x}\nabla^2 h_o\,.$$

It is difficult to show analytically that terms (5) and (6) are necessarily small. However, on the scale of motion under consideration (that is, the large-scale features of the tropospheric flow pattern) numerical computations on actual charts indicate that the terms (5) and (6) are usually small compared with $\nabla^2\frac{\partial h'}{\partial t}$ and terms (1) to (4).

Using the transformations for terms (1) to (4) and writing D for terms (5) and (6), it is seen that equation (22B) may now be written:

$$\nabla^2\frac{\partial h'}{\partial t} + u_o\frac{\partial}{\partial x}\nabla^2 h' + v_o\frac{\partial}{\partial y}\nabla^2 h' - u'\frac{\partial}{\partial x}\nabla^2 h_o - v'\frac{\partial}{\partial y}\nabla^2 h_o + D = 0$$

which is equation (23).